

AD-754 320

CONSTRUCTION AND DESIGN OF ROCKET  
ENGINES (SELECTED ARTICLES)

V. A. Volodin

Foreign Technology Division  
Wright-Patterson Air Force Base, Ohio

27 October 1972

DISTRIBUTED BY:



National Technical Information Service  
U. S. DEPARTMENT OF COMMERCE  
5285 Port Royal Road, Springfield Va. 22151

AD 754320

FTD-HT-23-1442-72

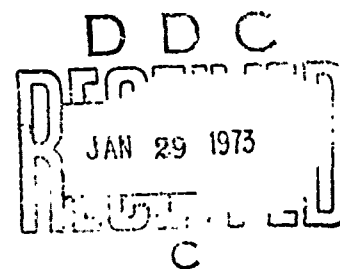
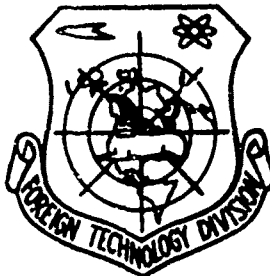
## FOREIGN TECHNOLOGY DIVISION



CONSTRUCTION AND DESIGN OF ROCKET ENGINES  
(SELECTED ARTICLES)

by

V. A. Volodin



Approved for public release;  
distribution unlimited.

145

Reproduced by  
NATIONAL TECHNICAL  
INFORMATION SERVICE  
U S Department of Commerce  
Springfield VA 22151

UNCLASSIFIED

Security Classification

DOCUMENT CONTROL DATA - R & D

(Security classification of title, body of abstract and indexing annotation must be entered when the overall report is classified)

1. ORIGINATING ACTIVITY (Corporate author)		2a. REPORT SECURITY CLASSIFICATION UNCLASSIFIED	
Foreign Technology Division Air Force Systems Command U. S. Air Force		2b. GROUP	
3. REPORT TITLE  CONSTRUCTION AND DESIGN OF ROCKET ENGINES (SELECTED ARTICLES)			
4. DESCRIPTIVE NOTES (Type of report and inclusive dates) Translation			
5. AUTHOR(S) (First name, middle initial, last name)  Volodin, V.A.			
6. REPORT DATE 1971		7a. TOTAL NO. OF PAGES 138-145	7b. NO. OF REPS 52
8. CONTRACT OR GRANT NO.		9a. ORIGINATOR'S REPORT NUMBER(S) FTD-HT-23-1442-72	
9. PROJECT NO. JDH		9b. OTHER REPORT NO(S) (Any other numbers that may be assigned to this report)	
10. DISTRIBUTION STATEMENT  Approved for public release; distribution unlimited.			
11. SUPPLEMENTARY NOTES		12. SPONSORING MILITARY ACTIVITY Foreign Technology Division Wright-Patterson AFB, Ohio	
13. ABSTRACT  This textbook gives a general survey, classification, and brief description of rocket engines and their working substances. It presents briefly the history of the development of rocket engines*. It examines the theory of thermal rocket engines* and presents the principles for the construction and design of rocket engines operating on liquid and solid chemical propellants. Some information is given on nuclear and electric rocket engines*. The textbook is intended for students at machine-construction technical schools. It can be useful to engineering and technical personnel engaged in rocket engine construction.			
*Those parts so marked are not included in the translation [Translator's note].			

DD FORM 1 NOV 68 1473

UNCLASSIFIED

Security Classification

~~UNCLASSIFIED~~

~~Security Classification~~

16. KEY WORDS	LINK A		LINK B		LINK C	
	ROLE	WT	ROLE	WT	ROLE	WT
Rocket Engine Thermal Rocket Engine Solid Propellant Engine Liquid Propellant Engine						

ib

~~CLASSIFIED~~

~~Security Classification~~

FTD-HT- 23-1442-72

# EDITED TRANSLATION

FTD-HT-23-1442-72

CONSTRUCTION AND DESIGN OF ROCKET ENGINES  
(SELECTED ARTICLES)

By: V. A. Volodin

English pages: 138

Source: Konstruktsiya i Proyektirovaniye  
Raketnykh Dvigateley, Izd-vo  
Mashinostroyeniye, Moscow, 1971, pp.  
131-139, 139-159, 159-187, 187-207,  
239-243, 244-269

Requester: FTD/PDTA

Translated by: John A. Miller

Approved for public release;  
distribution unlimited

THIS TRANSLATION IS A RENDITION OF THE ORIGINAL FOREIGN TEXT WITHOUT ANY ANALYTICAL OR EDITORIAL COMMENT. STATEMENTS OR THEORIES ADVOCATED OR IMPLIED ARE THOSE OF THE SOURCE AND DO NOT NECESSARILY REFLECT THE POSITION OR OPINION OF THE FOREIGN TECHNOLOGY DIVISION.

PREPARED BY:

TRANSLATION DIVISION  
FOREIGN TECHNOLOGY DIVISION  
WP-AFB, OHIO.

FTD-HT- 23-1442-72

1C

Date 27 Oct 1972

## TABLE OF CONTENTS

Abbreviations and acronyms used in the translation . . . . .	iii
CHAPTER IX. Typical schemes for liquid-propellant rocket engines . . . . .	1
§9.1. Features of LPRE schemes . . . . .	1
§9.2. Selecting optimum pressure $p_K$ . . . . .	8
CHAPTER X. Liquid chemical propellants . . . . .	12
§10.1. Simple oxidizers and fuels . . . . .	14
§10.2. Particular requirements of liquid chemical propellants . . . . .	16
§10.3. Characteristics of liquid propellants . . . . .	19
§10.4. Liquid oxidizers and fuels of rocket propellants	20
§10.5. Characteristics of two-component propellants (bipropellants) . . . . .	21
§10.6. Selecting the optimum oxidizer excess coefficient $\alpha_{OK}$ . . . . .	29
§10.7. Liquid monopropellants . . . . .	30
§10.8. Metal-containing fuels and tripropellants . . . . .	32
CHAPTER XI. Heat transfer and LPRE cooling . . . . .	34
§11.1. Forms of transfer of heat flows . . . . .	34
§11.2. Convection heat transfer . . . . .	36
§11.3. Radiation heat transfer . . . . .	39
§11.4. Heat transfer due to thermal conductivity of the wall material . . . . .	41
§11.5. Characteristics of heat transfer through a chamber wall . . . . .	43
§11.6. Requirements on the engine chamber cooling system . . . . .	46
§11.7. The influence of various factors on the heat flux from the combustion products to the wall . . . . .	48
§11.8. The influence of the parameters of the inner chamber wall on its cooling . . . . .	50

§11.9. The influence of the type of coolant and the parameters of external circulation cooling on the chamber cooling regime . . . . .	54
§11.10. Calculating coolant heating in the chamber cooling loop . . . . .	57
§11.11. Structural features of chamber cooling systems. . . . .	59
CHAPTER XII. The chambers of liquid-propellant rocket engines . . . . .	70
§12.1. The general characteristics of chambers . . . . .	70
§12.2. Shapes of the combustion chamber (afterburner) . . . . .	72
§12.3. Injectors . . . . .	75
§12.4. Chamber heads . . . . .	79
§12.5. Ways of positioning the injectors on flat heads. . . . .	82
§12.6. Calculating a chamber head . . . . .	84
§12.7. Selecting the volume and relative area of combustion chambers (afterburners) . . . . .	92
CHAPTER XIII. Systems for feeding liquid propellant components . . . . .	96
§13.13. Basic turbine parameters . . . . .	96
§13.14. Turbine efficiency and selection of the ratio $U/c_1$ . . . . .	98
§13.15. Liquid gasifiers . . . . .	100
CHAPTER XIV. Systems for LPRE start-up, mode change, and shutdown. Systems for creating controlling forces and moments . . . . .	103
§14.1. Systems for LPRE start-up . . . . .	103
§14.2. Ignition systems . . . . .	113
§14.3. Systems for changing the operating mode . . . . .	117
§14.4. Systems for creating controlling forces and moments . . . . .	125
§14.5. Systems for LPRE shutdown . . . . .	132
REFERENCES . . . . .	137

## ABBREVIATIONS AND ACRONYMS USED IN THE TRANSLATION

ад - adiabatic	н.п - heated surface
всп - auxiliary	ок - oxidizer
вх - inlet	о.п - cooled surface
вых - exit	опт - optimum
г - fuel	о.т - cooling loop
газ - gas	ох - coolant
газ.в - gas recovery	п - vacuum
г.в - gas vortex	пл - melting
гид - hydraulic	пос - [unidentified]
дУ - power plant	потр - required
ж - liquid, fluid	пр - reduced
з - ground, surface	р - rocket, missile
з.в - ignition delay	раб - working, operating
к - chamber	расп - available
к.в - kinematic viscosity	с - nozzle
к.з - swirl chamber	ср - mean, average
кип - boiling	ст - wall
кон - convection, convective	т - propellant
кон.н - convection-heated	турб - turbine
кр - critical	уд - specific
л - radiation, radiant	усл - arbitrary
л.н - radiation/chamber	φ - injector
нас - pump	э - effective
нач - initial	эк - equivalent

ERE - electric rocket engine [ЭРД, ERD]
ETJE - electrothermal jet engine [ЭТРД, ETRD]
LOX - liquid oxygen
LPRE - liquid-propellant rocket engine [ЖРД, ZhRD]
MMH - methylhydrazine [ММГ, MMG]
NRE - nuclear rocket engine [ЯРД, YaRD]
TPA - turbopump assembly [ТНА, TNA]
UDMH - uns. dimethylhydrazine [НДМГ, NDMG]

## CHAPTER IX

### TYPICAL SCHEMES FOR LIQUID-PROPELLANT ROCKET ENGINES [LPRE]

#### §9.1. Features of LPRE schemes

Liquid-propellant rocket engines with a *displacement system* of feeding propellant to the chamber can be subdivided, based on the method of producing the displacing gas, into engines with compressed-gas accumulators, with liquid gasifiers, and with solid-fuel gasifiers (see Chapter VIII). The simplest scheme of one such LPRE was examined in §1.2; they will be described in detail in Chapter XIII.

LPRE's with a *pump system* of propellant feed are classified according to the aggregate state of the propellant components entering the chamber and by the features of removal of the working medium after it has operated in the turbine; often the working medium is *generator gas*, i.e., it is generated in a gasifier.

As will be shown below, it is desirable to design an engine such that it operates without the use of additional propellant components. Therefore, in what follows we will examine only those schemes for LPRE's whose turbines operate on gas obtained from one or two basic propellant components. Usually, the chamber is cooled by the fuel; this is taken into consideration in all the schemes examined in this chapter.

LPRE's with exhausting of spent generator gas to the ambient medium (Fig. 9.1). The oxidizer and fuel enter the combustion chambers of such engines in the liquid state, i.e., the engine operates on the scheme "liquid-liquid," while the spent generator gas is exhausted through the nozzle of the exhaust pipe of the turbine to the ambient medium. Exhausting of this gas reduces the specific thrust of the engine. Although the nozzle of the turbine exhaust pipe, as already noted above, develops a certain thrust, its specific thrust, because of the low temperature of the generator gas and its low expansion ratio, is comparatively low. In the examined LPRE scheme, the generator gas is products of the incomplete combustion of a two-component propellant containing a large excess of oxidizer ( $\alpha_{OH} \gg 1$ ) or fuel ( $\alpha_{OH} \ll 1$ ). A liquid gasifier operating with  $\alpha_{OH} \gg 1$  is called an *oxidizing gasifier*, while one operating with  $\alpha_{OH} \ll 1$  is called a *reducing gasifier*.

An LPRE with feed of the spent generator gas to the combustion (afterburner) chamber. In such LPRE's the gas passing through the turbine is directed along the gas guide to the chamber as one of the basic propellant components; engines can operate on the "gas-liquid" and "gas-gas" schemes. Their common feature is high gas pressure at the turbine exit: it exceeds pressure  $p_{\infty}$  by the value of the hydraulic losses in the gas guide and the pressure differential in the gas injectors of the chamber.

In addition to the generator gas generated in a one- or two-component liquid gasifier, the working fluid of the turbine may be the gas that forms as a result of heating of one of the basic propellant components (e.g., hydrogen) in the chamber's cooling loop.

An LPRE with a one-component liquid gasifier can be created if one of the basic propellant components can decompose with the release of heat.

Let us examine the scheme of an LPRE in which the working fluid of the turbine is the products of decomposition of the oxidizer (e.g.,

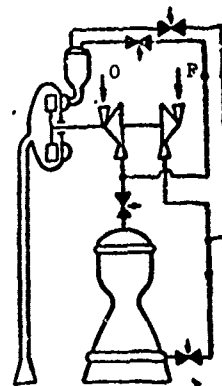


Fig. 9.1. LPRE with exhausting of spent generator gas to ambient medium.

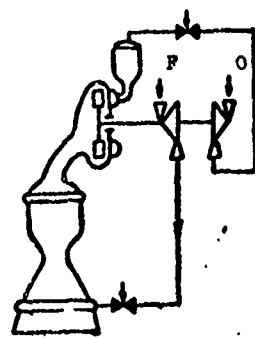


Fig. 9.2. LPRE operating on the scheme "gas-liquid" with oxidizing single-component liquid gasifier.

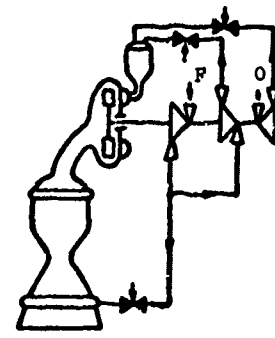


Fig. 9.3. LPRE operating on the scheme "gas-liquid" with oxidizing two-component liquid gasifier.

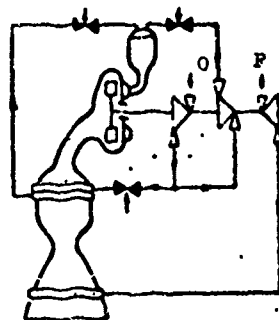


Fig. 9.4. LPRE operating on the scheme "gas-liquid" with reducing two-component liquid gasifier.

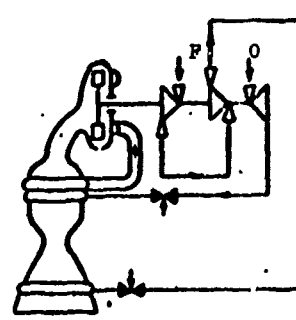


Fig. 9.5. LPRE operating on the scheme "gas-liquid" with gasification of working fluid of turbine in chamber cooling loop

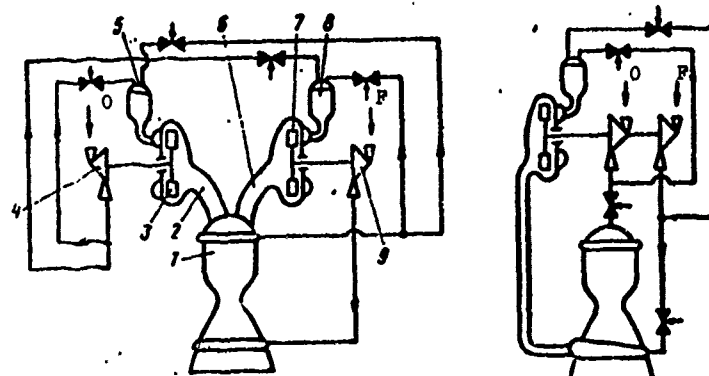


Fig. 9.6. LPRE operating on the scheme "gas-gas"; 1 - afterburner section; 2, 6 - gas guides; 3 - turbine of oxidizer TPA; 4 - oxidizer pump; 5 - oxidizing liquid gasifier; 7 - turbine of fuel TPA; 8 - reducing liquid gasifier; 9 - fuel pump.

Fig. 9.7. LPRE with introduction of working fluid, after operation in the turbine, into the expanding part of the nozzle.

hydrogen peroxide  $H_2O_2$ ) (Fig. 9.2). The total oxidizer flow is fed to the gasifier of such an engine. The gaseous decomposition products that form enter the turbine and then, along the gas guide, to the combustion chamber. The fuel flows through the cooling loop of the chamber, cooling it, and then, in the liquid state, enters the combustion chamber. The gasifier of such an engine is an *oxidizing* gasifier.

It is possible to use LPRE's with a one-component *reducing liquid gasifier*; here the liquid oxidizer and the combustion products of the fuel (e.g., ammonia  $NH_3$  or hydrazine  $N_2H_4$ ) are fed to the combustion chamber.

In an LPRE with an *oxidizing two-component liquid gasifier* (Fig. 9.3), the total flow of oxidizer from the pump and a relatively small part of the fuel are fed to the gasifier; the main portion of the fuel flows along the cooling loop and enters the chamber in liquid form; unlike the above-examined schemes, this is an *afterburner* chamber. Therefore, such LPRE's are called engines with *afterburning of the generator gas*.

These also include LPRE's with a *reducing two-component liquid gasifier* (Fig. 9.4); the chamber of such an engine is fed the spent reducing generator gas and the liquid oxidizer, while to the liquid gasifier is fed the total flow of fuel (after passing through the cooling loop of the chamber) and a relatively small amount of oxidizer.

Since the pressure in the liquid gasifiers of these examined engines is greater than pressure  $p_K$ , the pressure of that part of the propellant component directed to the liquid gasifier should be greater than that of the basic portion of component fed directly to the chamber. For this purpose, behind the main pump (the first-stage pump) an auxiliary ("booster") pump, also called the second-stage pump, is installed (see Figs. 9.3 and 9.4).

Let us compare LPRE's with oxidizing and reducing liquid gasifiers. Usually, for two-component LPRE's the coefficient  $\kappa$  is greater than one, i.e., the flow of oxidizer is greater than that of the fuel. The available turbine power, as will be shown in 13.13, depends on the gas flow through the turbine and on the product  $RT$  of the indicated gas. Therefore, from the standpoint of gas flow to drive the turbine, LPRE's with oxidizing liquid gasifiers have an advantage over those with reducing liquid gasifiers. However, the oxidizing gas, having a high temperature, has a strong oxidizing influence on the structural materials; therefore, its temperature must be lowered. On the whole, however, it is more advantageous to use an oxidizing liquid gasifier in an LPRE.

The product  $RT$  of the reducing liquid gasifier gas of hydrogen LPRE's has a high value because of the high gas constant of hydrogen; therefore, in these it is more advisable to use a reducing liquid gasifier.

*LPRE's with gasification of the working fluid of the turbine in the chamber cooling loop* can be created if liquid hydrogen is used as the fuel. Here it is not necessary to have a liquid gasifier, which simplifies the engine scheme.

One possible scheme for such an engine is shown in Fig. 9.5. Liquid hydrogen passes through two pumps in succession, after which it enters the chamber cooling loop. The gaseous hydrogen formed is directed to the turbine and then, along the gas guide, to the combustion chamber. The oxidizer (e.g., LOX) is fed to the chamber by the pump; this pump can be on a separate shaft and driven using a gear from the shaft containing the two hydrogen pumps and the turbine.

An outstanding feature of such LPRE's is the low temperature of the gas at the turbine inlet, approximately  $200-275^{\circ}\text{K}$ . In engines with liquid gasifiers this temperature is substantially higher ( $\approx 800-1075^{\circ}\text{K}$ ).

A disadvantage of LFRE's with gasification of the working fluid of the turbine in the chamber cooling loop is the relatively low pressure  $p_h$  (40-50 bars [ $\approx 40-50 \text{ kgf/cm}^2$ ]).

In LPRE's operating on the "gas-gas" scheme (Fig. 9.6), both propellant components are used completely to drive the turbopump assemblies [TPA's], while in LPRE's operating on the "gas-liquid" scheme, one of the components is either not used at all or only a small part of it is used for this purpose.

LPRE's operating on the scheme "gas-gas" have two TPA's and two liquid gasifiers each. The combustion products of reducing liquid gasifier 8 serve as the working fluid of turbine 7 of the fuel TPA; from the turbine it is fed along gas guide 6 to afterburner chamber 1. Similarly, the combustion products of the oxidizing liquid gasifier enter turbine 3 of the oxidizer TPA and then, along gas guide 2, also to the afterburner chamber.

Pump 9 feeds the main portion of the fuel to the reducing liquid gasifier, and the rest to the oxidizing gasifier. From pump 4 the main part of the oxidizer enters the oxidizing liquid gasifier, while the rest goes to the reducing gasifier.

As can be seen, LPRE's operating on the scheme "gas-gas" are engines with afterburning of the generator gases in the chamber. Such LPRE's can have higher pressure of the combustion products in the afterburner chamber as compared with LPRE's operating on the scheme "gas-liquid," or identical high pressure in the afterburner chamber with lower required pressures of the propellant components at the exit from the pumps.

An LPRE with input of working fluid, after operation in the turbine, to the expanding part of the nozzle (Fig. 9.7). If the engines operates on the scheme "liquid-liquid," but the working fluid, after operation in the turbine, is not sent to the ambient medium but to the expanding part of the nozzle, the specific impulse

of the engine increases; however, it is less than that of LPRE's operating on the scheme "gas-liquid" or "gas-gas." An example of an engine with introduction of the working fluid, after operation in the turbine, into the expanding part of the nozzle is the F-1 engine of the first stage of the American Saturn-5 booster.

A power plant with an LPRE includes systems, units, and assemblies to assure the following:

- a) disposition and storage of the liquid propellant components (tanks);
- b) propellant feed to the chamber;
- c) engine start-up;
- d) propellant ignition (for engines with nonhypergolic propellant);
- e) chamber cooling;
- f) change of engine operating mode;
- g) creation of forces and moments for rocket vehicle flight control;
- h) engine shutdown.

Certain systems are in many ways similar for various heat rocket engines, while certain are similar for all types of rocket engines. For example, to create forces for controlling the flight of a rocket vehicle any type of engine, including electric, can be tilted a certain angle, which causes a corresponding deflection of the reaction jet.

The systems for feeding the liquid propellant components to power plants with LPRE's (see Chapter XIII), other heat rocket engines, and, in particular, electric engines, are also analogous.

All types of rocket engines with relatively high temperature of the combustion and decomposition products and heating or plasma tem-

peratures have a cooling system, i.e., a system for removing the heat flows that enter the chamber walls.

The operating mode of most rocket engines is changed by changing the flow of working fluid (for chemical rocket engines - by changing the flow of the propellant components).

### §9.2 Selecting optimum pressure $p_K$

In §2.4 it was shown that to obtain a high velocity characteristic for a rocket vehicle there must be high values of specific impulse of the power plant and high ratio of the initial to final mass of the vehicle.

The degree of perfection of a power plant can be estimated by the ratio  $I_{\Sigma}/m_{\text{ды}}$ . Optimum pressure  $p_K$  is that for which this ratio has maximum value for given  $I_{\Sigma}$ .

The optimum pressure  $p_K$  depends mainly on the system for feeding the propellant components to the chamber.

For each type of displacement feed (using a high-pressure gas container, a liquid gasifier, or a solid-fuel gasifier), with an increase in pressure  $p_K$  to a certain value the ratio  $I_{\Sigma}/m_{\text{ды}}$  increases, while with a further increase in  $p_K$  it decreases.

Let us clarify this. We will start with the conditions  $m_{\text{ды}} = \text{const}$  and  $p_C = \text{const}$ . For a rocket-engine chamber an increase in specific impulse with rising pressure  $p_K$  is characteristic, but as the pressure increases the rise in specific impulse is noticeably slowed down (see §5.4).

Simultaneously with an increase in pressure  $p_K$  there must be a rise in pressure in the tanks which requires, in turn, an increase in thickness of the walls and, consequently, their mass. In addition, the mass of the chamber nozzle increases in connection with an increase

in the values of  $\epsilon_c$  and  $\bar{f}_c$ . Therefore, with a rise in pressure  $p_h$ , to assure the condition  $m_{\Delta y} = \text{const}$  the mass of propellant in the tanks of the power plant must be decreased.

The increase in the ratio  $I_{\Sigma}/m_{\Delta y}$  with a rise in pressure  $p_h$  is explained by the fact that in this interval of pressure  $p_h$  the specific impulse increases greatly, and the value of  $I_{\Sigma}$  increases despite the decreased mass of propellant.

With an increase in pressure  $p_h$  above optimum, ratio  $I_{\Sigma}/m_{\Delta y}$  begins to decrease, which indicates a greater influence of the decreased propellant mass due to an increase in the mass of the tanks and displacement system compared with the influence of an increase in specific impulse due to a rise in pressure  $p_h$ .

The lower the mass of the tanks and the displacement system for feeding a given quantity of propellant components from the tanks to the engine chamber, the better the power plant.

With improvement of the feed system, the ratio  $I_{\Sigma}/m_{\Delta y}$  and the optimum pressure  $p_h$  increase. For example, a displacement feed system using a liquid gasifier is more efficient than a system with a high-pressure gas container (Fig. 9.8).

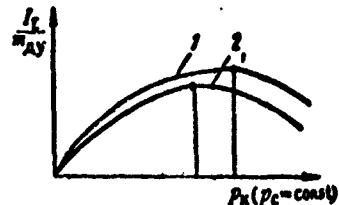


Fig. 9.8. Dependence of the ratio  $I_{\Sigma}/m_{\Delta y}$  on pressure  $p_h$  for LPRE's with displacement feed with a high-pressure gas container (2) and a liquid gasifier (1) ( $m_{\Delta y} = \text{const}$ ;  $p_c = \text{const}$ ).

Ordinarily, pressure  $p_h$  for an LPRE with a displacement propellant-component feed system is within the limits of 15-30 bars [ $\approx 15-30 \text{ kgf/cm}^2$ ]. The LPRE's of space vehicles, in a number of cases, use lower pressures (7-8 bars [ $\approx 7-8 \text{ kgf/cm}^2$ ]), making it possible to refrain from using external circulation cooling and to achieve

the possibility of a considerable change in thrust, in addition to high engine reliability.

For a power plant with a pump system for feeding propellant

components to the chamber there is also an optimum pressure  $p_K$  which depends on a number of factors, including the power-plant scheme.

In a power plant including an LPRE with exhausting of the working fluid, after operation in the turbine, into the ambient medium, a rise in pressure  $p_K$  increases the required pressure of the propellant components at the pump exit, which makes it necessary to increase turbine power (in §13.13 it will be shown that the turbine power can be increased basically by increasing the flow of gas through it; however, in this case, the engine specific impulse is reduced - see §9.1).

Within a certain range of pressure  $p_K$ , the specific impulse of the engine increases as pressure increases: the rise in specific impulse of the chamber due to a rise in pressure  $p_K$  exceeds the decrease in specific impulse of the engine due to the increased gas flow through the turbine.

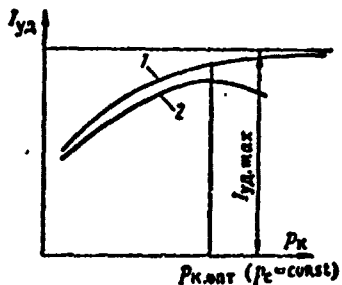


Fig. 9.9. Dependence of specific impulse of the chamber (1) and engine (2) with exhausting of the working fluid, after operation in the turbine, into the atmosphere on the pressure  $p_K$  ( $p_t = \text{const}$ ).

A certain pressure  $p_K$  assures maximum specific impulse for the engine, while with a further rise in  $p_K$  the specific impulse decreases (Fig. 9.9). In this case the drop in engine specific impulse due to increased gas flow through the turbine exceeds the increase in specific impulse due to the rise in pressure  $p_K$ .

The optimum pressure  $p_K$  for an LPRE with a pump feed system should also be selected from the condition of maximum ratio  $I_{\Sigma}/m_{dy}$ , not from the condition of maximum engine specific impulse.

In a power plant with an LPRE operating on the scheme "gas-liquid" or "gas-gas," the specific impulse of the chamber and engine is identical. For such engines, with a rise in pressure  $p_K$

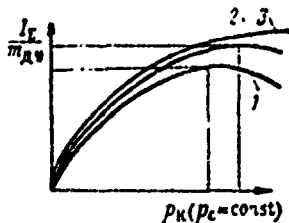


Fig. 9.10. Pressure  $p_h$  vs. the ratio  $I_e/m_{dy}$  for an LPRE with exhausting of the generator gas into the atmosphere with a liquid gasifier using auxiliary propellant components (1), basic propellant components (2), and for an LPRE with afterburning of the generator gas (3).

with LPRE's operating on the scheme "gas-liquid" or "gas-gas." It is particularly suitable to use such engines with high pressures  $p_h$  for high-thrust power plants.

In §5.4 it was shown that chamber dimensions decrease and its construction is simplified with an increase in  $p_h$ .

The use of high pressure  $p_h$  involves certain engine-design difficulties. These include: the need for more efficient cooling, difficulties in assuring tightness of the joints, and also difficulties in assuring engine unit strength and efficiency. However, these difficulties have been successfully overcome. Disadvantages in using high pressure  $p_h$  also include an increase in cost of the engines and a certain reduction in their reliability.

Pressure  $p_h$  for most modern LPRE's with pump feed systems is 50-100 bars [ $\approx 50-100$  kgf/cm<sup>2</sup>]; for certain LPRE's it reaches 200 bars [ $\approx 200$  kgf/cm<sup>2</sup>]. The expediency of using higher pressures  $p_h$  has been studied: 280-350 bars [ $\approx 280-350$  kgf/cm<sup>2</sup>] and higher.

## CHAPTER X

### LIQUID CHEMICAL PROPELLANTS

In §1.2 it was shown that "chemical propellant" is the name used for substances which, when they enter into chemical reaction, release heat and form basically gaseous products. The most typical chemical propellants consist of an oxidizer and a fuel. The oxidizer is a substance consisting mainly of oxidizing elements, while the fuel consists of fuel elements. During the chemical reaction there is electron exchange in the outer electron shell of the atoms:

the atoms of the fuel elements give their electrons to the atoms of the oxidizer elements.

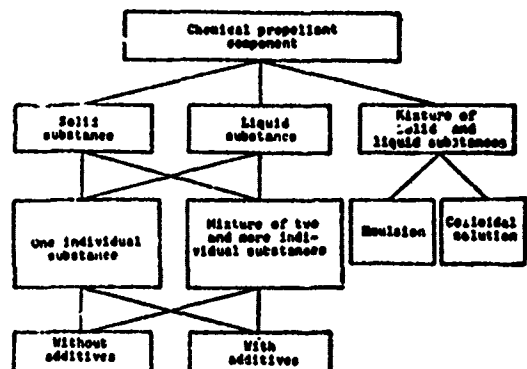


Fig. 10.1. Classification of chemical propellant components.

A *chemical propellant component* (Fig. 10.1) is a liquid substance stored in a separate tank and fed along a separate line to the engine chamber. The chemical propellant component (CPC) can also be a solid substance located directly in the chamber. The CPC can also be a combination of individual liquid or solid substances, or a mixture of individual liquid and solid substances.

rectly in the chamber. The CPC can also be a combination of individual liquid or solid substances, or a mixture of individual liquid and solid substances.

In certain cases the propellant component includes special additives (from tenths of a percent to several percent) in order to improve some one of its properties.

Liquid propellant components containing solid metal particles are called metal-containing, or metallized, components; there are two types of such components - suspensions and colloidal solutions.

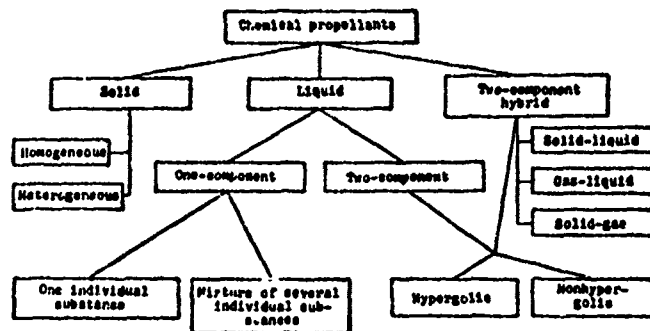


Fig. 10.2. Classification of chemical propellants.

A *suspension* is a liquid component containing uniformly distributed fine solid metal particles. A *colloidal solution* differs from a suspension in the smaller sizes of the metal particles.

Chemical propellants (Fig. 10.2) are classified by the following criteria:

- the number of basic components - mono-, bi-, and tripropellants;
- by the aggregate state of the basic propellant components - solid, liquid, and solid-liquid (hybrid) propellants;
- by the features of the interaction of the propellant components upon their immediate contact - hypergolic and nonhypergolic propellants.

Hypergolic propellants ignite  $(3-8) \cdot 10^{-3}$  seconds after their components come into contact (this time is called the self-ignition delay period). A special system is required to ignite nonhypergolic propellants.

Tripropellants include, in particular, those containing oxidizer, fuel, and a component with small  $\mu$  (e.g., liquid hydrogen), sometimes called a *diluent*.

Solid propellants can be homogeneous (uniform) or heterogeneous (nonuniform, or mixed). A *homogeneous* propellant is a chemical substance whose molecule contains both oxidizer and fuel; a solid solution of two such chemical substances can also be a homogeneous propellant. A *heterogeneous* propellant is a mechanical mixture of oxidizer (usually crystalline) and fuel, which at the same time acts as the binder, thus assuring creation of a solid propellant charge with the necessary mechanical characteristics. Solid propellants are examined in Chapter XVI.

#### §10.1. Simple oxidizers and fuels

Chemical propellant components contain both oxidizer and fuel elements. Propellant components consisting of oxidizer or fuel elements of a single type are called simple oxidizers or fuels, respectively.

The *oxidizers* include oxygen and the halogens: fluorine, chlorine, bromine, and iodine. Oxygen and, in particular, fluorine have the best oxidizing ability. They are used as simple oxidizers and in combination with other, less effective, oxidizing elements. Certain properties of simple oxidizers are given in Table 10.1.

Table 10.1. Certain properties of simple oxidizers  
[35, 37]

Oxidizer	Chemical formula	Atomic number	$\mu$	Density in liquid state	$T_{\text{пп}}$	
					at standard pressure	$^{\circ}\text{K}$
				kg/m <sup>3</sup>		
Oxygen	$\text{O}_2$	8	31,999	1144 (at $T_{\text{пп}}$ )	54,35	90,18
Fluorine	$\text{F}_2$	9	37,997	1507 (at $T_{\text{пп}}$ )	53,53	85,02
Chlorine	$\text{Cl}_2$	17	70,906	1557 (at $T_{\text{пп}}$ )	171,85	238,45; 239,05
Bromine	$\text{Br}_2$	35	159,808	3102 (at 298°, 15K)	265,85	331,05; 331,93
Iodine	$\text{I}_2$	53	253,809	3960 (at 393°, 15K)	386,85	453,95; 457,50

The basic fuels of chemical rocket propellants are hydrogen, lithium, beryllium, boron, carbon, magnesium, aluminum, and silicon; other fuel elements - sodium, calcium, phosphorus, titanium, and zirconium - are less effective. Table 10.2 gives the basic properties of simple fuels.

Table 10.2. Certain properties of simple fuels  
[35, 37]

Fuel	Chemical formula	Atomic number	$\mu$ kg kmole	g		$T_{f.s.}$	$T_{KHN}$
				in solid state	in liquid state		
Hydrogen	H <sub>2</sub>	1	2,016	—	70.97 (at $T_{KHN}$ )	13.94	20.39
Lithium	Li	3	6,939	534°	507 (at 473°, 15K)	453.65	1620.15
Beryllium	Be	4	9,012	1850°	—	1556.15	2757.15
Boron	B	5	10,811	2300°	—	2300.15	3950.15
Carbon (graphite)	C	6	12,011	2250	—	3873; 3973	≈ 4473
Magnesium	Mg	12	24,305	1740°	—	923.15	1381.15
Aluminum	Al	13	26,982	2700°	2289 (at 1273°, 15K)	932.15	2740.15
Silicon	Si	14	28,086	2000 (amorphous)	—	—	≈ 2873

\*At 298.15°K.

Propellants using fluorine as the oxidizer are more efficient than oxygen-based propellants. This is explained by the following features of oxides (the end products of fuel/oxygen interaction) and fluorides (end products of fuel/fluorine interaction).

1. The heat of formation of fluorides for most of the examined fuel elements is greater than that of the oxides.

2. The boiling and melting points of the fluorides are substantially lower than those of the oxides. Therefore, in most cases the fluorides leave the nozzles of chemical rocket engine chambers in the gaseous state, while many oxides (particularly  $\text{BeO}$  and  $\text{Al}_2\text{O}_3$ ) leave in the liquid or solid states.

Hydrogen, upon interaction with oxygen and fluorine, does not give the highest heat of formation of the corresponding oxide ( $\text{H}_2\text{O}$ ) and fluoride (HF), but these compounds have low molecular mass and low values of  $T_{\text{KIN}}$  and  $T_{\text{INL}}$ , which makes propellants using oxygen and fluorine as the oxidizer and hydrogen as the fuel very efficient.

Metals and metal-containing compounds with low molecular mass (Li, Be, B) are also highly-efficient fuels. Carbon is one of the relatively low-efficiency fuel elements.

#### §10.2. Particular requirements of liquid chemical propellants

The general and specific requirements of chemical propellants have been examined in §§3.2 and 3.3.

In accordance with equation (5.10), propellants should assure high thrust-coefficient values  $K_p$  (see §5.3) and  $\beta$  (see §4.5). These coefficients, as well as velocity  $W_c$  (see §4.5), increase with increasing temperature and gas constant of the combustion products at the nozzle inlet, and also with increasing expansion ratio  $\epsilon_c$  and decreasing index  $n_p$ .

A substantial influence is exerted by temperature  $T_k$ , which is a function of the working heating capacity  $H_{\text{pa6}}$ , determined by the type and ratio of the propellant components.

The chemical propellant component, like all working fluids of the rocket engine (see §3.2), should have *high density*. This is particularly important for the oxidizer, since it is its density which basically determines the density of the propellant.

In connection with the fact that the values of  $I_{ydh}$  and  $\rho_T$  have varying influence on the characteristic velocity of a rocket vehicle, the need arises for a combination estimate parameter, such as the expression  $I_{ydh} \rho_T^c$ , where  $c$  is an exponent whose value is defined by the equation

$$c = \frac{m_T/m_{Na4}}{\lg \frac{1}{1 - m_T/m_{Na4}}}.$$

Here  $m_T$  is the mass of the propellant components.

The maximum value of the expression  $I_{ydh} \rho_T^c$  corresponds to the maximum characteristic velocity of the rocket vehicle. Exponent  $c$ , which defines the influence of propellant density on the rocket vehicle characteristic velocity, is less than one. Therefore, the specific impulse, rather than the propellant density, has a greater influence on the characteristic velocity. With a decrease in exponent  $c$  (i.e., with an increase in the ratio  $m_T/m_{Na4}$ ), the influence of the density  $\rho_T$  decreases. With  $m_T/m_{Na4} = 0.8$ , characteristic of ballistic missiles,  $c = 0.5$ .

For the upper stages of rockets the influence of the propellant density decreases, while that of the specific impulse increases. Therefore, for these stages we recommend use of the propellant LOX + liquid hydrogen, despite the extremely low density of liquid hydrogen ( $\rho \approx 71 \text{ kg/m}^3$ ).

The stability with which combustion or decomposition occurs, and the starting properties, are also important characteristics of a chemical propellant.

The *stability of combustion* or decomposition of the propellant is determined mainly by the amplitude of oscillations of pressure  $p_K$ ; the greater the amplitude, the less stable the chemical reactions in the chamber and the lower its operational reliability (see §15.1).

Propellants with *good starting properties* assure stable engine

start-up regimes (without large oscillations of pressure  $p_K$ ). For example, two-component propellants with good starting properties ignite easily and reliably over a broad range of change of coefficient  $\kappa$ , which is explained by their following features:

- a) easy evaporability;
- b) low ignition point;
- c) small amount of heat required for ignition;
- d) short ignition delay period  $\tau_{s.s.}$ .

From the standpoint of ensuring good starting properties and stable combustion, and also to simplify engine design, hypergolic propellants are usually preferred over nonhypergolic propellants.

The following additional requirements are imposed on liquid propellant components:

- a) low viscosity and as little a change in it as possible in the engine operation temperature range;
- b) low surface tension;
- c) low saturated vapor pressure.

With low viscosity of the propellant components there is a decrease in the hydraulic resistance of the engine lines, which results in decreased power expenditures for feeding the components to the chamber.

With low viscosity and surface tension of the propellant components their atomization is improved, i.e., they break up into finer particles as they enter the chamber, facilitating more complete combustion.

Low saturated vapor pressure decreases the amount of components lost to evaporation and has a favorable influence on certain other parameters of the engine and of the vehicle as a whole.

If the engine chamber has external circulating cooling, one of the propellant components should have good cooling properties.

We must point out that there are no propellants that can be used equally effectively for various types of rocket engines with varying thrust. Therefore, the propellant should be very carefully selected in each specific case.

### §10.3. Characteristics of liquid propellants

LPRE's use mainly *bipropellants*. Such propellants are also called separate-feed propellants, since the oxidizer and fuel are stored in separate tanks and fed to the chamber along different lines.

LPRE's operating on a *monopropellant* (or unitary propellant) are simpler in design and operation.

Monopropellants, a blend of oxidizer and fuel or solutions of fuel in oxidizer, can have sufficiently high power characteristics, but such propellants tend to explode. The same can be said of a monopropellant consisting of one substance whose molecule contains both oxidizer and fuel elements (e.g., nitromethane  $\text{CH}_3\text{NO}_2$ ).

Monopropellants consisting of one individual substance (e.g., hydrazine  $\text{N}_2\text{H}_4$ ) and releasing heat as a result of decomposition in the presence of a *catalyst* are stable enough, but have relatively low power characteristics.

Both solid and liquid catalysts are used. The solid catalyst is located directly in the chamber; its mass remains practically unchanged during engine operation.

The liquid catalyst is located in a separate tank and is fed directly to the chamber along a special line.

An example of a starting propellant component for an LPRE is triethylaluminum  $Al(C_2H_5)_3$ , a liquid that ignites in air; it is used to ignite nonhypergolic propellants.

When designing an LPRE and any other type of rocket engine we tend to eliminate, as much as possible, starting and auxiliary propellant components. The use of only basic propellant components simplifies the design of a rocket vehicle and the fueling units of launch complexes, facilitates filling of the tanks, etc.

Above we indicated that additives are introduced into rocket propellants in a number of cases, additives which assure the following, in particular:

- a) prolonged chemical stability of the propellant component (inhibitors);
- b) reduction in the corrosion activity of the propellant component (deactivators);
- c) a decrease in the value of  $\tau_{3.8}$  (catalysts);
- d) self-ignition of the propellant (this can be achieved, e.g., by introducing liquid fluorine into LOX).

#### §10.4. Liquid oxidizers and fuels of rocket propellants

The oxidizers usually make up the bulk of the propellant. Simple oxidizers ( $O_2$ ,  $F_2$ ) or combinations of oxidizing elements (oxygen fluoride  $OF_2$ , halogen fluorides:  $ClF_3$ ,  $ClF_5$ ,  $BrF_3$ ,  $BrF_5$ ,  $IF_5$ , and others, perchloryl fluoride  $ClO_3F$ , and others) consist entirely of oxidizing elements.

Certain oxidizers contain nitrogen in the molecule together with the oxidizing element; this is a neutral element (nitrogen tetroxide  $N_2O_4$ , nitrogen fluorides  $NF_3$  and  $NF_4$ , and others). Certain oxidizers contain fuels and neutral elements simultaneously (nitric acid  $HNO_3$ , tetrannitromethane  $C(NO_2)_4$ , perchloric acid  $HClO_4$ , and others).

Hydrogen peroxide  $H_2O_2$  includes oxidizer and fuel elements.

The following oxidizers are most widely used in LPRE's: oxygen, nitric acid, nitrogen tetroxide, and hydrogen peroxide. The physico-chemical properties of the basic oxidizers are given in Table 10.3.

The most efficient fuels are those consisting entirely of fuel elements. The presence of nitrogen or some oxidizer element in the fuel, as a rule, lowers the power characteristics of the propellant.

The fuels used and foreseen for liquid propellants can be divided into the following groups:

1. Liquid hydrogen and nitrogen-hydrogen fuels: hydrazine  $N_2H_4$ , ammonia  $NH_3$ .
2. Fuels containing hydrogen, nitrogen, and carbon, and which are hydrazine derivatives: methylhydrazine (MMH)  $H_2N-NH(CH_3)$ , unsymmetrical dimethylhydrazine (UDMH)  $H_2N-N(CH_3)_2$ , and aerozine-50, a 1:1 blend of hydrazine and UDMH.
3. Hydrocarbon fuels: kerosene (a blend of hydrocarbons produced during petroleum distillation); methane  $CH_4$  (liquefied hydrocarbon, a basic component of natural gas); ethane  $C_2H_6$  and propane  $C_3H_8$  (also liquefied hydrocarbons); and others.
4. Fuels containing hydrogen, carbon, and oxygen (alcohols): ethyl alcohol  $C_2H_5OH$ , methyl alcohol  $CH_3OH$ , and others.

The physicochemical properties of the basic fuels are given in Table 10.4.

#### **§10.5. Characteristics of two-component propellants (bipropellants)**

The characteristics of basic bipropellants are given in Table 10.5.

Table 10.6 shows the hypergolic and nonhypergolic propellants.

Table 10.3. Certain properties of liquid oxidizers [2, 23, 35]

Oxidizer	Chemical formula	$\mu$ kg /mole	$T_{\text{m}}$	$T_{\text{bo}}$	$\epsilon^*$	$I_{\text{e}}^{\text{**}}$	Chemical stability	Maximum possible concentration in air
			at standard pressure	°K				
					kg m <sup>3</sup>	KJ kg		kg m <sup>3</sup>
Oxygen	O <sub>2</sub>	31,999	54,35	90,18	1144	-300	Stable	Non-toxic
Hydrogen peroxide	H <sub>2</sub> O <sub>2</sub>	34,015	272,26	423,35	1442	-5530	Unstable	1,0
Nitric acid	HNO <sub>3</sub>	63,014	231,56	357,25	1504	-2753	"	5,0
Nitrogen tetroxide	N <sub>2</sub> O <sub>4</sub>	92,011	261,96	294,3	1442	-209	Stable	5,0
Fluorine	F <sub>2</sub>	37,997	33,53	85,02	1507	-335	Stable	0,03
Oxygen fluoride	OF <sub>2</sub>	63,006	49,35	127,85	1521	222	Stable	0,01
Chlorine trifluoride	ClF <sub>3</sub>	92,448	196,83	284,00	1800	-2000	Stable	Highly toxic
Chlorine pentafluoride	ClF <sub>5</sub>	130,457	—	—	1750	—	"	Slightly toxic
Nitrogen trifluoride	NF <sub>3</sub>	71,008	66,36	144,14	1531	-2050	"	Highly toxic
Tetrafluorohydrazine	N <sub>2</sub> F <sub>4</sub>	104,016	105,15	200,15	1500 (at 173°K)	—	"	"
Bromine trifluoride	BrF <sub>3</sub>	136,916	261,92	308,9	2797	—	"	Toxic
Bromine pentafluoride	BrF <sub>5</sub>	174,916	210,65	313,45	2465	-2625	"	"
Perchloryl fluoride	ClO <sub>3</sub> F	102,457	125,41	226,45	1601	-300	"	Slightly toxic
Perchloric acid	HClO <sub>4</sub>	100,465	161,18	403,18	1773	-460	Unstable	Toxic

<sup>a</sup>Values at 298.15°K; for low-boiling oxidizers — at the boiling point.

<sup>\*\*</sup>Values at 293°K; for low-boiling oxidizers — at the boiling point.

Table 10.4. Certain properties of liquid fuels  
[2, 23, 35]

Fuel	Chemical formula	$\mu$	$T_{\text{na}} / T_{\text{KHN}}$		$q^*$	$i_{\text{u}}^{**}$	Chemical stability	Max. poss. conc. in air
			kg kmole	°K				
Hydrogen	H <sub>2</sub>	2,016	13.94	20.39	70.97	-3628	Stable	Nontoxic
Hydrazine	N <sub>2</sub> H <sub>4</sub>	32,048	274.68	386.65	1004	1573	*	Toxic
Ammonia	NH <sub>3</sub>	17,032	195.39	239.73	682	-4180	*	20-50
Methylhydrazine (MMH)	H <sub>2</sub> N—NH(CH <sub>3</sub> ) <sub>2</sub>	46,075	220.75	360.65	874	1222	*	Toxic
UDMH	H <sub>2</sub> N—N(CH <sub>3</sub> ) <sub>2</sub>	60,102	215.95	336.25	784	774	*	*
Aerozine-50	—	45,584	265.85	343.25	899	1173	*	*
Kerosene	C <sub>7.21</sub> H <sub>12.29</sub> (cond. form.)	—	200-220	450	820-850	-1728	*	300
Methane	CH <sub>4</sub>	16,047	89.15	111.65	424	-5439	*	Slightly toxic
Ethyl alcohol	C <sub>2</sub> H <sub>5</sub> OH	46,070	159.05	251.47	785	-6025	*	1000
Diborane	B <sub>2</sub> H <sub>6</sub>	27.67	107.65	180.65	430	438	Stable in hermetic tank	Highly toxic
Pentaborane	B <sub>5</sub> H <sub>9</sub>	63.27	226.34	335.15	618	361	*	0.01

\*Values at 298.15°K; for low-boiling fuels - at boiling point.

\*\*Values at 293°K; for low-boiling fuels - at the boiling point.

LOX-based propellants. During the initial development period of LPRE's and during World War II, the propellant liquid oxygen O<sub>2</sub> + ethyl alcohol C<sub>2</sub>H<sub>5</sub>OH was widely used. The comparatively low heating capacity of this propellant led to its replacement with O<sub>2</sub> + kerosene.

The propellant O<sub>2</sub> + kerosene is cheap and reliable, and its production and use is very familiar. Certain difficulties in cooling the chamber due to the high temperature of the combustion products, and the comparatively low percentage of fuel in the propellant, have been successfully overcome, and the propellant O<sub>2</sub> + kerosene is widely used in modern LPRE's. LPRE's have been developed which pro-

Table 10.5. Theoretical characteristics of certain bipropellants [35] ( $p_{\infty} = 68.946$  bars [68.046 atm(phys)];  $p_c = 1.013$  bars [1 atm(phys)];  $\kappa = \kappa_{\text{ONR}}$ ;  $p_h = p_c$ ; equilibrium expansion)

Characteristic	Fuel	Oxidizer									
		O <sub>2</sub>	H <sub>2</sub> O <sub>2</sub>	HNO <sub>3</sub>	N <sub>2</sub> O <sub>4</sub>	F <sub>2</sub>	OF <sub>2</sub>	ClF <sub>3</sub>	ClF <sub>5</sub>	N <sub>2</sub> F <sub>4</sub>	ClO <sub>3</sub> F
$\kappa$	H <sub>2</sub>	4.00	7.33	6.14	5.25	8.00	5.67	11.50	11.50	11.50	6.14
	N <sub>2</sub> H <sub>4</sub>	0.92	2.03	1.50	1.33	2.37	1.50	2.71	2.70	3.25	1.50
	UDMH	1.70	4.26	3.00	2.57	2.45	2.00	2.83	3.00	3.17	2.70
	B <sub>3</sub> H <sub>8</sub>	2.12	2.23	3.00	3.00	4.66	4.00	6.60	7.33	6.60	3.76
$\sigma_r$ kg/m <sup>3</sup>	H <sub>2</sub>	284	435	393	353	468	375	605	616	517	403
	N <sub>2</sub> H <sub>4</sub>	1065	1261	1254	1217	1314	1263	1458	1507	1103	1327
	UDMH	975	1244	1223	1170	1190	1214	1325	1381	1028	1288
	B <sub>3</sub> H <sub>8</sub>	897	1021	1107	1084	1199	1179	1413	1493	1027	1239
$T_x$ °K	H <sub>2</sub>	2977	2419	2474	2640	3088	3547	3705	3134	3814	3001
	N <sub>2</sub> H <sub>4</sub>	3406	2927	3021	3247	4727	4047	4157	3001	4481	3167
	UDMH	3608	3008	3147	3415	4464	4493	4003	3700	4226	3637
	B <sub>3</sub> H <sub>8</sub>	4160	2980	3588	3013	5080	5000	4656	4447	4840	4242
$\eta_p$	H <sub>2</sub>	1.932	1.247	1.258	1.260	1.237	1.230	1.200	1.061	1.230	1.333
	N <sub>2</sub> H <sub>4</sub>	1.184	1.187	1.190	1.191	1.177	1.166	1.220	1.237	1.061	1.160
	UDMH	1.144	1.160	1.172	1.166	1.149	1.167	1.189	1.196	1.186	1.171
	B <sub>3</sub> H <sub>8</sub>	1.111	1.112	1.120	1.121	1.150	1.136	1.150	1.152	1.155	1.123
$\tau$ N·s/kg	H <sub>2</sub>	2431.1	2011.3	2001.5	2134.9	2553.7	2362.5	2145.7	2022.1	2272.2	2133.5
	N <sub>2</sub> H <sub>4</sub>	1890.7	1753.4	1714.2	1779.9	2112.4	2091.8	1928.0	1827.0	2026.4	1791.6
	UDMH	1856.4	1714.2	1654.4	1725.0	2087.8	2136.0	1826.0	1735.0	1930.4	1754.4
	B <sub>3</sub> H <sub>8</sub>	1804.6	1632.9	1753.4	1781.9	2175.1	2163.3	1850.3	1751.3	2013.3	1764.8
$I_{yA,0}$ N·s/kg	H <sub>2</sub>	3835.4	3161.7	3135.2	3311.1	4038.4	4012.3	3363.7	3145.0	3564.7	3173.5
	N <sub>2</sub> H <sub>4</sub>	3068.5	2813.5	2737.0	2854.7	3373.5	3392.1	3050.7	2880.0	3282.3	2693.9
	UDMH	3037.1	2782.1	2671.3	2796.0	3111.7	3153.9	2923.3	2750.6	3147.9	2840.0
	B <sub>3</sub> H <sub>8</sub>	3135.2	3031.2	2880.2	2935.1	3530.2	3548.1	3026.3	2846.0	3273.4	2163.1
$I_{yA,n}$ N·s/kg	H <sub>2</sub>	4471.8	3675.5	3636.3	3672.6	4683.7	4600.5	3687.4	3620.6	4118.8	3680.9
	N <sub>2</sub> H <sub>4</sub>	3625.5	3310.7	3210.7	3333.8	4210.0	4000.9	3547.7	3312.0	3827.6	3106.8
	UDMH	3610.8	3294.1	3153.8	3304.8	4050.1	4085.5	3411.2	3239.1	3826.1	3351.9
	B <sub>3</sub> H <sub>8</sub>	3777.5	3659.8	3454.9	3526.5	4224.7	4248.2	3616.7	3402.9	3809.1	3323.5

duce, using this propellant, thrusts up to 7000 kN [ $\approx$ 700 tons].

The propellants O<sub>2</sub> + NH<sub>4</sub>, O<sub>2</sub> + NH<sub>3</sub>, O<sub>2</sub> + MMH, and O<sub>2</sub> + UDMH have better starting characteristics and more stable burning as compared with O<sub>2</sub> + kerosene. Of these propellants, O<sub>2</sub> + UDMH is the most widely used. For these propellants, and also for O<sub>2</sub> + H<sub>2</sub>, despite their high heating capacity, a reduced temperature of the combustion products is characteristic, which facilitates chamber cooling.

Table 10.6. Characteristics of ignition of certain propellants

Fuel	Oxidizer					
	O <sub>2</sub>	H <sub>2</sub> O <sub>2</sub>	HNO <sub>3</sub>	N <sub>2</sub> O <sub>4</sub>	F <sub>2</sub>	ClF <sub>3</sub>
H <sub>2</sub>	N	N	N	N	H	H
N <sub>2</sub> H <sub>4</sub>	N	C	H	H	H	H
NH <sub>3</sub>	N	N	C	C	H	H
MMH	N	N	H	H	H	H
UDMH	N	N	H	H	H	H
C <sub>2</sub> H <sub>5</sub> OH	N	N	N	N	H	H

Note: N - nonhypergolic propellants; H - hypergolic propellants; C - propellants that self-ignite in the presence of a catalyst

The greatest specific impulse (up to 4800 N·s/kg [ $\approx$ 480 kgf s/kg]) of all modern propellants that have been developed is provided by the propellant LOX + liquid hydrogen (O<sub>2</sub> + H<sub>2</sub>). LPRE's have been developed which, using this propellant, yield thrusts of up to 1000 kN [ $\approx$ 100 tons]; work is being carried out in the US on creation of an LPRE with a thrust of up to 7000 kN [ $\approx$ 700 tons]. Despite the low density of the propellant O<sub>2</sub> + H<sub>2</sub> ( $\rho_T \approx 320 \text{ kg/m}^3$ ), its use for LPRE's in the upper stages of booster rockets makes it possible to substantially increase the mass of the payload.

When up to 5% of liquid fluorine is added to LOX, all LOX-based propellants become hypergolic.

When the propellant O<sub>2</sub> + H<sub>2</sub> is replaced by (70% O<sub>2</sub> + 30% F<sub>2</sub>) + H<sub>2</sub>, the engine specific impulse increases. The mixture O<sub>2</sub> + F<sub>2</sub> can be used with UDMH, kerosene, and liquefied hydrocarbons (methane, ethane, and propane).

**Hydrogen peroxide-based propellants.** Hydrogen peroxide was widely used as an oxidizer in LPRE's during World War II.

However, during that period, hydrogen peroxide was used in the form of an 80% aqueous solution, which reduced the heating capacity of the propellant. With the development of methods for stabilizing

hydrogen peroxide, it became possible to increase its concentration to 90%, and in certain cases to 98%.

Propellants on a highly-concentrated hydrogen peroxide base are just as good as nitric acid-based propellants as far as density is concerned, and at the same time they assure a somewhat greater specific impulse at a substantially lower combustion temperature. An additional advantage over nitric acid and nitric acid-based oxidizers is the lower corrosion activity of hydrogen peroxide.

The propellant  $H_2O_2$  + kerosene is the most widely used;  $H_2O_2$  + UDMH,  $H_2O_2$  +  $NH_3$ , and  $H_2O_2$  +  $N_2H_4$  are used more rarely. The concentration of  $H_2O_2$  in all these propellants is 90%. Prospective hydrogen peroxide-based propellants include  $H_2O_2$  +  $B_2H_6$  and, in particular,  $H_2O_2$  +  $B_5H_9$ . An important advantage of the latter is that it consists of high-boiling compounds.

**Nitric acid-based propellants.** The heating capacity of such propellants is less than that of LOX-based propellants, but unlike the latter they have high density and can be stored for a prolonged time in a fully fueled rocket.

Nitric acid (100% concentration) is an unstable product. Therefore, LPRE's use concentrated nitric acid containing about 2%  $H_2O$  and 0.5% nitrogen oxides  $NO_2$  (this is called white fuming nitric acid [WFNA]) or a solution of concentrated nitric acid and nitrogen tetroxide  $N_2O_4$  (this solution is called red fuming nitric acid [RFNA]). The latter oxidizer is more efficient. RFNA-based propellant, using UDMH as the fuel, is an example of a hypergolic propellant with prolonged storage capability, good starting characteristics, and stable burning.

However, nitric acid-based propellants have basically been replaced by nitrogen tetroxide-based propellants.

*Nitrogen tetroxide-based propellants.* The propellants  $N_2O_4$  +

+  $N_2H_4$ ,  $N_2O_4$  + MMH, and, in particular,  $N_2O_4$  + aerozine-50 and  $N_2O_4$  + UDMH are the most widely used, especially when prolonged storage is required. They are not quite as good as  $O_2$  + kerosene as far as the specific impulse that can be developed by the engine, but their density is higher.

The propellants  $N_2O_4$  + aerozine-50 and  $N_2O_4$  + UDMH make it possible to create reliably operating LPRE's with high specific impulse and very high thrust in a single chamber. The propellants  $N_2O_4$  +  $N_2H_4$  and  $N_2O_4$  + MMH are used for engines having relatively low thrust; the latter propellant has the best starting properties.

**Fluorine-based propellants.** Liquid fluorine is best used in combination with such fuels as ammonia, hydrazine, pentaborane, and in particular liquid hydrogen. The propellant  $F_2$  +  $H_2$  is 4-5% better than  $O_2$  +  $H_2$  as far as the mass specific impulse developed by the engine, 70% better as far as volume specific impulse is concerned, and 55% better in density. It is most suitable for the LPRE's of the upper stages of booster rockets and for the LPRE's of space vehicles having a relatively short flight time and high required total thrust [1].

The disadvantages of  $F_2$  +  $H_2$  include: 1) high temperature of the combustion products, which complicates chamber cooling; 2) the high cost of fluorine; and 3) the high toxicity of fluorine and its combustion products (HF).

The high values of the volume specific impulse developed by an engine using fluorine-based propellants can be judged from Table 10.7.

The LPRE's of space vehicles can use the following propellants:  $F_2$  +  $NH_3$ ,  $F_2$  +  $N_2H_4$ ,  $F_2$  + MMH,  $F_2$  +  $CH_4$ ,  $F_2$  +  $B_2H_6$ , and others.

**Propellants based on fluorine-containing oxidizers.** Oxygen fluoride  $OF_2$  is best used in combination with liquid hydrogen, UDMH, MMH, hydrazine, ammonia, and methane. For the LPRE's of space

Table 10.7. Volume specific impulse of oxygen and fluorine LPRE's at sea level ( $p_{\infty} = 66.7$  bars [68 kgf/cm<sup>2</sup>];  $p_c = 0.981$  bars [1 kgf/cm<sup>2</sup>];  $\kappa = \kappa_{\text{crit}}$ ; equilibrium expansion)

Fuel	Oxidizer			
	$O_2$		$F_2$	
	$I_{\text{sp}}, \text{sec}$			
	N·s/m <sup>3</sup>	kgf·s/liter	N·s/m <sup>3</sup>	kgf·s/liter
$H_2$	1,069	109	1,834	187
$NH_3$	2,569	262	4,119	420
$N_2H_4$	3,258	335	4,678	477

vehicles it is possible to use the propellant  $OF_2 + B_2H_6$ . The mass and volume specific impulses of engines using oxygen fluoride-based propellants are higher than those for LPRE's using LOX-based propellants. All oxygen fluoride-based propellants are hypergolic and have, except for  $OF_2 + H_2$ , comparatively high density.

Because of the high cost of oxygen fluoride, in a number of cases it is advisable to use  $F_2 + O_2$ , whose efficiency is only somewhat lower.

The propellants  $ClF_3 + N_2H_2$  and, in particular,  $ClF_5 + N_2H_4$  are very promising as long-storage hypergolic propellants. One of the difficulties arising when using  $ClF_5 + N_2H_4$  is the formation of a solid deposit on the inner surface of the chamber walls.

The propellant  $BrF_5 + B_5H_9$  is highly efficient; its density is 1990 kg/m<sup>3</sup>. The volume specific impulse of an engine operating on such a propellant is 4.81 N·s/m<sup>3</sup> [489 kgf·s/liter] when  $p_{\infty} = 68.7$  bars [76 kgf/cm<sup>2</sup>] and  $p_c = 0.981$  bars [1 kgf/cm<sup>2</sup>] with equilibrium expansion and optimum coefficient  $\kappa$ .

Among the efficient propellants are those on a nitrogen trifluoride  $NF_3$  and, in particular, tetrafluorohydrazine  $N_2F_4$  base using hydrazine, pentaborane, and liquid hydrogen as the fuels. However, the use of tetrafluorohydrazine is hampered by its high cost.

## §10.6. Selecting the optimum oxidizer excess coefficient $\alpha_{OK}$

After selecting the propellant components, we calculate the optimum value of the coefficient for the propellant component ratio  $\kappa$  or the coefficient  $\alpha_{OK}$ . In these calculations we find the maximum of the expression  $I_{y\Delta h} \rho_T^c$ .

The engine specific impulse and the propellant density depend on the coefficient  $\alpha_{OK}$ , i.e.,  $I_{y\Delta h} = f(\alpha_{OK})$  and  $\rho_T = f(\alpha_{OK})$ .

The specific impulse has maximum value with an excess of fuel, i.e., when  $\alpha_{OK} < 1$ , and not with a stoichiometric propellant component ratio, since with a fuel excess the combustion products contain an increased amount of gases with low molecular mass (CO, H<sub>2</sub>, and others) compared with the content of gases with higher molecular mass (CO<sub>2</sub>, H<sub>2</sub>O, and others). In addition, when  $\alpha_{OK} < 1$  the temperature of the combustion products is lowered, which results in decreased expenditure of chemical energy of the propellant on dissociation. Chamber cooling is facilitated at the same time: it is easier to cool a chamber, using a greater fuel flow, in which at the same time the combustion products have reduced temperature.

As the temperature of the combustion products increases, the value of the coefficient  $\alpha_{OK}$  for which maximum specific impulse is assured decreases.

Usually the oxidizer density is greater than that of the fuel, i.e.,  $\rho_{OK} > \rho_T$ . Therefore, with decreasing coefficients  $\alpha_{OK}$  and  $\kappa$  the density of the propellant  $\rho_T$  decreases.

Because of the influence of propellant density, the value of the coefficient  $\alpha_{OK}$  for which maximum characteristic velocity of the rocket vehicle is achieved is shifted from the value of the coefficient  $\alpha_{OK}$  corresponding to the maximum specific impulse, toward lower values.

Table 10.8. Values of coefficient  $\mu$  for certain propellants used in LPRE's

Propellant		$\mu$
oxidizer	fuel	
O <sub>2</sub>	H <sub>2</sub>	4,50-5,50
O <sub>2</sub>	Kerosene	2,20-2,38
O <sub>2</sub>	NH <sub>3</sub>	1,25
F <sub>2</sub>	H <sub>2</sub>	8,00-12,00
N <sub>2</sub> O <sub>4</sub>	H <sub>3</sub> N-NH(CH <sub>3</sub> )	1,64-2,54
N <sub>2</sub> O <sub>4</sub>	Aerozine-50	1,50-2,00
85%	Kerosene	8,2
H <sub>2</sub> O <sub>2</sub>		

The optimum values of coefficients  $\alpha_{OK}$  and  $\mu$  also depend on the gas expansion ratio  $\epsilon_c$ . For a chamber with a large gas expansion ratio  $\alpha_{OK,OPT} \rightarrow 1$  (usually  $\alpha_{OK,OPT} = 0.95-0.98$ ) as a result of the more complete recombination reactions. Table 10.8 gives the values of the coefficient  $\mu$  used for certain LPRE propellants.

### §10.7. Liquid monopropellants

The most widely used LPRE monopropellants are hydrogen peroxide and hydrazine, substances which can decompose with the release of heat in the presence of a catalyst.

A high-concentration (90-98%) aqueous solution of hydrogen peroxide, when used as a monopropellant, assures an LPRE specific impulse of 1500-1900 N·s/kg [ $\sim 150-190$  kgf·s/kg]; here the vapor-gas temperature in the decomposition chamber is 875-1250°K. With great expansion of the hydrogen peroxide decomposition products in the chamber nozzle the water vapors condense, which causes a certain lowering of the engine specific impulse.

Hydrazine is a more efficient monopropellant than hydrogen peroxide is. It decomposes on heating to 750°K, forming the gaseous products NH<sub>3</sub>, H<sub>2</sub>, and N<sub>2</sub> (with complete decomposition - only H<sub>2</sub> and N<sub>2</sub>).

The hydrazine decomposition products have rather high temperature (to 1475°K), low molecular mass, and do not tend to condense. Hydrazine assures an engine specific impulse of 2200-2400 N·s/kg [ $\sim 220-240$  kgf·s/kg].

Monopropellant LPRE's operating on hydrogen peroxide or hydrazine have lower specific impulse but their operational reliability is higher than bipropellant LPRE's. Therefore, hydrogen peroxide

or hydrazine are usually used as propellants for auxiliary LPRE's with low thrusts, including those in satellites and space vehicles. In particular, we should note the creation of a hydrazine liquid retrorocket engine with multiple ignition and variable thrust developed in the US for a soft landing on Mars [1].

The addition of nitric acid or hydrazine nitrate  $N_2H_5NO_3$  (components with oxidizing properties) to hydrazine increases the engine specific impulse and the density of the propellant, and also lowers the freezing point (e.g., to  $253^{\circ}K$  [ $-20^{\circ}C$ ] with the addition of 24%  $N_2H_5NO_3$ ).

A monopropellant blend of 75%  $N_2H_4$ , 24%  $N_2H_5NO_3$ , and 1%  $H_2O$  assures an engine specific impulse of up to  $2600 \text{ N}\cdot\text{s}/\text{kg}$  [ $\approx 260 \text{ kgf}\cdot\text{s}/\text{kg}$ ] and a density of  $1110 \text{ kg/m}^3$ , i.e., the power characteristics are close to the mean-power bipropellants of the type  $N_2O_4 + \text{aerozine-50}$ .

Table 10.9. Certain characteristics of LPRE's operating on bipropellants

propellant	Upper limit of thermal stability temperature	$T_K$	$I_{y.d.n}$ at $p_K = 9.81 \text{ bars}$ [ $10 \text{ kgf/cm}^2$ ]	
			$\text{N}\cdot\text{s}/\text{kg}$	$\text{kgf}\cdot\text{s}/\text{kg}$
80% $H_2O_2$	—	1150	1765	180
98% $H_2O_2$	383	1240*	1893*	193*
$N_2H_4$	533	1345*	2422**	247**
$N_2H_4$ (75%) + $N_2H_5NO_3$ (24%) + $H_2O$ (1%)	491	1615**	2569**	262**

\*The values are given considering condensation of water vapors as they move through the nozzle.  
\*\*The values are given for the condition that 40% of the ammonium that forms decomposes into nitrogen and hydrogen.

Table 10.9 gives the values of  $T_K$  and  $I_{y.d.n}$  for LPRE's operating on various monopropellants [1].

In monopropellant LPRE's it is possible to use other propellants, including ammonia, UDMH, isopropyl nitrate  $(CH_3)_2CHONO_2$ , and others.

Products of the decomposition of hydrazine, hydrogen peroxide, and UDMH are also used as the gaseous working fluid for the turbine in bipropellant LPRE's with pump feed.

#### §10.8. Metal-containing fuels and tripropellants

One of the ways to increase LPRE specific impulse and propellant density is to use metals (Li, Be, Al, Mg), their hydrides (LiH, BeH<sub>2</sub>, and others), and also boron. They can be used:

- a) in the form of a suspension or a colloidal solution of metal in fuel;
- b) in the form of a third component stored in a separate tank and fed to the chamber along a separate line.

For each propellant we must select the type of metal and its optimum content. For example, to the propellant O<sub>2</sub> + H<sub>2</sub> it is advisable to add beryllium, while lithium can be added to F<sub>2</sub> + H<sub>2</sub>. The component ratios of the propellants O<sub>2</sub> + Be + H<sub>2</sub> and F<sub>2</sub> + Li + H<sub>2</sub> are best selected such that the chemical reaction occurs between the oxidizer (O<sub>2</sub>, F<sub>2</sub>) and the metal (Be, Li), while the hydrogen is used as an inert working fluid, lowering the molecular mass of the gases discharging from the nozzle.

In place of the propellant F<sub>2</sub> + Li + H<sub>2</sub> we can use F<sub>2</sub> + LiH + H<sub>2</sub>; lithium hydride evaporates better than lithium.

After methods have been developed for stabilizing liquid ozone, the most powerful chemical propellant will probably be O<sub>3</sub> + Be + H<sub>2</sub>.

The use of propellants with metal-containing fuels is hampered by the following.

1. The difficulties in mixing metal powders and liquid fuels, particularly cryogenic fuels.
2. The metal particles settle during shipment and with prolonged storage. It is possible to mix the fuel and the powdered

metal directly at the launch site, but this presents great operational inconveniences. The particles settle to a lesser extent with an increase in viscosity and density of the fuel (e.g., with the addition of wax or paraffin), and also with a decrease in the particle dimensions (to 1-40  $\mu\text{m}$ ).

3. The production of powder metals, especially beryllium (i.e., Be and  $\text{BeH}_2$  powder), is complex and expensive. In addition, powdered Be and  $\text{BeH}_2$  are highly toxic, which eliminates the possibility of using them as additives to the fuel for engines of the first stages of booster rockets.

4. When a metal-containing fuel is fed to the chamber, the injectors may become clogged. Certain difficulties are caused in the organization of combustion of metal particles.

When a tripropellant is used the metal can be fed to the chamber in atomized form, e.g., by a compressed inert gas. Tests of an experimental chamber operating on the tripropellant  $\text{F}_2 + \text{Li} + \text{H}_2$  with 10-12% Li yielded a vacuum specific impulse of more than 5000 N·s/kg [ $\approx 500 \text{ kgf}\cdot\text{s/kg}$ ] [1]. The metal can be introduced into the chamber along a separate line or directly in the form of a finely-disperse powder which, however, involves great difficulties.

The disadvantages of LPRE's using tripropellants is the complexity of design and changes in the operating mode.

The use of metal-containing fuels and tripropellants leads to an increase in heat flows to the chamber walls, which complicates chamber cooling and increases the requirements on the structural materials. LPRE's operating on such propellants are most advantageously used for space vehicles and the last stages of boosters.

## CHAPTER XI

### HEAT TRANSFER AND LPRE COOLING

#### §11.1. Forms of transfer of heat flows

During operation of most rocket engines, the walls of their chambers receive a considerable amount of heat from the products of combustion or decomposition of the propellant components or the products of heating of the working fluid. To assure reliable operation of the chamber, and the engine as a whole, this heat must be removed in some manner or other.

Quantitatively, the transmission of heat (also called *heat transfer*) is determined by the values of the heat flux and the specific heat flux.

The *heat flux* is the quantity of energy transmitted in the form of heat per unit time across any surface  $F$ . The heat flux is measured in watts [joules/second; kilocalories/second] and is designated by the letter  $Q$ .

The *specific heat flux* (or the *heat flux density*) is the heat flux arriving per unit surface area. The specific heat flux characterizes the intensity of heat transfer; it is designated by  $q$ .

Consequently,

$$q = \frac{Q}{F}. \quad (11.1)$$

The specific heat flux has the dimensions  $W/m^2$  [ $J/s \cdot m^2$ ; kcal per  $hr \cdot m^2$ ].

The region of the nozzle throat is the most thermally stressed. For certain types of LPRE's the specific heat flux in this section reaches  $70 \cdot 10^6 W/m^2$  [ $60.2 \cdot 10^6$  kcal/ $hr \cdot m^2$ ].

The heat fluxes can be transmitted by convection, thermal radiation, and thermal conductivity of the medium (substance) (for more detail see [17] and [18]).

The specific *convection* flux is designated  $q_{\text{con}}$ , while the radiation flux is  $q_{\text{rad}}$ .

The relative values of convection and radiation fluxes in various types of rocket engines differ significantly.

In the chambers of LPRE's with a cooling loop, the basic form of heat transfer is convection heat fluxes from the combustion products to the inner wall of the chamber, and from it to the coolant (a propellant component).

Heat transfer by means of thermal radiation is of much less significance in LPRE's. However, the final sections of the nozzles of certain LPRE's have no cooling loops. The thermal regime of this section of the nozzle is determined by the heat transfer from the combustion products to the nozzle wall and radiation heat transfer from the wall into the surrounding space and to the combustion products.

Nuclear rocket engines [NRE] and electrothermal jet engines [ETJE] are characterized by higher gas temperatures than for chemical engines. Therefore the role of radiation noticeably increases

in NRE's and ETJE's. In addition, convection heat transfer performs the complex task of removing heat from the fuel elements to the working medium.

Electric rocket engines [ERE] are distinguished by the very low pressure of the plasma in their chambers. Therefore, the convection heat fluxes, which depend on the pressure of the gas in the chamber, are also low and the thermal regimes of these engines are determined basically by radiation fluxes from the plasma to the chamber walls and from them to outer space.

### §11.2. Convection heat transfer

Let us examine the equations from which we can determine the specific convection flux from the gas to the wall surface and from the wall to the coolant.

Let us introduce the following designations of the parameters for a chamber with a cooling loop:

$T_{\text{gas},s}$  – the gas recovery temperature, determining the heat transfer from the gas to the wall;

$T_{\text{H},\text{u}}$  – the temperature of the heated (heat-receiving) surface of the inner chamber wall;

$T_{\text{O},\text{u}}$  – the temperature of the cooled (heat-giving) surface of the inner chamber wall;

$T_{\text{ox}}$  – temperature of the coolant flowing through the cooling loop;

$q_{\text{KOH},\text{H}}$  – the specific convection heat flux transmitted from the gas to the heated surface of the inner wall;

$q_{\text{O},\text{u}}$  – specific convection heat flux transmitted from the cooled surface of the inner wall to the coolant;

$\alpha_{\text{H},\text{u}}$  – coefficient of convection heat transfer from the gas to the heated surface of the inner wall;

$\alpha_{o,n}$  - coefficient of convection heat transfer from the cooled surface of the inner wall to the coolant.

The coefficient of convection heat transfer expresses the quantity of heat transmitted by convection across a unit surface per unit time for each degree of difference of wall and fluid temperatures; this coefficient has the dimensions  $W/m^2 \cdot deg$  [ $kcal/hr \cdot m^2 \cdot deg$ ].

Therefore, the specific flux  $q_{H.O.H}$  is calculated from the equation

$$q_{H.O.H} = \alpha_{o,n} (T_{gas,s} - T_{w,s}). \quad (11.2)$$

while the specific flux  $q_{o,n}$  is calculated from the equation

$$q_{o,n} = \alpha_{o,n} (T_{o,n} - T_{w,n}). \quad (11.3)$$

Temperature  $T_{gas,s}$  is somewhat lower than the gas stagnation temperature, since part of the heat released during stagnation of the gas in the boundary layer is removed from it by convection and thermal conductivity.

All the difficulties involved in calculating convection heat transfer reduce to determining the heat-transfer coefficients  $\alpha_{H,n}$  and  $\alpha_{o,n}$ . They are calculated using the dependence among dimensionless criteria - the Nusselt, Reynolds, and Prandtl criteria:

$$Nu = f(Re, Pr). \quad (11.4)$$

These criteria determine the nature of the change in velocity and temperature in the boundary layer, which influences to a considerable extent the convection heat transfer.

Use of dependence (11.4) for heat transfer between combustion products of an LPRE chamber and its wall gives the following formula for calculating heat-transfer coefficient  $\alpha_{H,n}$ :

$$\alpha_{H,n} = B_1 \cdot \frac{\dot{m}^{0.8}}{A^2}. \quad (11.5)$$

where  $B_1$  is a set of thermophysical properties of the combustion products, a function of their composition and temperature;  $\sigma$  is a dimensionless coefficient, taking into account the influence of the change in temperature and Mach number  $M$  with boundary layer height;  $\dot{m}$  is the per-second mass flow rate of the combustion products; and  $d$  is the chamber diameter.

The coefficient  $\alpha_{H,n}$  depends on the product  $\rho W$ , and increases with it. This is explained by the fact that with increasing gas density the number of gas particles per unit volume increases, while

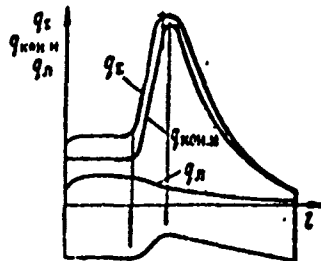


Fig. 11.1. Graphs of the distribution of specific heat fluxes  $q_t$ ,  $q_{KOH.H}$ , and  $q_n$  along the chamber.

with an increase in gas velocity the number of gas particles reaching the wall per unit time increases. With convection heat transfer, heat is transported by the particles. Therefore, with increasing gas density and velocity the process of heat transfer from the gas to the wall becomes more intense, i.e., the values of  $\alpha_{H,n}$  and  $q_{KOH.H}$  increase. The product  $\rho W$  has maximum value at the throat (see

§4.5); consequently, the values of  $\alpha_{H,n}$  and  $q_{KOH.H}$  are also maximum in this section (Fig. 11.1).

Use of dependence (11.4) for heat transfer between the wall and the coolant with high heat-flux values characteristic of LPRE chambers gives the following formula for calculating heat-transfer coefficient  $\alpha_{o,n}$ :

$$\alpha_{o,n} = B_2 \beta \left( \frac{\dot{m}_{ox}}{f_{o,n}} \right)^{0.8} \frac{1}{d_{res}^{0.2}}, \quad (11.6)$$

or, considering equation (4.9),

$$\alpha_{o,n} = B_2 \beta (Q_{ox} W_{ox})^{0.8} \frac{1}{d_{res}^{0.2}}, \quad (11.7)$$

where  $B_2$  is a set of thermophysical properties of the coolant, a function of the type of coolant and its temperature;  $\beta$  is a coefficient which takes into account the change in thermophysical properties of the coolant with boundary layer height;  $\dot{m}_{ox}$ ,  $\rho_{ox}$ , and  $W_{ox}$

are the per-second mass flow rate, the density, and the velocity of the coolant, respectively;  $f_{0,T}$  is the area of the cooling-loop cross section;  $d_{ГИД}$  is the hydraulic (equivalent) diameter of the cooling loop, defined by the equation

$$d_{ГИД} = \frac{4f_{0,T}}{l_s}.$$

where  $l_s$  is the total (wetted) perimeter of the cooling-loop cross section.

### §11.3. Radiation heat transfer

Solids emit and absorb waves of all lengths, from  $\lambda = 0$  to  $\lambda = \infty$ , i.e., their radiation is characterized by a *continuous* spectrum.

Gases emit and absorb electromagnetic energy only within specific wavelength bands  $\Delta\lambda$ , i.e., the radiation and absorption of gases are characterized by a so-called *line* spectrum. Such radiation and absorption are called *selective*. The simpler the structure of the molecule or atom, the more clearly expressed is the line structure of the radiation spectrum, and the more necessary it is to consider such spectral structure when calculating radiation.

Selective radiation is completely inherent in the working media of ERE's, i.e., the monatomic gases cesium, lithium, argon, etc.; it is very difficult to calculate their radiation. However, calculations that have been done show a sharp increase in radiant fluxes  $q_{\lambda}$  with increasing temperature of the gases.

Of the gases making up the combustion products of chemical propellants, energy is mainly radiated and absorbed by the polyatomic gases having asymmetric molecular structure, mainly water vapor  $H_2O$  and carbon dioxide  $CO_2$ . The radiating capacity and absorptivity of monatomic and diatomic gases can be disregarded.

Solids usually radiate and absorb energy on the surface, while

gases radiate and absorb throughout. Therefore, the radiating capacity and absorptivity of gases containing  $H_2O$  and  $CO_2$  are determined not only by the gas temperature and the  $H_2O$  and  $CO_2$  partial pressures, but also by the shape of the combustion chamber; the latter, in turn, is characterized by the mean free beam path  $l$ .

The radiation of water vapor and carbon dioxide is subject, with certain allowances, to the Stefan-Boltzmann law; to calculate the radiation heat flux from these gases to the chamber wall we can use the equation

$$q_s = \epsilon_{CT,s} \left[ \epsilon_{ras} c_0 \left( \frac{T_{ras}}{100} \right)^4 - \epsilon'_{ras} c_0 \left( \frac{T_{H,n}}{100} \right)^4 \right]. \quad (11.8)$$

where  $\epsilon_{CT,s}$  is the effective degree of blackness of the heated surface of the inner chamber wall;  $\epsilon_{ras}$  and  $\epsilon'_{ras}$  are the degrees of blackness of the gas at temperatures  $T_{ras}$  and  $T_{H,n}$ , respectively.  $c_0$  is the radiation coefficient of an absolutely black solid, equal to  $5.67 \text{ W/m}^2 \cdot \text{deg}^4$  [ $4.96 \text{ kcal/hr} \cdot \text{m}^2 \cdot \text{deg}^4$ ].

The value  $\epsilon_{CT,s}$  is a function of the degree of blackness of the wall and the gas ( $\epsilon_{CT}$  and  $\epsilon_{ras}$ , respectively). The value of  $\epsilon_{CT}$ , determined by the material of the wall and the state of its heated surface, is taken from tables [17].

The value of  $\epsilon_{ras}$  for combustion products containing water vapor and carbon dioxide is equal to

$$\epsilon_{ras} = \epsilon_{H_2O} + \epsilon_{CO_2} - \epsilon_{H_2O} \epsilon_{CO_2}. \quad (11.9)$$

The presence of the last term in (11.9) is explained by the partial mutual absorption of  $H_2O$  and  $CO_2$  radiation.

The values of  $\epsilon_{H_2O}$  and  $\epsilon_{CO_2}$  are functions of the temperature of the gas and of the product of its partial pressure times the mean free beam path  $l$ , while the values of  $\epsilon_{H_2O}$  are also functions of the pressure of the combustion products  $p_{\Sigma}$ . Special graphs [17] are used to determine  $\epsilon_{H_2O}$  and  $\epsilon_{CO_2}$ .

The distribution of specific radiation heat fluxes  $q_n$  along the chamber is shown in Fig. 11.1; they are maximum in the combustion chamber, since in it the pressure (and, consequently, the values  $p_{H_2O}$  and  $p_{CO_2}$ ) and temperature  $T_{ras}$  have maximum values.

Considering the approximate nature of the radiation calculations, it is recommended that  $q_n$  be calculated only for the flow core in the combustion chamber (let us designate this value by  $q_{n.K}$ ), while the values of  $q_n$  in the other sections are taken as follows:

- 1) directly at the fire plate of the head

$$q_n = 0.8 q_{n.K}$$

- 2) in the section 50-100 mm from the fire plate to the convergent part of the nozzle with diameter  $d = 1.2d_{kp}$ , the value of  $q_n$  is constant and equal to  $q_{n.K}$ ;

- 3) at the throat

$$q_n = 0.5q_{n.K}$$

- 4) in the divergent part of the nozzle with diameter  $d = 1.5d_{kp}$ ,  $q_n = 0.1q_{n.K}$ ;

- 5) in the last section of the nozzle with diameter  $d = 2.5d_{kp}$ ,  $q_n = 0.02q_{n.K}$ .

Connecting these points with a smooth curve we get the distribution of the radiation heat flux along the chamber.

With a combustion-product temperature of  $2000^{\circ}\text{K}$ ,  $q_n$  is small compared with the specific convection flux  $q_{\text{кон.н}}$ , but with a combustion-product temperature of  $3000-4000^{\circ}\text{K}$ ,  $q_n$  can reach 30% of the total heat flux to the wall.

#### §11.4. Heat transfer due to thermal conductivity of the wall material

If, as the engine operates, there is assured in some manner or other a difference of the chamber wall surface temperatures, heat

is transmitted through the wall because of the thermal conductivity of the wall material. In this case the specific heat flux is determined from the equation

$$q_{ct} = \frac{\lambda_{ct}}{\delta_{ct}} (T_{n,n} - T_{o,n}), \quad (11.10)$$

where  $\delta_{ct}$  is the wall thickness;  $\lambda_{ct}$  is the coefficient of thermal conductivity of the wall material, characterizing its capability to conduct heat.

With identical wall thickness  $\delta_{ct}$ , to assure a given flux  $q_{ct}$  through the wall the required wall-temperature difference is the less, the greater the coefficient  $\lambda_{ct}$ . On the other hand, with a small coefficient  $\lambda_{ct}$  the wall-temperature difference  $T_{n,n} - T_{o,n}$  can be rather great on a thin chamber wall. For example, with a moderate specific heat flux through a wall  $q_{ct} = 11.6 \cdot 10^6 \text{ W/m}^2$  [ $10 \cdot 10^6 \text{ kcal/hr} \cdot \text{m}^2$ ] the difference in temperatures on a wall 1 mm thick made of stainless steel is

$$T_{n,n} - T_{o,n} = \frac{q_{ct} \delta_{ct}}{\lambda_{ct}} = \frac{11.6 \cdot 10^6 \cdot 1 \cdot 10^{-3}}{23.3} = 500 \text{ deg.}$$

Of all materials, except for the noble metals, pure copper has the highest thermal conductivity coefficient.

For copper containing impurities, and for alloys of copper with other metals (e.g., bronze of some composition or other), the value of  $\lambda$  is noticeably lower.

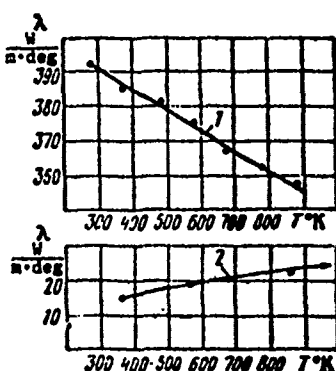


Fig. 11.2. Dependence of the coefficient of thermal conductivity for pure copper (1) and stainless steel (2) on temperature.

The coefficient of thermal conductivity of metals and other materials is a function of their temperature. Figure 11.2 shows graphs  $\lambda = f(T)$  for pure copper and stainless steel.

Taking this dependence into account, the coefficient of thermal conductivity in (11.10) must be taken at the average wall temperature

$$T_{ct,av} = \frac{T_{n,n} + T_{o,n}}{2}.$$

### §11.5. Characteristics of heat transfer through a chamber wall

During engine operation, the chamber walls receive both convective as well as radiant heat fluxes. Therefore, the total specific heat flux entering the chamber walls is

$$q_1 = q_{n,n} = q_{n,n,n} + q_s. \quad (11.11)$$

The specific heat flux  $q_{n,n}$  can also be written as follows:

$$q_{n,n} = a'_{n,n} (T_{res,n} - T_{n,n}), \quad (11.12)$$

where  $a'_{n,n}$  is some effective heat-transfer coefficient which takes into account both convection as well as radiation heat transfer between the combustion products and the wall.

On the basis of equations (11.2), (11.11), and (11.12), the heat-transfer coefficient  $a'_{n,n}$  is equal to

$$a'_{n,n} = a_{n,n} + \frac{q_1}{T_{res,n} - T_{n,n}}. \quad (11.13)$$

The graph of the distribution of the total specific heat flux  $q_{\Sigma}$  along the chamber is shown in Fig. 11.1. Because of the influence of the radiant flux, the maximum of the total specific heat flux is shifted somewhat from the critical section toward the chamber head. From the graph in Fig. 11.1 it follows that the region of the critical section is the most thermally-stressed section of the chamber; therefore, reliable cooling of it causes great difficulties.

The heat fluxes entering the walls from the combustion products pass through the wall and are transmitted to the coolant flowing through the cooling loop.

At the start of engine operation, the coolant is transmitted not the entire heat flux entering the wall from the combustion products, but only part of it; the rest is used to heat the chamber walls, as a result of which the chamber wall temperature continually

increases. As the wall temperature increases, that part of the heat flux expended on heating the walls continually decreases. Consequently, the initial period of engine operation is characterized by a *nonsteady-state* cooling regime. If specific conditions are satisfied, after a certain period of time (for an LPRE chamber this is short) equilibrium is established. It is characterized by the fact that the entire heat flux entering the wall from the combustion products is transmitted from the wall to the coolant. Therefore, if we consider that the areas of the heated and cooled wall surfaces are equal to one another, the following equality is guaranteed:

$$q_{\text{E},\text{R}} = q_{\text{C},\text{R}} = q_{0,\text{R}} = \text{const.}$$

Over the entire section of heat-flux transfer – from the boundary layer of the combustion products to that of the coolant – a constant temperature distribution is established (Fig. 11.3), such

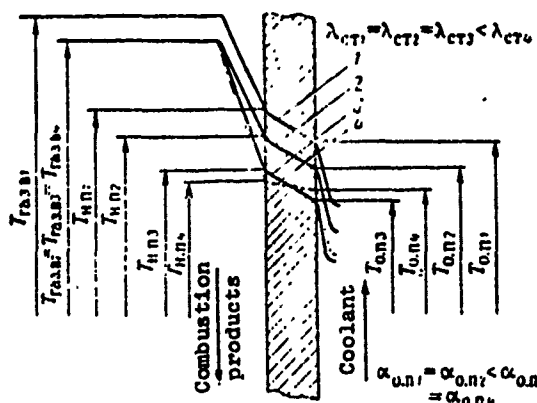


Fig. 11.3. Graphs of the distribution of temperature through the inner wall and in the boundary layers for various gas, coolant, and inner-wall parameters

that the temperatures  $T_{H,n}$ ,  $T_{o,n}$ , and  $T_{ox}$  remain constant despite the presence of the heat flux. Consequently, in this case a *steady-state* chamber cooling regime is assured. This heat flux, with a steady-state cooling regime, will henceforth be designated  $q_{\Sigma}$ , by analogy with equation (11.11). Consequently,

$$q_{\alpha_1} = q_{\alpha_2} = q_{\alpha_3} = q_{\alpha_4}$$

Therefore, equations (11.12), (11.10), and (11.3) can be written in the following form:

$$q_2 = a'_{1,1}(T_{2,1,1} - T_{2,1,2});$$

$$q_2 = \frac{\lambda_{ct}}{\rho_{ct}} (T_{u,n} - T_{o,n});$$

$$q_i = a_{i,n} (T_{e,n} - T_{ex}),$$

From this,

$$T_{H,n} = T_{gas,s} - \frac{q_\Sigma}{\alpha'_{H,n}}; \quad (11.14)$$

$$T_{o,n} = T_{o,n} + \frac{q_\Sigma \delta_{cr}}{\lambda_{cr}}; \quad (11.15)$$

$$T_{o,n} = T_{ox} + \frac{q_\Sigma}{\alpha_{o,n}}. \quad (11.16)$$

Substituting (11.16) into (11.15) we get

$$T_{H,n} = T_{ox} + \frac{q_\Sigma}{\alpha_{o,n}} + \frac{q_\Sigma \delta_{cr}}{\lambda_{cr}}. \quad (11.17)$$

The above equations are conveniently used for analyzing the influence of various parameters on the chamber cooling regime. A change of any of these parameters causes, to some extent or other, a change in the graph of temperature distribution in the boundary layer on the part of the combustion products, and throughout the wall and in the boundary layer on the part of the coolant (see Fig. 11.3).

For example, if the temperature of the combustion products  $T_{gas,s}$  is increased, temperatures  $T_{H,n}$  and  $T_{o,n}$  rise (see curves 1 and 2), with a simultaneous increase in temperature  $T_{ox}$ . If the wall material is replaced by a material having a higher coefficient of thermal conductivity  $\lambda_{cr}$ , temperature  $T_{H,n}$  drops but temperature  $T_{o,n}$  rises somewhat (see curves 3 and 4). The same effect is observed with a decrease in the thickness of the inner wall  $\delta_{cr}$ . If, in some manner or other (e.g., by increasing the coolant velocity  $W_{ox}$ ), the removal of heat fluxes from the wall to the coolant is intensified, temperatures  $T_{H,n}$  and  $T_{o,n}$  simultaneously drop (see curves 2 and 3).

As can be seen from equations (11.14)-(11.16), the difference in temperatures and, consequently, the slope of the temperature distribution curve decrease

a) for the boundary layer of the combustion products, in which their temperature drops from  $T_{gas,s}$  to  $T_{H,n}$  - with a decrease in  $q_\Sigma$  and an increase in the heat-transfer coefficient  $\alpha'_{H,n}$ ;

b) for the wall - with an increase in the coefficient of thermal conductivity of its material  $\lambda_{CT}$ ;

c) for the coolant boundary layer, in which its temperature drops from  $T_{o.n}$  to  $T_{ox}$  - with a decrease in  $q_{\Sigma}$  and an increase in the heat-transfer coefficient  $\alpha_{o.n}$ .

The influence of the parameters of the combustion products, wall, coolant, and cooling loop on the cooling regime will be examined in greater detail in §§11.7-11.9.

#### §11.6. Requirements on the engine chamber cooling system

If the heat fluxes are not removed from the wall, within a short period of time the wall overheats and there is an inadmissible reduction in the strength of the material of which it is made, or burnout occurs, which can lead to destruction of the chamber.

Because of the high velocity of the combustion products, particularly in the expanding part of the nozzle, the chamber walls are subjected to erosion. Wall erosion becomes especially noticeable during overheating, since in this case the erosion resistance of the material decreases. Therefore, for reliable engine chamber operation the temperature of its walls should not exceed the value allowed for the selected wall material based on strength and erosion-resistance conditions, i.e.,

$$T_{cr} < T_{ew}$$

while for a chamber with external circulating cooling

$$T_{ew} < T_{ew}$$

A system of external circulating cooling should maintain the following standards.

1. The temperature of the cooled surface of the wall  $T_{o.n}$  in all sections of the chamber should not exceed the value at which so-called film boiling sets in; the presence of film boiling leads to a substantial decrease in the heat flux from the wall to the coolant,

and to its burnout (see p. 53).

2. The temperature of the coolant should not reach those values at which it begins to decompose with formation of solid, resinous, or gaseous decomposition products. Solid and resinous particles are deposited on the wall, forming a layer with a low coefficient of thermal conductivity. In this case, heat transfer from the wall to the coolant is reduced, causing a rise in the temperature of the wall, and the wall can burn out. In addition, solid and resinous particles can clog the openings in the chamber injectors, which is not permissible.

With overheating of certain propellant components ( $H_2O_2$ ,  $N_2O_4$ , UDMH) used as coolants, effects equivalent to explosions can occur.

3. For LPRE's operating in the scheme "liquid-liquid," the temperature of the coolant coming from the cooling loop to the chamber injectors should not exceed the boiling point of the coolant, i.e.,

$$T_{ox} < T_{\text{кип}}$$

where  $T_{\text{кип}}$  must be taken for the pressure of the coolant at the exit from the cooling loop.

If the condition  $T_{ox} < T_{\text{кип}}$  is not observed, the coolant enters the injectors as a vapor or emulsion. In this case the operating regime for injectors designed to atomize the liquid is abruptly curtailed, and the chamber can explode. In addition, the removal of heat is sharply reduced from those sections of the chamber walls to be cooled by vaporized coolant, and they can burn out.

4. The velocity of the coolant must not be too high. As it increases, heat-transfer coefficient  $\alpha_{\text{о.н}}$  increases and temperature  $T_{\text{кип}}$  decreases [see equation (11.17)], but there is a simultaneous increase in the required power of the system for feeding the propellant components to the chamber and, consequently, in the mass of this system.

5. The chamber cooling loop should be practical to produce, i.e., its dimensions and shape should be such that no great difficulties arise in serial manufacture of the chambers.

#### §11.7. The influence of various factors on the heat flux from the combustion products to the wall

The *temperature of the combustion products* has a substantial influence on the values of  $q_{\text{HOH},H}$  and  $q_{\text{J}}$ , causing them to increase as it increases, which is evident from equations (11.2) and (11.8). The tendency of the temperature of combustion products to rise in the LPRE chamber is due to the use of more efficient propellants (with high heating capacity) to obtain high specific impulse. An increase in specific impulse causes a lowering of the required flow of propellant components, bringing about additional difficulties when cooling the chamber, since the coolant is one of the propellant components.

The *coefficient  $\kappa$*  influences the heat fluxes through the temperature of the combustion products and, in part, through their composition. With an increase in the deviation of coefficient  $\kappa$  from the stoichiometric value, the heat fluxes from the combustion chamber to the walls are reduced.

The values of  $q_{\text{HOH},H}$  and  $q_{\text{J}}$  are greatly influenced by the *pressure  $p_{\text{K}}$* . The dependence of heat flux  $q_{\text{HOH},H}$  on pressure  $p_{\text{K}}$  can be shown using the critical section as an example; for it, in accordance with equation (11.5),

$$a_{\text{HOH},\text{Kp}} = B_1 \frac{\dot{m}^{0.8}}{d_{\text{Kp}}^{1.5}}.$$

Substituting into this equation the value of  $\dot{m}$  from equation (4.14) and considering the relationship  $f_{\text{Kp}} = \pi d_{\text{Kp}}^2/4$ , after certain transformations we get

$$a_{\text{HOH},\text{Kp}} = B'_1 \frac{p_{\text{K}}^{0.8}}{p^{0.8} d_{\text{Kp}}^{0.5}}. \quad (11.18)$$

As can be seen from equation (11.18), the value of  $\alpha_{\text{KOH.H.KP}}$  and, consequently, the value of  $q_{\text{KOH.H.KP}}$  increase with a rise in pressure  $p_K$  to the 0.8 power.

The value of  $q_n$  also increases with increasing pressure  $p_K$  in connection with a rise in the partial pressures  $p_{\text{CO}_2}$  and  $p_{\text{H}_2\text{O}}$  which determine radiation heat transfer. The greater the heat fluxes to the chamber walls, the higher the temperature of the coolant flowing along the cooling loop. Consequently, a transition to higher pressures in the combustion chamber causes increased difficulties in cooling the chamber. This dependence holds for a fixed coolant flow rate, since the examined increase in  $p_K$  is achieved by decreasing the area of the critical section, not by increasing the flow rate of the propellant components (and, consequently, the coolant flow).

The influence of the *total heat flux*  $q_{\Sigma}$  on the temperature of the heated surface of the chamber wall  $T_{\text{H.n}}$  can be estimated on the basis of equation (11.14). With increasing  $q_{\Sigma}$  the temperature  $T_{\text{H.n}}$  drops, and vice versa; in the limiting case, when  $q_{\Sigma} = 0$  (i.e., with no heat flux through the wall), temperature  $T_{\text{H.n}}$  becomes equal to the temperature of the combustion products  $T_{\text{gas.s}}$ . Consequently, with an increase in  $q_{\Sigma}$ , temperature  $T_{\text{H.n}}$  drops, if we consider the temperature of the combustion products  $T_{\text{gas.s}}$  as constant.

The influence of the *rated chamber thrust* on its cooling involves the fact that with a drop in thrust there is a directly proportional decrease in flow rate of the propellant components and, consequently, of the coolant. The chamber surface area to be cooled decreases to a lesser extent. Therefore, it is extremely difficult to create high-efficiency LPRE's having a thrust of less than 500 N [ $\approx 50$  kgf] and cooled using a coolant (particularly with prolonged engine operation).

The *engine operating regime* influences chamber cooling for the reason that a reduction in chamber thrust is achieved by reducing the flow rate of the propellant components (and, consequently, of

the coolant); here there is a significant reduction in  $p_K$  and  $q_{KOH.H}$ . Consequently, with a drop in  $p_K$  there is a simultaneous decrease in  $\dot{m}_{ox}$  and  $q_{KOH.H}$ .

In accordance with equations (11.18) and (4.14),

$$q_{KOH.H} \sim p_K^{0.8} \text{ and } \dot{m}_{ox} \sim p_K$$

i.e., with a drop in pressure  $p_K$  the coolant flow is reduced to a greater extent than is the convection heat flux. In addition, with a decrease in coolant flow there is a reduction in the velocity of the coolant in the cooling loop and a drop in coefficient  $\alpha_{o.n}$ . Therefore, with a reduction in engine thrust, temperatures  $T_{H.n}$  and  $T_{o.n}$  increase in accordance with equations (11.15) and (11.16). Consequently, as the engine thrust is decreased, the difficulties in cooling it increase. This is one of the essential drawbacks of chambers with external circulation cooling.

#### §11.8. The influence of the parameters of the inner chamber wall on its cooling

The influence of the temperature of the heated chamber wall surface  $T_{H.n}$  on the cooling regime. The permissible temperature  $T_{H.n}$  is determined by the heat resistance of the material of the inner chamber wall. The greater the temperature  $T_{H.n}$  that can be allowed, the lower the total heat flux  $q_{\Sigma}$  at the same temperature  $T_{ras.s}$  [see equation (11.14)]; here the required value of the coefficient  $\alpha_{o.n}$  decreases.

In §11.7 it was shown that if we set  $T_{H.n} = T_{ras.s}$ , then  $q_{\Sigma} = 0$ , i.e., there is no need for cooling the chamber walls. However, temperature  $T_{ras.s}$  is high for most LPRE's ( $T_{ras.s} = 2800-4000^{\circ}\text{K}$ ). Therefore, temperature  $T_{H.n}$  must be lowered, removing heat fluxes from the chamber wall. Equality of the temperatures of the combustion products and the wall can be achieved only for the chamber of monopropellant LPRE's.

The influence of the coefficient of thermal conductivity of the inner chamber wall material  $\lambda_{CT}$  on the cooling regime. As the coefficient  $\lambda_{CT}$  increases, the temperature difference  $T_{H,n} - T_{o,n}$  decreases, with fixed parameters of the combustion products and the coolant. If the coolant parameters are unchanged, with an increase in coefficient  $\lambda_{CT}$  the temperature  $T_{H,n}$  drops; this has some influence on temperature  $T_{o,n}$ . This influence is explained by the fact that with a drop in temperature  $T_{H,n}$ , there is a slight increase in heat fluxes  $q_{KOH,H}$  and  $q_n$ , which leads to a rise in coolant temperature; this latter, in accordance with equation (11.16), leads to a rise in temperature  $T_{o,n}$ .

If we compare two inner chamber wall materials, where  $\lambda_{CT2} > \lambda_{CT1}$ , the following relationships are valid:

$$T_{H,n2} < T_{H,n1} \text{ and } T_{o,n2} > T_{o,n1}.$$

The higher the coefficient  $\lambda_{CT}$ , the less the slope of the line of temperature distribution throughout the inner wall and the lower the temperature  $T_{H,n}$  for given temperature  $T_{o,n}$ . Therefore, for the inner chamber wall it is advisable to select materials with as high a coefficient of thermal conductivity  $\lambda_{CT}$  as possible. However, the following restrictions must be considered with using materials with high values of  $\lambda_{CT}$ .

1. With an increase in coefficient  $\lambda_{CT}$  the temperature difference  $T_{H,n} - T_{o,n}$  decreases, which increases the danger of overheating of the cooled inner wall surface. Therefore, in a number of cases this temperature difference must be artificially increased; this is done, as will be shown below, by increasing the thickness  $\delta_{CT}$  of the inner wall.

2. Usually, materials with higher  $\lambda_{CT}$  have lower heat resistance, i.e., for them it is necessary to select lower temperatures  $T_{H,n}$ , in connection with which the difficulties in cooling the chamber increase.

Let us explain this influence, using as our example chambers with steel and copper walls.

The permissible temperature for copper ( $575^{\circ}\text{K}$ ) and bronze ( $1075^{\circ}\text{K}$ ) is lower than for stainless steel ( $1475^{\circ}\text{K}$ ). Therefore, when using a copper or bronze wall at identical temperature  $T_{\text{gas.s.}}$ , the total heat flux  $q_{\Sigma}$  increases, i.e., a greater quantity of heat must be removed from the wall to the coolant. The required value of  $\alpha_{\text{o.n}}$  for a copper wall is approximately 2.0-2.5 times greater than for a wall of stainless steel (for identical wall thickness) [7].

Let us write equation (11.10) in the following form:

$$q_{\Sigma} = \frac{\lambda_{\text{ct}} \Delta T}{\delta_{\text{ct}}}. \quad (11.19)$$

As can be seen from equation (11.19), with identical thickness  $\delta_{\text{ct}}$  the wall can pass a greater heat flux, the larger the product  $\lambda_{\text{ct}} \Delta T$ . Calculations show that with identical thickness, a wall of copper or bronze is capable of passing 2.5-3.0 times greater heat fluxes than a wall of stainless steel can. Therefore, with intense cooling of a chamber with copper walls, an elevated boundary-layer temperature is permitted.

The influence of chamber inner wall thickness  $\delta_{\text{ct}}$  on the cooling regime. A decrease in wall thickness  $\delta_{\text{ct}}$  influences the heat transfer in the same manner as an increase in the coefficient of thermal conductivity  $\lambda_{\text{ct}}$ . In accordance with equation (11.19), with a decrease in thickness  $\delta_{\text{ct}}$  there is an increase in the heat flux which the wall can transmit with the identical temperature difference  $T_{\text{H.n}} - T_{\text{o.n.}}$ .

The optimum value to which it is advisable to reduce the wall thickness depends on the total heat flux  $q_{\Sigma}$ . With increasing  $q_{\Sigma}$  the temperature  $T_{\text{H.n}}$  drops. Therefore, in the region of the critical section, in which the heat fluxes have maximum value, the wall is made the thinnest, but it should assure the required chamber strength

and be technologically feasible.

The influence of the temperature of the cooled wall surface  $T_{o.n}$  on the cooling regime. With a decrease in total heat flux  $q_{\Sigma}$  the temperature  $T_{H.n}$  rises, approaching the temperature  $T_{ras.s}$ ; the value of  $T_{o.n}$  rises correspondingly with the value  $T_{H.n}$ . But the value of  $T_{o.n}$  is limited by the coolant temperature. Temperature  $T_{o.n}$  can exceed the coolant temperature only by some slight permissible value. Otherwise, decomposition or boiling of the coolant can occur. Therefore, with low heat fluxes  $q_{\Sigma}$  and high temperature  $T_{H.n}$ , the thickness of the wall must be increased to obtain the permissible temperature  $T_{o.n}$ .

To exclude the possibility of the coolant's boiling on the cooled surface of the chamber inner wall, temperature  $T_{o.n}$  should be below the boiling point of the coolant at the given pressure.

However, in most cases, for intensification of external circulation cooling provisions are made for raising the temperature  $T_{o.n}$  10-55° above the boiling point of the coolant, which leads to the coolant's starting to boil on the cooled wall surface, and the formation of bubbles ("nucleate boiling"). Because of flow turbulence of the coolant, the bubbles are removed to colder layers, further away from the wall, where they condense. Therefore, with nucleate boiling, the heat fluxes are removed more intensely from the wall to the coolant; with unchanged coolant velocity, the heat-transfer coefficient  $\alpha_{o.n}$  increases by a factor of two or more.

However, with a further rise in temperature  $T_{o.n}$  above the boiling point of the coolant there is an abrupt increase in the number of forming bubbles; they cannot be washed away by the coolant and condense in its colder layers, but join together, forming a continuous film of vapor on the wall surface ("film boiling"). In this case the heat-transfer coefficient  $\alpha_{o.n}$  and the heat flux from the wall to the coolant abruptly decrease (by a factor of 10 or more), resulting in an inadmissible rise in temperatures  $T_{H.n}$  and  $T_{o.n}$  and

to burnout of the chamber wall.

### §11.9. The influence of the type of coolant and the parameters of external circulation cooling on the chamber cooling regime

For efficient external circulation cooling of the chamber it is necessary to select the optimum type of coolant, the optimum temperature at the inlet to the cooling loop, and also the most suitable shape for the cooling loop to assure the necessary distribution of coolant velocity along the cooling loop.

The influence of the type of coolant on the cooling regime. Analysis of equation (11.7) shows that the heat-transfer coefficient  $\alpha_{o.n}$  and, consequently, the cooling capacity of various fluids with an identical cooling loop depend essentially on the type of coolant. Given the coolant velocity, and also technologically feasible dimensions and shape for the cooling loop, for each type of coolant we can determine a value of coefficient  $\alpha_{o.n}$  called the *available* value; let us designate this as  $\alpha_{o.n.pacn}$ .

The *required* value of the coefficient,  $\alpha_{o.n.notp}$ , can be determined from equation (11.16), substituting in it the permissible temperatures  $T_{o.n}$  and  $T_{ox}$ .

Normal cooling is assured under the condition

$$\alpha_{o.n.pacn} > \alpha_{o.n.notp}$$

To estimate the cooling properties of a coolant, significant factors include the value of the specific heat of the coolant, the temperature range of its liquid state, and also the percentage of coolant in the propellant, defined by coefficient  $\kappa$ .

The temperature range for the liquid state of a coolant is determined by the difference in temperatures  $T_{\text{ким}} - T_{\text{пл}}$ ; the boiling point must be taken for the pressure of the coolant in the cooling loop. The cooling ability of a coolant increases with an increase in this temperature difference and the specific heat of the coolant.

In a rocket vehicle, only the propellant components can be used for external circulation cooling of the chamber. The flow of propellant components (and, consequently, the coolant) is restricted, and besides, not all components have sufficiently good cooling properties.

Of all fluids, water has the best cooling power. The heat-transfer coefficient  $\alpha_{o.n}$  of nitrogen tetroxide and nitric acid is 1.5-2.0 times lower, while that of kerosene and UDMH is three times lower, than that of water. Ordinarily, the coolant for an LPRE chamber is the fuel (kerosene, ammonia, UDMH, hydrogen, etc.), while if the fuel does not guarantee the required cooling, the oxidizer is used (e.g., nitric acid, nitrogen tetroxide, and hydrogen peroxide).

The advantage of using the oxidizer as the coolant is that its flow rate is usually 2-4 times that of the fuel, i.e.,  $\kappa = 2-4$ . However, if the oxidizer is used as the coolant, the material of the inner wall should be stable in an oxidizing medium at elevated temperatures.

**The influence of coolant temperature on the cooling regime.** Analysis of equation (11.17) shows that with decreasing coolant temperature, the temperature of the heated surface of the inner wall  $T_{H.n}$  also drops; this, as shown in §11.8, is desirable, despite a slight increase in the total heat flux  $q_{\Sigma}$ .

The coolant temperature can be lowered by reducing the value of  $q_{\Sigma}$  (see §11.11). It can be supercooled to a temperature below that of the ambient medium, using a special system included in the launcher.

**The influence of coolant velocity on the cooling regime.** The coolant velocity  $W_{ox}$  determines, to a considerable extent, the heat-transfer coefficient  $\alpha_{o.n}$  [see equation (11.7)] and, consequently, the heat transfer from the cooled wall surface to the coolant. In accordance with equation (11.3), with an increase in coefficient  $\alpha_{o.n}$ , the value of  $q_{\Sigma}$  also increases, but temperatures  $T_{o.n}$  and  $T_{H.n}$

are lowered (see §11.8).

The velocity of the coolant in the chamber cooling loop can be increased by raising its per-second flow rate  $\dot{m}_{ox}$  with  $f_{o.r} = \text{const}$  or by decreasing the area of the throughput section of the cooling loop  $f_{o.r}$  with  $\dot{m}_{ox} = \text{const}$ . Area  $f_{o.r}$  is decreased by selecting the appropriate dimensions and shape of the cooling loop (see §11.11).

With an increase in coolant velocity there is an increase in the hydraulic resistance of the cooling loop  $\Delta p_{o.r}$ , which is undesirable. Usually, the value of  $\Delta p_{o.r}$  is 5-20 bars [ $\approx 5-20 \text{ kgf/cm}^2$ ]. Therefore, it is important to select the optimum coolant velocity  $W_{ox}$  in various sections of the cooling loop. The heat fluxes have maximum value in the critical section, and velocity  $W_{ox}$  here should be maximum; it can reach 50-60 m/s.

The influence of the area of the cooled surface on the cooling regime. If we disregard the thickness of the inner wall  $\delta_{cr}$ , then for the simplest shape of the cooling loop (an annular slot between the outer and inner walls of the chamber) the area of the heated surface of the inner wall  $F_{H.n}$  is equal to the area of its cooled surface  $F_{o.n}$ , i.e.,  $F_{H.n} = F_{o.n}$ .

Cooling efficiency can be increased when  $F_{o.n} > F_{H.n}$ , which is assured when there are some type of ribs on the cooled surface of the inner wall [7].

In a steady-state cooling regime the value of the heat flux, equal to the sum  $Q_{KOH.H} + Q_{L}$ , is time constant. Therefore, when  $F_{o.n} > F_{H.n}$  we have the inequality  $q_{o.n} < q_{H.n}$ , where  $q_{H.n} = q_{\Sigma} = q_{KOH.H} + q_{L}$ .

A decrease in the value of  $q_{H.n}$  as compared with  $q_{o.n}$  is defined by the relationship

$$\frac{q_{H.n}}{q_{o.n}} = \frac{F_{o.n}}{F_{H.n}}.$$

By using ribbing on the cooled surface of the inner wall we can increase the area  $F_{o.m}$  a factor of 1.4-1.8 and more as compared with the area  $F_{n.m}$ ; there is an identical decrease in the required value of the heat-transfer coefficient  $a_{o.m}$  as compared with  $a_{n.m}$  for the simplest shaped cooling loop (without ribbing).

#### §11.10. Calculating coolant heating in the chamber cooling loop

As the coolant moves along the chamber cooling loop it continually absorbs the heat fluxes, so that its temperature continually increases along the loop and reaches its maximum value before entering the chamber head. Depending on the chamber dimensions and the heating capacity of the propellant, the cooling temperature in the cooling loop is raised by 100-300°.

The heating of the coolant in each section of the loop is defined by the equation

$$T_{ox,nu} = T_{ox,ex} + \Delta T_{ox}. \quad (11.20)$$

The value of  $\Delta T_{ox}$  is calculated as follows. The quantity of heat absorbed by the coolant in the  $i$ -th section of the chamber is

$$Q_i = q_{\Sigma i} F_i,$$

where  $q_{\Sigma i}$  is the total specific heat flux in the  $i$ -th section, defined by the graph  $q_{\Sigma} = f(l)$  (see Fig. 11.1), which should be constructed ahead of time based on results of calculating the heat fluxes to the wall;  $F_i$  is the surface of the wall of the  $i$ -th section, through which the heat flux is transmitted to the coolant.

If in the  $i$ -th section of the chamber the temperature of the coolant, with heat capacity  $c_{ox}$  at flow rate  $\dot{m}_{ox}$ , increases by  $\Delta T_{ox,i}$ , the heat flux absorbed by the coolant in the given section can be written as follows:

$$Q_i = \dot{m}_{ox} c_{ox} \Delta T_{ox,i}. \quad (11.21)$$

Consequently,

$$\Delta T_{ox,l} = \frac{Q_l}{m_{ox} c_{ox}}. \quad (11.22)$$

The heat capacity of the coolant  $c_{ox}$  is a function of its temperature, which changes along the cooling loop. Therefore, the heating in each section is calculated from the average temperature of the coolant by the method of successive approximations; in the first approximation we assume that the coolant temperature along the entire length of the given section is constant and equal to its temperature at the inlet to the given section.

The temperature of the coolant at the exit from the cooling loop is

$$T_{ox,out} = T_{ox,in} + \frac{\sum_{l=1}^{l=n} Q_l / c_{ox,l}}{m_{ox}}.$$

Temperature  $T_{ox,BHx}$  in most cases should not exceed the boiling point of the coolant; the latter, as already indicated, should be selected for the pressure of the coolant at the exit from the loop.

On the basis of equation (11.21), the maximum heat-absorption capacity of the coolant is

$$Q_{max} = \dot{m}_{ox} c_{ox} (T_{ox,out} - T_{ox,in}). \quad (11.23)$$

Examination of (11.23) lets us indicate the following ways for increasing the heat-absorption capacity of the coolant:

- a) lower the temperature  $T_{ox,in}$ , i.e., use a coolant in the supercooled state;
- b) use both propellant components as the coolant.

In a number of cases, with insufficient heat-absorption capacity of the coolant we seek ways of lowering the heat fluxes to the chamber walls, i.e., reduce the value of  $\sum_{l=1}^{l=n} Q_l / c_{ox,l}$ .

### §11.11. Structural features of chamber cooling systems

In the previous sections we examined basically external circulation cooling. Using this cooling method, the heat fluxes are removed from the chamber walls using a coolant flowing through a cooling loop of some shape or other. After leaving the loop the coolant (propellant component) passes through the chamber head into the combustion chamber.

External circulation cooling is also called *regenerative* [*closed-cycle*] cooling, since practically all the heat entering the inner wall and removed from it by the coolant is returned to the combustion chamber and efficiently used (regenerated). In addition, preheating of the propellant component facilitates its more rapid evaporation and more complete combustion in the chamber.

External circulation cooling is only comparatively rarely used in its pure form. Usually the chamber as a whole, or at least some part of it, is additionally cooled by some other method. Such cooling is called *combination* (hybrid) cooling.

As an example, we have cooling of the main part of the chamber by external circulation cooling, while the nozzle tip is cooled by radiation.

#### Design of the chamber cooling loops

The efficiency of external circulation cooling depends essentially on the dimensions and shape of the cooling loop; these should assure the required values for coolant velocity and heat-transfer coefficient  $\alpha_{o,n}$  along the loop.

We distinguish two types of cooling loops:

- a) a smooth annular cooling loop in which the outer and inner walls of the chamber are not connected along the chamber;
- b) a cooling loop with ribbing (fins), in which the outer and

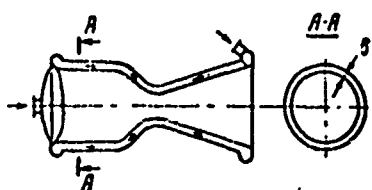


Fig. 11.4. Chamber with smooth annular cooling loop ( $\delta$  - height of the cooling-loop channel).

high coolant flow rates.

inner walls of the chamber are connected by some type of fins along the entire chamber.

A smooth annular cooling loop (Fig. 11.4) is of simple design and has low hydraulic resistance. Such a loop can be used for low pressures and rather

*Cooling loops with ribbing* are very efficient. Loops with ribbing and *axial* movement of the coolant include the following:

- a) a loop with longitudinal fins;
- b) a loop with a spacer having longitudinal corrugations;
- c) a loop made of longitudinal pipes, welded together on their sides.

Loops with ribbing and *helical* movement of the coolant include those with helical fins and those formed by helical pipes.

If the inner and outer walls are interconnected, the outer wall is relieved of much of its load. Chambers with such a cooling loop are strong and rigid, which makes it possible to use thin walls with relatively high pressure in the cooling loop. It is easier to assure high coolant velocity in ribbed loops than in smooth annular loops.

In §11.9 it was shown that fins increase the heat-transfer coefficient  $\alpha_{o,n}$ . Channels (longitudinal or helical) distribute the coolant more uniformly across the loop. Therefore, ribbed cooling loops are widely used in LPRE chambers, despite their design complexity.

*Loops with longitudinal fins* (Fig. 11.5a) are made by milling the longitudinal fins on the outer surface of the inner chamber wall and then connecting the tops of the fins to the outer wall

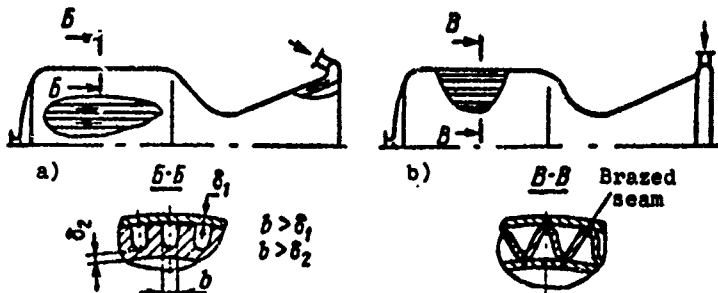


Fig. 11.5. Chambers with milled longitudinal channels (a) and corrugated spacer (b).

by seam welding or brazing.

The *loop with a corrugated spacer* (Fig. 11.5b) consists of the outer and inner walls, with a spacer and longitudinal corrugations

inserted into the annular space between them. The tops of the corrugations are brazed to the walls. The corrugated spacer makes it possible to separate the coolant flow into two flows, thus increasing the velocity of the coolant. In addition, in this case the collector for the coolant (fuel) is located not at the nozzle tip but approximately in the middle of the expanding part of the nozzle, which decreases the length of the line feeding the fuel to the chamber. In such a cooling loop a small portion of the coolant (20-30%) flows along the channels formed by the spacer and the outer chamber wall, up to the outlet section, and then along the channels formed by the spacer and the inner wall, toward the critical section. The main portion of the flow passes immediately to the critical section along the channels formed by the spacer and the outer wall. Both flows converge in a special collector at the inlet to the critical section and then uniformly enter the channels between the spacer and the outer wall, and also between the spacer and the inner wall.

*Loops made of longitudinal pipes* (Fig. 11.6) are a version of the ribbed cooling loop. The most widely used shape of the pipe cross section is rectangular or trapezoidal with rounded edges. The pipes are shaped around the chamber profile. The pipes have differing widths and cross-sectional areas.

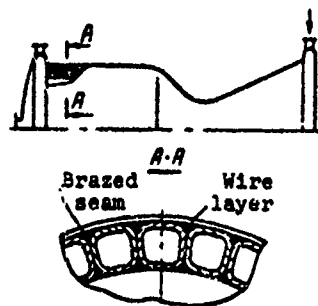


Fig. 11.6. Chamber brazed of shaped longitudinal pipes and wound with a layer of wire.

The ends of the pipes are welded into collectors for feeding and removing the coolant. One of the advantages of the pipe chamber is the possibility of introducing the coolant into the loop and removing the coolant from it at the same end. In such a chamber the feed and discharge collectors are located at the chamber head. The coolant makes two passes: in each neighboring pair of pipes the coolant passes along one pipe from the head to the nozzle, and in the other pipe - in the opposite direction.

The longitudinal walls of the pipes are brazed together, forming the chamber wall.

To increase the strength of pipe chambers, several shrouds (reinforcing rings) are positioned along them, or the chamber is wound with bands or wires of steel or high-strength alloys, or fiberglass.

Pipe chambers are very strong and rigid with relatively small mass; they can be reliably cooled as a result of the ribbing and the thin walls. In chambers with ribs or corrugated spacers the

solder can flow into the channels and clog them, while in pipe chambers this drawback is eliminated because of the location of the welded seams outside the coolant channels.

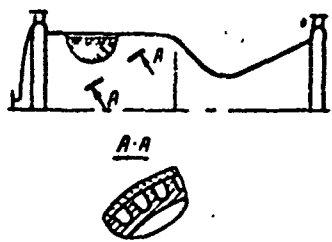


Fig. 11.7. Chamber with a cooling loop having helical channels.

heat-transfer coefficient  $\alpha_{0,n}$ . The helical channel can be single- or multiple-entry. The effect of using helical channels is that for identical values of channel height and coolant flow rate, the velocity is greater than that in a longitudinal channel; this difference increases with a decrease in the number of entries. In addition, the surface of the fins in a loop with helical channels is also larger than in a loop with longitudinal channels, which increases the efficiency of cooling even more.

However, the cooling loop with helical channels is characterized by high hydraulic resistance and complications in making the channels, particularly in chamber sections with variable cross section. Therefore, such cooling loops are used on only the most thermally-stressed parts of the chamber, mainly the region of the critical section.

Chambers with helical pipes have not been widely accepted because of the considerable hydraulic resistance and the difficulty of assuring a smooth contour of the inner surface (along the generatrix of the chamber).

#### Methods of reducing heat fluxes to the chamber wall

Heat fluxes from the combustion products to the chamber wall can be reduced by using internal cooling or a layer of heat-insulating material coated onto the inner surface of the chamber wall.

*Internal cooling.* Cooling in which the coolant is introduced into the chamber and creates a boundary layer of gas with reduced temperature is called internal, or film, cooling.

For the required lowering of the boundary-layer temperature, the flow rate of the fed fuel is less than the required oxidizer flow. This can be explained by the greater steepness of the curve of the function  $T_{gas} = f(\alpha_{OK})$  in the region  $\alpha_{OK} < 1$  than in the region  $\alpha_{OK} > 1$  (Fig. 11.8). In addition, the working conditions of a heated surface of the chamber wall are better in a reducing than an oxidizing medium.

Fig. 11.8. Dependence of temperature of the combustion products of the propellant  $O_2 +$  kerosene on the coefficient  $\alpha_{OK}$ .

The coolant used for internal cooling should have high heat capacity in the liquid and gaseous states, and also high values of the boiling point, the heat of evaporation, and dissociation.

The efficiency of internal cooling increases if only gaseous products with low molecular mass are formed upon decomposition of the coolant. A number of fuels ( $H_2$ ,  $NH_3$ , MMH, and others) satisfy this requirement to a considerable extent. The chemical energy of the propellant component that is excess in the boundary layer is not completely used. Therefore, internal cooling decreases the specific impulse of the chamber to a certain extent.

The coolant used for internal cooling (the fuel) is fed onto the heated surface of the chamber wall by the following methods:

- through auxiliary fuel injectors located on the periphery of the chamber head;
- through screen bands;
- through bands of porous inserts.

The first method is the simplest, designwise; it is usually used in combination with the second method (with the screen band). This is explained by the fact that the boundary layer with excess coolant is displaced, as it moves from the head to the nozzle, with the combustion products.

Usually, there are no more than three screen bands; they are positioned ahead of the thermally-stressed sections of the chamber,

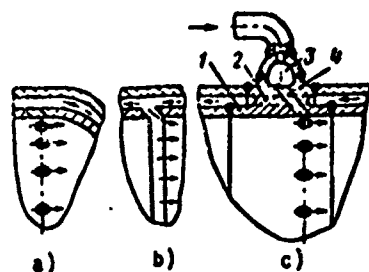


Fig. 11.9. Diagrams of coolant input to the chamber for setting up internal cooling: a - through the band of openings in the inner wall; b - through the slotted screen band; c - through openings in the screen ring. 1 - screen ring; 2 - longitudinal openings; 3 - screen collector; 4 - screen openings.

The screen bands consist of a number of fine and, for the most part, tangential (to the chamber cylinder) openings located about the periphery in a given section of the chamber, or an annular slot (Fig. 11.9).

The coolant is fed to the openings of the bands directly from the cooling loop or the collector, to which special lines are fed (see Fig. 11.9). In the latter case, the screen ring has two groups of openings

staggered about the periphery. The coolant is fed into the chamber through the radial (or tangential) openings, those of the screen band. Axial openings (in Fig. 11.9c the dashed line shows one such opening) assure coolant flow along the cooling loop through the screen ring.

Low-thrust LPRE chambers (50-5000 N [ $\approx$ 5-500 kgf]), including those with multiple ignition, can also be cooled by internal cooling (without external circulation cooling). The cooling efficiency depends on the properties of the propellant components (particularly the component used as the coolant), and also on the heat resistance of the chamber wall material. The lower the temperature of the combustion products, the more efficient the coolant and the lower the required coolant flow rate and its associated losses in specific impulse.

The terminal section of the nozzle of the chamber of certain LPRE's (e.g., the F-1) is cooled by the working fluid of the turbine, which is introduced into the nozzle through a collector which is far enough away from the outlet section of the nozzle to assure that the pressure of the working fluid will be greater than that of the combustion products in the given nozzle section. Gas is fed from the collector to the nozzle through several slotted screen bands or bands with tangential openings (tangential gas feed increases cooling efficiency).

With screen cooling, the terminal section of the nozzle can be made of ordinary stainless steel, including those for LPRE's with multiple ignition and a considerable total operating time. A certain disadvantage of such cooling is the need for raising the pressure at the turbine exit, which reduces the power developed by it (see §13.13).

The coolant can be fed into the chamber through a wall made of a porous material. In this case the coolant, under pressure, continuously enters the numerous fine pores uniformly distributed

throughout the wall and creates, on the heated wall surface, a layer of liquid or vaporized coolant. Such cooling is called *porous*.

The difficulties in creating a chamber with porous cooling are explained by the complexities in obtaining uniform wall porosity, the low strength of porous materials, and the possibility that the pores will become clogged during engine operation. Therefore, it is advisable to use such cooling only for chambers that have high thermal stresses.

*Coating a layer of heat-insulating material on the inner surface of the chamber.* The effect created by using a layer of heat-insulating material as a supplement to external circulation cooling is as follows. If the heat-insulating materials have a high melting point, there can be high heating of the surface of its layer in contact with the combustion products, which decreases the heat fluxes to the wall and heating of the coolant in the cooling loop. In addition, because of the low coefficient of thermal conductivity, the temperature of the layer of heat-insulating material drops abruptly with thickness. Therefore, the temperature of the wall surface onto which this layer is coated is noticeably lower than that of a chamber without heat insulation (Fig. 11.10).

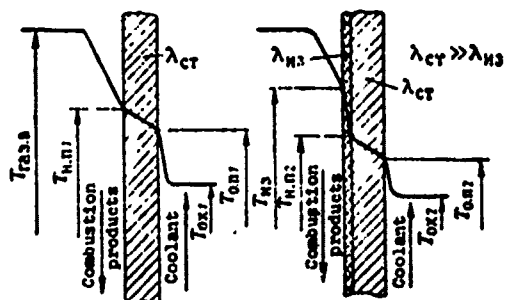


Fig. 11.10. Graphs of the distribution of temperature throughout the wall of a chamber with and without a layer of thermal insulation.

Heat-insulating materials include the oxides of refractory metals (zirconium dioxide  $ZrO_2$ , magnesium oxide  $MgO$ , aluminum oxide  $Al_2O_3$ ) and their carbides, molybdenum disulfide  $MoSi_2$ , etc.

The thickness of a layer of such materials, applied most often by the method of plasma spraying,

is 0.3-0.6 mm. For better adhesion of the layer to the chamber surface, the surface is first coated with a sublayer of chromium or nickel up to 0.1 mm thick.

Heat-insulating coatings of zirconium dioxide and molybdenum disulfide are the ones that have been best developed.

The heat-insulating layer operates under severe conditions. Therefore, it is very difficult to create a chamber with a layer of heat insulation; cracks and pitting often occur in a number of sections of such a layer. Coating a layer of heat insulation onto the inner surface of the chamber complicates its manufacture and increases its cost and mass.

#### **Other methods of cooling chamber walls**

Let us examine ablation and radiation cooling of the terminal section of a nozzle or of the entire chamber.

*Ablation cooling.* Ablation cooling is the name given to cooling accomplished by a layer of material coated onto the inner surface of the chamber and subjected to so-called ablation during chamber operation. *Ablation* is a complex group of processes occurring with the absorption of heat and leading to destruction of the surface layer. Such processes include those with phase conversions (melting, vaporization, sublimation) and decomposition processes; the heat expended on these processes is called the *heat of ablation*. Ablation results in the formation of gaseous and solid products which create a boundary layer with reduced temperature and are carried off by the flow of the combustion products. Therefore, the thickness of the layer of material coated onto the wall continually decreases during chamber operation.

Material subjected to ablation is called *ablating* (or disintegrating) material.

The heat fluxes entering the layer of ablating material are used basically to support ablation, so that the heat flux that passes through the layer of ablating material is not great. A relatively

low temperature (several hundreds of degrees), depending on the composition of the ablating material, is established on the surface of this layer.

The ablating material can be fibers or fabric made of silicon oxide, graphite, carbon, asbestos, or quartz impregnated with phenolic resin. Chambers with ablation cooling have a number of advantages over chambers with external circulation cooling, including

- a) the absence of a cooling loop, which simplifies chamber design, lowers the hydraulic losses in the line of one of the propellant components, and reduces the possibility of its freezing in outer space;
- b) the permissibility of a substantially greater change in coefficient  $\mu$ , the temperature of the propellant components, and the pressure of the combustion products (and, consequently, chamber thrust) under reliable cooling conditions.

However, chambers with ablation cooling have the following inherent and substantial drawbacks:

- a) limitation on the value of specific impulse; as it increases the thickness (and, consequently, the mass) of the layer of ablating material should be increased;
- b) limitation on the engine operating time; a thick layer of ablating material is required for prolonged engine operation;
- c) the need for considering an increase in nozzle cross-sectional area (particularly the throat) caused by decreased thickness of the layer of ablating material.

Ablation cooling is mainly used for chambers with low thrust and pressure  $p_K$ .

*Radiation cooling.* With radiation cooling, the heat from the chamber walls is removed to the ambient space by radiation. The heat fluxes passing through the wall of such a chamber and radiated

into ambient space are comparatively low. Therefore, in accordance with equation (11.14), the wall can have a rather high temperature (up to 1800°K and higher).

Chambers with radiation cooling are characterized by long (up to 60 seconds and longer) periods of operation in the nonsteady-state cooling regime. At the end of this period, equilibrium temperature of the wall is established, since the heat fluxes entering the wall and removed from it are equal.

The use of radiation cooling in a number of cases makes it possible to substantially decrease the mass of the chamber (compared not only with other chambers but also with a chamber having ablation cooling), particularly with prolonged engine operation time.

Disadvantages of radiation cooling include the need for using expensive refractory alloys from which it is difficult to make parts. In addition, these alloys are brittle and chemically are not very stable to combustion products. To prevent oxidation of such alloys by the combustion products, the inner wall of the chamber is coated with a special covering; e.g., a wall of niobium alloy is coated with a layer of organosilicon compounds.

In a number of cases, the coating not only protects the wall surface against oxidation but increases its radiating capacity, which makes it possible to additionally lower the wall temperature. Such properties are exhibited, in particular, by a layer of aluminum oxide coated onto the surface of a nickel-alloy wall.

*Uncooled chambers with massive walls.* Normal chamber operating conditions can be assured by utilizing the heat capacity of the wall material. If the chamber wall has great mass and its material has high heat capacity and thermal conductivity, the wall can absorb heat fluxes distributed over the entire mass until the temperature of the wall reaches the maximum value allowed for the given material. Such chambers (they are also called uncooled, or cooled using "sponge" cooling) are used mainly in bench-test LPRE's.

## CHAPTER XII

### THE CHAMBERS OF LIQUID-PROPELLANT ROCKET ENGINES

#### §12.1. The general characteristics of chambers

The LPRE chamber is its basic and most thermally-stressed unit; to a considerable extent it determines the development and reliability of the engine and the power plant as a whole.

The chamber of an LPRE operating on the scheme "liquid-liquid" consists of a head, a combustion chamber, and a nozzle.

The *head* should introduce the propellant components into the chamber such that the chemical reactions of their interaction occur completely and within a short period of time.

Vaporization, blending of the propellant components, and their combustion (decomposition) occur in the *combustion* (decomposition) *chamber*. The volume of the combustion chamber should be as small as possible, but sufficient to assure complete combustion of the propellant components before entering the nozzle. The combustion-chamber volume is measured from the inside (fire plate) of the head to the critical section. The length of the combustion chamber also influences the completeness of burning of the propellant components, but to a lesser extent than does the volume.

The nozzle accelerates the combustion products up to maximum velocity to produce high chamber specific impulse.

The most widely used type of chamber for bipropellant LPRE's operating on the scheme "liquid-liquid" is a cylindrical chamber with a cooling loop and a head having three faces (Fig. 12.1). The oxidizer is fed through inlet pipe 1 to cavity a between the outside of the head 2 and the head midsection 3; from here it goes through injectors 11 into the combustion chamber.

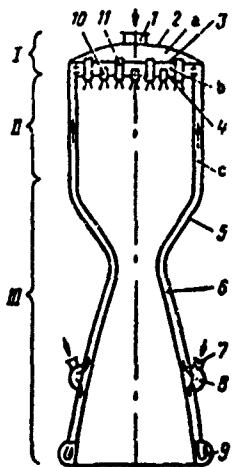


Fig. 12.1. Diagram of a cylindrical chamber with a cooling loop: 1 - head; II - combustion chamber; III - nozzle; 1 - oxidizer inlet pipe; 2 - outside of head; 3 - midsection of head; 4 - inside (fire plate) of head; 5 - outer wall; 6 - inner wall; 7 - fuel inlet pipe; 8 - fuel input collector; 9 - fuel swivel collector; 10 - fuel injector; 11 - oxidizer injector.

The fuel passes through inlet pipes 1 (there are usually two of them) into collector 8 which is usually positioned some distance away from the nozzle outlet section (see §11.11). Flowing along the collector, the fuel enters cooling loop c formed by outer wall 5 and inner wall 6 of the chamber. The fuel flow is divided into two parts: the main portion is fed to the chamber head, while the remainder goes to swivel collector 9 at the end of the nozzle; the collector turns, and the fuel is fed along the appropriate channels, also to the head. From the cooling loop the fuel is fed to cavity b between head midsection 3 and fire plate 4, and from this cavity it goes through injectors 10 into the combustion chamber.

The chamber of LPRE's operating on the scheme "gas-liquid" and "gas-gas" consists of a head, an afterburner (in some cases a combustion chamber), and nozzle.

As was shown in §9.1, for the scheme "gas-liquid" the afterburner is fed generator gas and the liquid propellant component, while for the scheme "gas-gas" it is fed the reducing and oxidizing gases from the liquid gasifier.

When designing and building a chamber, the following are the main considerations:

- a) high reliability;
- b) high specific impulse;
- c) low mass with sufficient strength;
- d) small size, particularly length, since the length of the chamber determines the length of the engine as a whole.

LPRE chambers differ from one another in the shape of the combustion chamber, the type of head and the injectors used in it, the type of nozzle (see Chapter VI), the method of cooling (see Chapter IX), and other features.

#### §12.2. Shapes of the combustion chamber (afterburner)

Combustion chambers (afterburners) are divided by geometric shape into cylindrical, shaped, spherical, and annular (Fig. 12.2).

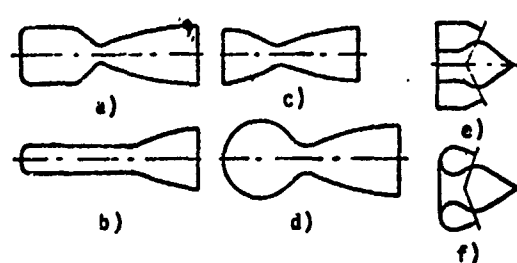


Fig. 12.2. Combustion chamber shapes: a - cylindrical; b - semi-elliptical nozzle; c - in the form of a shaped convergent section; d - spherical; e - annular cylindrical, with central body; f - annular toroidal, with central body.

*Cylindrical* combustion chambers (Fig. 12.3) are the most widely used for engines having the most diverse thrusts. They are simple to design and uncomplicated to manufacture. The constancy of the cross-sectional area along such chambers makes it possible to organize efficient combustion of

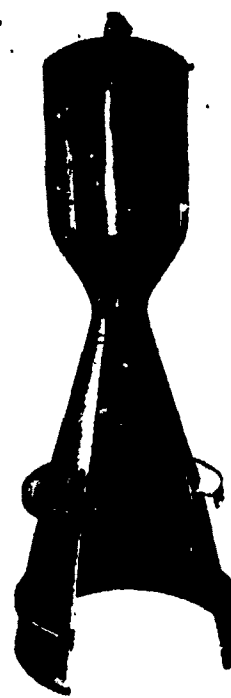


Fig. 12.3. Chamber of the RD-107 "Vostok" LPRE.

the propellant components; in particular, the formation of stagnation zones, in which combustion does not occur, is eliminated. The relatively small outside diameter of cylindrical combustion chambers facilitates their use in multichamber LPRE's or in power plants consisting of several single-chamber engines.

The drawbacks of cylindrical chambers as compared with spherical ones are as follows:

- a) reduced strength characteristics, forcing an increase in wall thickness;
- b) greater hydraulic resistance of the cooling loop;
- c) increased wall surface which must be cooled.

Two types of chambers can be distinguished: pressure and velocity. Pressure chambers are those in which the pressure of the combustion products remains approximately constant along the chamber; the ratio of the cross-sectional area to that of the critical section for such chambers  $f_K/f_{Kp} > 3$ .

This ratio is called the *relative area* of the combustion chamber and is designated by  $\bar{f}_K$ , i.e.,

$$\bar{f}_K = \frac{f_K}{f_{Kp}}. \quad (12.1)$$

Chambers with  $\bar{f}_K < 3$  are called *velocity* chambers. They have so-called *thermal resistance*: the gas stagnation pressure at the end of such combustion chambers is less than at the beginning; this effect is caused by the feeding of heat to the gas flow moving in a cylindrical tube [28]. With a decrease in  $\bar{f}_K$ , the velocity of the gas and the thermal resistance of the chamber increase, resulting in a corresponding decrease in its specific impulse. In addition, with an increase in the velocity of the combustion products there are increased pressure losses due to friction with movement in the combustion chamber. Therefore, to assure identical pressure of the combustion products at the nozzle inlet, with a decrease in  $\bar{f}_K$  there must be a corresponding increase in the pressure at which the com-

ponents are fed to the combustion chamber.

Limited use is made of cylindrical combustion chambers in which the value of  $\bar{F}_H$  is equal to one (see Fig. 12.2b); these are called *semi-thermal nozzles*.

As LPRE's are improved, the pressure  $p_H$  is raised, chamber cooling and head design are improved and the outside diameter is simultaneously decreased, and new propellant components and structural materials are used. This entails a decrease in chamber volume and an increase in nozzle size.

Some use is made of *shaped* convergent combustion chambers, in which there is simultaneous combustion of the propellant components and acceleration of the combustion products to critical velocity (see Fig. 12.2c).

*Spherical* combustion chambers (see Fig. 12.2d) have the least surface for a given volume, which facilitates chamber cooling and allows its mass to be decreased, also as a result of thinner required thickness of the walls. However, in such combustion chambers it is most difficult to assure uniform distribution of the flow rate of the combustion products across the chamber, while stagnant zones can form in the region of the head.

*Pear-shaped* and *elliptical* combustion chambers can be used in addition to spherical ones. The injectors for such chambers are located on a flat plate or in precombustion chambers, which makes it possible to increase the injector-placement surface.

Because of the relative complexity of design and the technology of manufacturing spherical combustion chambers, and the fact that they have no appreciable advantages over cylindrical ones, spherical chambers have been used only to a limited extent in LPRE's.

*Annular* combustion chambers are shaped like rings (Fig. 12.2e) or toruses (Fig. 12.2f).

Annular combustion chambers together with an external-expansion nozzle (or a nozzle with a central body) have a number of substantial advantages over the ordinary chambers. The basic ones are examined in Chapter VI. Other advantages include convenience in positioning the units of the propellant-component feed system inside the central body of the chamber and the possibility of creating forces to control the flight of the rocket vehicle (with sectional design of the combustion chamber).

Maximum efficiency for LPRE's with annular combustion chambers is assured by their operation on high-energy propellants (mainly  $O_2 + H_2$  or  $F_2 + H_2$ ).

### §12.3. Injectors

The liquid propellant components are fed into the combustion chamber through injectors which atomize the propellant components with a significant increase in the surface of the drops.

There are two basic types of injectors - jet and centrifugal.

Jet injectors are small precisely-made openings in the fire plate of the head. Such injectors can also be made as individual items and then be welded to the head; in this case the injectors are practically identical.

Jet injectors spray the fluid in the form of parallel or impinging jets (Fig. 12.4).

The outlet opening of the injector is called the nozzle. The fluid jet emerging from the nozzle is, at some distance from it, a solid cone with small ( $5-20^\circ$ ) apex angle. The jet is broken down into small drops as a result of friction of the jet against the combustion products and the transverse oscillations arising in it.

The basic advantage of a head with jet injectors is its relative simplicity and high throughput.

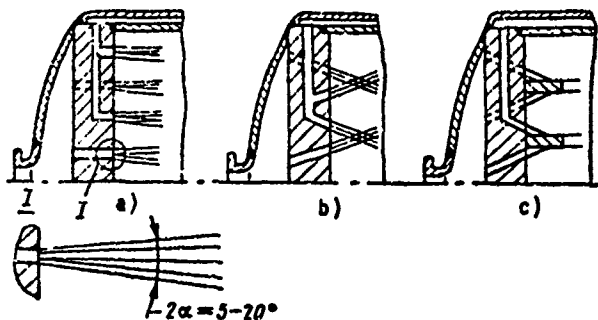


Fig. 12.4. Flat injector heads with jet injectors:  
a - with parallel jets; b - with impinging jets;  
c - with reflecting plates.

placed per unit surface of the head as compared with centrifugal injectors. In addition, the flow coefficient of jet injectors (see p. 86) is 2.5-3.0 times greater than that of centrifugal injectors. Jet injectors assure a relatively greater hitting range of the jets and a wider spray than the centrifugal injectors provide.

Injectors with impinging jets (see Fig. 12.4b) give a finer spray and a shorter spray zone than injectors with parallel jets. But the throughput of a head with impinging jets is less than for a head with parallel jets.

The group of injectors with impinging jets can consist of two, three, four, or five jet injectors; here we can use:

- a) oxidizer injector units;
- b) fuel injector units;
- c) units with oxidizer and fuel injectors; in a number of cases these insure better characteristics as compared with the other two.

An injector unit containing only oxidizer injectors or only fuel injectors is actually a *single-component* injector, while an oxidizer-and-fuel injector unit is a *two-component* injector.

Jets of oxidizer and fuel can be fed to a flat reflecting plate (see Fig. 12.4c); the thin fluid films that form as the pro-

The *throughput* of a head is the flow rate of the propellant components passing across a unit of surface of its plate with a given pressure differential in the injector. The jet injector is smaller than the centrifugal one. Therefore, a greater number of jet injectors can be

pellant component jet flows over the plate run together, assuring good breakup and mixing

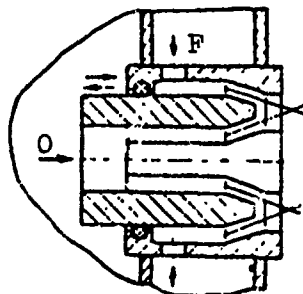


Fig. 12.5. Two-component slotted injector with impinging cones and variable injection area (the mechanism for moving the rod is not shown).

One version of the jet injector is the *slotted* injector; its nozzle has the shape of an annular slot, not a circle.

In two-component-slotted injectors (Fig. 12.5) the annular slots are angled to the injector axis, so that the jets of liquid collide with one another in the form of two hollow spray cones.

Jet injectors are most often used for hypergolic propellants, and also for chambers with small head area. They are more suitable for atomizing propellant components having relatively low viscosity.

*Centrifugal* injectors are those in which twisting of the liquid occurs; the jets of liquid coming from the nozzles are thin conical films with vertex angles of up to  $120^\circ$  that easily break down into very fine drops.

Centrifugal injectors are divided into tangential and screw-type. In *tangential* injectors (Fig. 12.6b) the liquid is twisted by passing it through one or several tangential openings, i.e., openings whose axes are tangent to the cylinder of the inner cavity, called the *twisting chamber*.

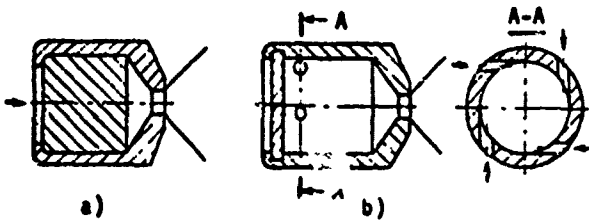


Fig. 12.6. Centrifugal injectors: a - screw (with swirl); b - tangential.

In *screw-type* injectors (or injectors with swirlers) (see Fig. 12.6a) the liquid is twisted by moving it along helical channels cut in the screw (or swirler); the liquid enters them from the back of the screw.

Centrifugal injectors assure a finer atomization and a shorter spray zone than do jet injectors. Disadvantages include relative structural complexity and low throughput.

Centrifugal injectors, like jet injectors, can be divided into *single-component* and *two-component* injectors. In two-component centrifugal injectors (Fig. 12.7) the propellant components are mixed both inside the injector (internal mixing) as well as outside it (external mixing). Injectors with internal mixing are often used for chambers operating on nonhypergolic propellants.

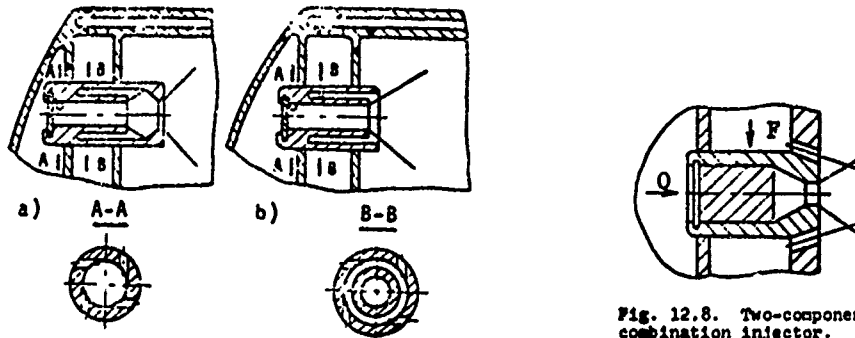


Fig. 12.7. Two-component centrifugal injectors: a - with internal displacement; b - with external displacement.

Combination two-component injectors combine jet and centrifugal injectors; in the injector shown in Fig. 12.8 the slotted fuel injector is placed around the centrifugal oxidizer screw injector.

Screw-type injectors are examples of combination injectors; in these there is an axial opening, the jet injector, with a small spray cone and a great hitting range.

The use of two-component injectors reduces the length of the spray zone, since the propellant components are mainly mixed in the liquid phase and therefore burn more rapidly. In addition, the throughput of a head with two-component injectors is higher than that of a head with single-component centrifugal injectors.

However, two-component injectors are structurally quite complex; use of them leads to more severe temperature conditions for head operation, since the flame front is closer to the head because of the reduced length of the spray zone.

The flow rate of propellant component through a single-component injector is within the limits of 30-300 g/s, while for two-component injectors it can reach 2.5-3 kg/s. Peripheral injectors usually have a greater hitting range and a 20-30% lower flow rate as compared with the main injectors. Flow through the oxidizer injectors located on the periphery of the head is also less than the flow through the main injectors.

All the above-examined injectors have *fixed nozzle area*. For engines whose thrust must be changed over a wide range, injectors with *variable nozzle area* are used; in these, the pressure differential can be kept approximately constant with a substantial decrease in flow rate of the propellant components. The area of a nozzle in such injectors can be changed by moving a special rod within the injector along its axis and closing off the injector nozzle to some extent. In a two-component slotted injector, the moving of one rod changes the area of the oxidizer and fuel nozzles (see Fig. 12.5). It is possible to use other designs for injectors with variable nozzle area.

#### §12.4. Chamber heads

The chamber head serves for introduction and uniform distribution of the propellant components across the combustion chamber.

For efficient vaporization, mixing, and combustion of the propellant components, and reliable chamber operation, the head should assure

- a) a fine uniform spray of the propellant components, i.e., their atomization into fine particles whose dimensions differ as little as possible from one another;

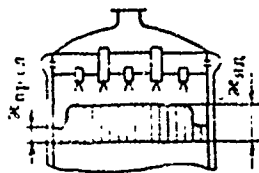


Fig. 12.9. Graph of the change in coefficient  $n$  along the radius of the combustion chamber  $r_n$  ( $n_{nA}$  and  $n_{np, ch}$  are coefficients  $n$  for the flow core of the combustion products and the boundary layer, respectively).

b) identical value of coefficient  $n$  over the entire cross section except for the boundary layer (Fig. 12.9).

The value of coefficient  $n$  in the boundary layer, corresponding to fuel excess, should also be as constant as possible around the combustion chamber.

To satisfy these conditions, the greatest possible number of injectors must be appropriately positioned on the head.

An important requirement imposed on the chamber head is uniform flow intensity of the propellant components over the entire combustion chamber cross section.

The *average cross-sectional flow intensity* of a combustion chamber is the ratio of the per-second flow rate of the propellant components to the area of its section:

$$r = \dot{m}/f_n, \text{ kg/m}^2 \cdot \text{s.} \quad (12.2)$$

For a section of chamber with area  $\Delta f_i$  through which the flow rate of the propellant components is  $\Delta \dot{m}_i$ , the *local flow intensity*

$$r_i = \Delta \dot{m}_i / \Delta f_i.$$

The hydraulic losses associated with feed of the propellant components to the head injectors should be low. In addition, the head should be rather strong and rigid, despite the weakening of its face with a large number of openings for the injectors; it should also assure smooth start-up of the chamber (see §14.1) and stable burning in it (see §15.1).

Flat heads are the ones most widely used (see Fig. 12.3). These employ jet injectors with parallel or impinging jets (see Fig. 12.4), and also centrifugal injectors (see Fig. 12.7).

Flat heads are simple to design, not complicated to manufacture, and allow uniform flow intensity across the section and required distribution of coefficient  $\mu$  along the radius of the combustion chamber.

A certain disadvantage of flat heads is their relatively low strength and rigidity. This is particularly true for chambers with large diameter; therefore, annular and radial stiffeners are welded between their outer and middle faces, while the outer face is made in the form of a section of a sphere (see Fig. 12.3).

One of the ways of maintaining the necessary conditions of atomization and stable burning of the propellant in the combustion chamber with a considerable decrease in propellant flow and with fixed injector nozzle area is to feed an inert gas into the head cavity (i.e., directly into the propellant components). In this case, special grids are installed ahead of the injectors for uniform distribution and mixing of the liquid propellant components and the bubbles of inert gas.

The design of the head does much to determine the reliability and specific impulse of the chamber and the engine as a whole. With unsuccessful head designs we note the following chamber flaws and undesirable consequences:

- 1) erosion or burnout of the chamber walls, mainly in the critical section, and also excessive heat fluxes to the walls, attested to by traces of local overheatings of the wall;
- 2) erosion of the inner surface of the fire plate and the ends of the injectors due to the action of the hot combustion products on them;
- 3) unstable propellant burning;
- 4) reduced chamber specific impulse.

The influence of the head on the specific impulse and stability of the burning process increases with decreasing chamber dimensions and thrust.

To reduce the heat fluxes to the chamber walls a boundary layer of combustion products with reduced temperature is formed, as was shown in §11.11.

To eliminate erosion of the inner surface of the fire plate and the ends of the injectors we increase the number of fuel injectors at the points of erosion, we use a porous material for producing the fire plate and the injector housings, or we coat them with a layer of heat-insulating material.

The processes of atomization of the propellant components, as well as their vaporization, mixing, and combustion, have still not been investigated to the extent that it is possible to theoretically determine the optimum type of head. Therefore, when developing an engine we must test several versions of small-scale models and full-size heads, including fire-tests of the heads in the chamber.

For the initial tests we often select heads which provide only moderate specific impulse, but which are most reliable. This makes it possible to test the engine as a whole in parallel with final adjustment of the head and chamber. During final alignment, the head finally selected is that whose design makes it possible to obtain maximum specific impulse with stable propellant burning.

In a vast number of cases, the required burning stability and reliable chamber cooling are achieved only at the expense of a slight reduction in specific impulse.

Finalizing the design of a head is a complex and expensive stage in the creation of an engine.

#### §12.5. Ways of positioning the injectors on flat heads

Uniform distribution of oxidizer and fuel across the combustion chamber is achieved by appropriate placement of the injectors on the head. There are several ways of doing this: staggered, honeycomb, in concentric circles, and in groups.

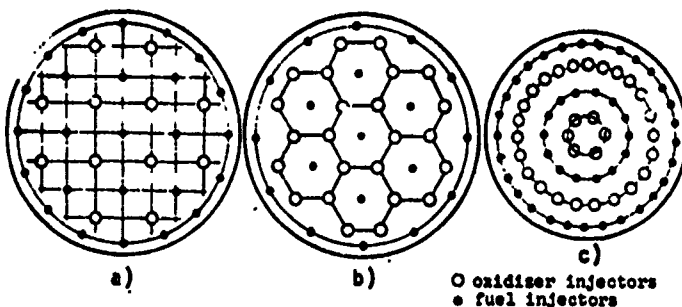


Fig. 12.10. Types of injector placement on flat heads: a - staggered; b - honeycomb; c - in concentric circles.

times that of the fuel, with staggered placement the flow rates through the fuel and oxidizer injectors differ considerably, which has an unfavorable influence on mixing.

With *honeycomb* placement (Fig. 12.10b), each fuel injector is surrounded by several oxidizer injectors: for each fuel injector there are two ( $6 \times 1/3$ ) oxidizer injectors. The flow rates through the injectors differ relatively slightly, which improves the mixing of the propellant components.

When the injectors are placed in *concentric circles* (see Fig. 12.10c), the head contains alternating circles of fuel injectors and oxidizer injectors. The peripheral circle contains fuel injectors, creating a boundary layer of reduced temperature.

With *group* arrangement the injectors are formed into groups containing a specific number of oxidizer and fuel injectors (e.g., in a 4:1 or 3:2 ratio) in identical mutual arrangements.

Two-component injectors are usually arranged in concentric circles.

The distance between centrifugal injectors is determined by the dimensions of the injector itself, and also by head strength conditions, the strength being reduced by the holes for the injectors.

With *staggered* positioning (Fig. 12.10a) of the fuel and oxidizer injectors, there are approximately the same number of each: for one fuel injector there is one ( $4 \times 1/4$ ) oxidizer injector. Since the mass flow rate of oxidizer is usually 2-4

This distance is usually 12-30 mm. The jet injectors are located much closer together - 3-4 mm.

#### §12.6. Calculating a chamber head

To calculate a head we must know the following:

- 1) the density and viscosity of the propellant components at the rated temperature at which they enter the injectors;
- 2) the total oxidizer and fuel flow rates;
- 3) the diameter of the chamber head; for a cylindrical chamber this equals the diameter of the combustion chamber;
- 4) the pressure differential at the injectors  $\Delta p_\phi$ , i.e., the difference in pressures in the oxidizer or fuel cavities of the head and in the combustion chamber.

The pressure differential in the injectors is usually selected within the limits of 3-5 bars [ $\approx 3-5 \text{ kgf/cm}^2$ ], and in certain LPRE's it can be up to 30 bars [ $\approx 30 \text{ kgf/cm}^2$ ]. With low pressure differentials, atomization of the propellant components is worsened and the burning process becomes unstable. On the other hand, an excessive increase in the value of  $\Delta p_\phi$ , without substantially worsening the atomization of the propellant components, makes it necessary to increase the power of the feed system.

In LPRE's with a wide range of change of propellant flow rate it is necessary to select high pressure differentials in the injectors, in order that the necessary atomization of the propellant jet be achieved when operating with low flow rate (and, consequently, a low value of  $\Delta p_\phi$ ).

The number of oxidizer and fuel injectors that can be positioned on the head with a given diameter is determined graphically, selecting the method of arranging the injectors and the distances between them (see §12.5).

Let us introduce the following designations:  $n_{OK}$  and  $n_f$  – the number of oxidizer and fuel injectors;  $\dot{m}_{OK,\phi}$  and  $\dot{m}_{f,\phi}$  – the per-second flow rate through the oxidizer injector and the fuel injector.

The values of  $\dot{m}_{OK,\phi}$  and  $\dot{m}_{f,\phi}$  are defined by the formulas

$$\dot{m}_{OK,\phi} = \frac{\dot{m}_{OK}}{n_{OK}}; \quad \dot{m}_{f,\phi} = \frac{\dot{m}_f}{n_f},$$

where  $\dot{m}_{OK}$  and  $\dot{m}_f$  are the per-second flow rates of oxidizer and fuel through the chamber head; these are known from its thermal calculation.

#### Calculating the jet injector

Let us use the following formulas, known from hydraulics, for the discharge of an incompressible fluid from an aperture:

$$W = \sqrt{\frac{2\Delta p_\phi}{\rho}}; \quad (12.3)$$

$$\dot{m} = \mu W f \rho, \quad (12.4)$$

where  $W$  is the velocity of injection of the liquid propellant component into the combustion chamber – usually  $W = 15-40$  m/s;  $\dot{m}$  is the per-second flow rate of liquid propellant component through the head;  $f$  is the total area of the injector nozzles;  $\mu$  is the flow-rate coefficient, taking into account the constriction of the jet and a decrease in the true velocity of injection compared with the theoretical, because of hydraulic resistances.

The flow-rate coefficient  $\mu$  of a jet injector is a function of the following factors:

- a) the geometry of the inlet edge of the opening; for a sharp edge, particularly with projecting edges, coefficient  $\mu$  is less than for a bevelled or smoothly rounded edge;
- b) the surface finish of the opening; very rough opening walls lead to a substantial reduction in  $\mu$ ;
- c) the ratio of injector length  $l_\phi$  to its nozzle diameter  $d_c$ , i.e., the ratio  $l_\phi/d_c$ .

With a sharp inlet edge and ratio  $l_\phi/d_c = 0.5-1.0$ , the flow coefficient  $\mu$  is 0.60-0.65. With an increase in the ratio  $l_\phi/d_c$  to 2-3, the value of  $\mu$  rises to 0.75-0.85; the losses to friction simultaneously increase. It is advisable to select those geometric characteristics of a jet injector which assure maximum flow coefficient. The injector opening shown in Fig. 12.11 satisfies this condition.



Fig. 12.11. Injector opening assuring maximum flow coefficient ( $\mu = 0.85-0.90$  when  $l_\phi/d_c > 3$ ).

To determine the area of fuel or oxidizer injection, let us substitute into equation (12.4) the expression for  $W$  from formula (12.3):

$$\dot{m} = \mu f \sqrt{2 \Delta p_\phi \rho}, \quad (12.5)$$

from which

$$f = \frac{\dot{m}}{\mu \sqrt{2 \Delta p_\phi \rho}}. \quad (12.6)$$

The diameter of the injector nozzle is usually selected within the limits  $d_c = 0.5-3.0$  mm. Smaller-diameter nozzles are difficult to engineer and, in addition, they can become clogged. However, studies have been run on microinjectors ( $d_c < 0.25$  mm) which assure best mixing of the propellant components and their more complete burning. When  $d_c > 3.0$  mm it is difficult to obtain fine atomization of the jet coming from the injector nozzle.

Having determined, by the graphic method examined above, the number of oxidizer and fuel injectors, we can calculate the area of their openings (nozzles):

$$f_{ox,t} = \frac{f_{ox}}{n_{ox}}; \quad f_{r,t} = \frac{f_r}{n_r}.$$

For a head with impinging oxidizer and fuel jets the angles  $\alpha_{ox}$  and  $\alpha_r$  (Fig. 12.12) are selected such that the resulting jets are parallel to the chamber axis. Since the flow rates through the oxidizer and fuel injectors, and also their spray velocities, differ from one another, the above-indicated condition reduces to

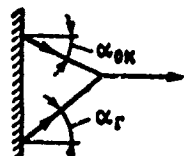


Fig. 12.12. Diagram of the impinging of oxidizer and fuel jets.

an equality resulting from the law of conservation of momentum:

$$\dot{m}_{r,k} W_{nk} \sin \alpha_{nk} = \dot{m}_{r,k} W_r \sin \alpha_r. \quad (12.7)$$

One of the angles is given arbitrarily, while the other is calculated from formula (12.7).

#### Calculation of a centrifugal injector

A feature of the operation of a centrifugal injector is that the liquid does not move through the entire cross section of the injector: due to twisting of the fluid along the injector axis there arises a gas vortex with pressure equal to that of the ambient medium, i.e., the pressure in the combustion chamber. The radius of the gas vortex  $r_{r,s}$  is less than that of the injector nozzle  $r_c$ . Consequently, the liquid discharges from the injector nozzle through an annular cross section with area

$$f_a = \pi (r_c^2 - r_{r,s}^2).$$

The velocity of the liquid discharging from a centrifugal injector can be divided into the axial component  $W_a$  and the tangential component  $W_u$ .

Component  $W_a$  determines the flow rate of the liquid through the injector, while  $W_u$  defines the twisting of the liquid by the injector.

Consequently, the volume flow of liquid through the nozzle of a centrifugal injector

$$\dot{v} = W_a f_a = W_a \pi (r_c^2 - r_{r,s}^2)$$

or

$$\dot{v} = W_a \varphi \pi r_c^2,$$

where  $\varphi$  is the clear-opening coefficient, determined from the formula

$$\varphi = 1 - \frac{r_{r,s}^2}{r_c^2}.$$

The mass flow rate of the liquid through the nozzle of a centrifugal injector can be determined from a formula which, to all external appearances, is analogous to the equation of flow through a jet injector (12.5):

$$\dot{m}_\phi = \mu f_c \sqrt{2\Delta p_\phi Q},$$

from which

$$f_c = \frac{\dot{m}_\phi}{\mu \sqrt{2\Delta p_\phi Q}}. \quad (12.9)$$

The flow coefficient  $\mu$  for a centrifugal injector is a function of the clear-opening coefficient  $\phi$ , i.e., of the area of the clear opening  $f_\phi$ .

The quality of spraying of the liquid by a centrifugal injector is influenced by twisting of the liquid, which defines the spray cone angle  $2\alpha$ ; atomization of the liquid improves with an increase in this angle, but at the same time the required injector dimensions increase.

The values of  $2\alpha$ ,  $\phi$ , and  $\mu$  of a centrifugal injector are functions of its *geometric characteristic*, a complex which connects the basic dimensions of the injector. The geometric characteristic of

a centrifugal injector (Fig. 12.13) is designated by the letter  $A$ , and is defined by the following formulas:

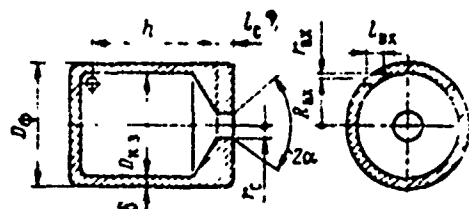


Fig. 12.13. Tangential injector (the drawing shows the basic geometric dimensions of the injector).

a) for an injector with one tangential opening

$$A = \frac{R_\phi r_c}{r_{\phi x}^2}; \quad (12.10)$$

b) for an injector with  $i$  tangential openings

$$A = \frac{R_\phi r_c}{i r_{\phi x}^2}; \quad (12.11)$$

c) for a screw-type injector

$$A = \frac{\pi R_\phi r_c}{i f_i} \sin \frac{\pi}{i}, \quad (12.12)$$

where  $R_{bx}$  is the average channel radius;  $f_1$  is the continuous section of one channel;  $i$  is the number of channels (or entries of the screw);  $\beta$  is the helix angle of the screw line.

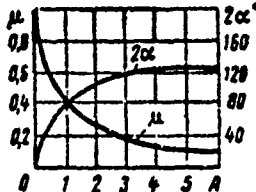


Fig. 12.14. The flow coefficient  $\mu$  and spray cone angle  $2\alpha^*$  vs. geometric characteristic  $A$ .

With an increase in  $A$ , coefficients  $\varphi$  and  $\mu$  decrease, while angle  $2\alpha$  increases.

In the limiting case (when  $A \rightarrow \infty$ ) we have

$$\varphi \rightarrow 0 \text{ and } \mu \rightarrow 0.$$

A graph of the dependence of  $\mu$  and  $2\alpha$  on the geometric characteristic is shown in Fig. 12.14.

*Consideration of the viscosity of the liquid.* The above-examined relationships are valid for a perfect fluid. The flow of a perfect fluid in a centrifugal injector is subject to the law of conservation of the moment of momentum, since the moment of the external forces acting on the fluid in the injector swirl chamber is equal to zero.

In a real fluid, friction forces arise due to the presence of viscosity forces. Their action has the result that the moment of momentum at the nozzle inlet is less than in the initial part of the injector swirl chamber, i.e., because of friction forces there is a decrease in the degree of swirl of the fluid and, as a result, the flow coefficient increases and the fluid spray angle decreases.

To take into account the viscosity of the fluid, instead of geometric characteristic  $A$  of the injector we use the equivalent characteristic  $A_{eq}$ , defined by the formula

$$A_{eq} = \frac{R_{bx} r_c}{4r_{bx}^2 + \frac{\lambda}{2} R_{bx} (R_{bx} - r_c)}. \quad (12.13)$$

Friction coefficient  $\lambda$  for conditions at the injector inlet is calculated from the equation

$$\lg \lambda = \frac{25,8}{(\lg Re_{sx})^{2,55}} - 2, \quad (12.14)$$

where  $Re_{sx}$  is the Reynolds number defined for injector inlet conditions.

The value of  $Re_{sx}$  is defined by the expression

$$Re_{sx} = \frac{4 \dot{m}_\phi}{\mu_{K.S.} \pi d_{sx} \gamma i}, \quad (12.15)$$

where  $\mu_{K.S.}$  is the coefficient of kinematic viscosity at the injector inlet.

*Sequence of the calculation.* A centrifugal injector is calculated in the following sequence.

1. Given the pressure differential in the injector  $\Delta p_\phi$  (see p. 84).
2. Select the spray cone angle  $2\alpha$  within limits  $2\alpha = 30-120^\circ$  ( $90-120^\circ$  in most cases).
3. Knowing angle  $2\alpha$ , from the graphs in Fig. 12.14 determine the geometric characteristic A and flow coefficient  $\mu$ .
4. Using equation (12.9), calculate the cross-sectional area of the injector nozzle  $f_c$ , and then the nozzle diameter from the formula

$$d_c = \sqrt{\frac{4}{\pi} f_c}$$

5. Select the dimensions of the injector.

There are usually 2-4 tangential openings or screw entries. More than 2-4 improves the distribution of flow intensity around the perimeter of the fluid jet circle.

The ratio  $R_{sx}/r_c$  is taken as approximately 2.5.

Using equation (12.11), determine radius  $r_{sx}$  from the selected

values of  $i$  and  $R_{bx}/r_c$ :

$$r_{bx} = \sqrt{\frac{R_{bx}r_c}{iA}}.$$

Usually, radius  $r_{bx}$  is selected within the limits of 0.25-1 mm.

6. From formulas (12.15) and (12.14), calculate the friction coefficient  $\lambda$  and then, from (12.13), the equivalent injector characteristic  $A_{3K}$ . If characteristics  $A$  and  $A_{3K}$  do not differ more than 5% from one another, this ends the calculation; in this case, the values of  $r_c$ ,  $R_{bx}$ , and  $r_{bx}$  of the first approximation serve as the final values.

If the discrepancy between  $A$  and  $A_{3K}$  is greater than 5%, we select as our basis the value of  $A_{3K}$  obtained in the first approximation and, from the graph given in Fig. 12.14, determine the flow coefficient  $\mu$  with consideration of viscosity, and then the dimensions  $r_c$ ,  $R_{bx}$ , and  $r_{bx}$  in the second approximation; from them we calculate the characteristic  $A_{3K}$  in second approximation. Usually the discrepancy of the values of  $A_{3K}$  obtained in the first and second approximations is insignificant, so that the dimensions  $r_c$ ,  $R_{bx}$ , and  $r_{bx}$  obtained in the second approximation can be used as final values.

7. Knowing  $r_c$ ,  $R_{bx}$ , and  $r_{bx}$ , select the remaining injector dimensions (see Fig. 12.13):

$$l_s = (1.5 - 3)d_{bx}; l_c = (0.25 - 1.0)d_c.$$

As the injector height (length)  $h$  we use the following:

- $h = R_{bx}$  and greater, for a tangential injector;
- $1/4$  to  $1/3$  the channel pitch or more, for a screw-type injector. The diameter of the swirl chamber

$$D_{s.s} = 2(R_{bx} + r_{bx}).$$

The outside diameter of the injector

$$D_o = D_{s.s} + 2\delta,$$

where  $\delta$  is the thickness of the swirl chamber wall.

The values of  $\delta$  and  $l_{sx}$  are interrelated; usually we select  $\delta = 1.5$  mm.

#### Features of the heads of afterburners

Injectors are divided into *liquid*, *gas*, and *gas-liquid*, depending on the aggregate state of the propellant component introduced into the afterburner. The term *gas-liquid* is used for two-component injectors, where one component enters in the liquid state and the other enters in the gaseous state.

Generator gas is fed into the afterburner through jet injectors.

The head of the chamber of LPRE's operating on the scheme "gas-liquid" can be a grid with radial and annular bridges; the openings serve as jet injectors for the generator gas, while the injectors for the liquid component are located at the bridge junctions.

The pressure differential in the generator-gas jet injectors is slight, while the pressure in the afterburner is high; therefore, the discharging of the gas from the injector is subcritical.

#### §12.7. Selecting the volume and relative area of combustion chambers (afterburners)

The volume of a combustion chamber (afterburner) should assure the required stay time for the propellant components, while at the same time the size and mass of the chamber should be small.

The volume of the combustion chamber is calculated from its reduced length  $l_{np}$  and the arbitrary stay time of the gas in the chamber  $\tau_{ycn}$ .

The reduced (or characteristic) length of the combustion chamber is the ratio of its volume to the area of the critical section:

$$l_{np} = \frac{V_k}{f_{np}}. \quad (12.16)$$

Time  $\tau_{ycn}$  can be obtained by dividing the mass of gas in the combustion chamber by its per-second flow rate:

$$\tau_{ycn} = \frac{m_{gas}}{\dot{m}} ;$$

disregarding the volume of the liquid propellant components in the combustion chamber and arbitrarily considering that the density of the gas is identical throughout, and equal to  $\rho_h$ , we get

$$\tau_{ycn} = \frac{V_h \rho_h}{\dot{m}} .$$

Let us substitute into this equation the expression for  $\rho_h$  from formula (4.4) and take relationships (4.14) and (12.16) into account. Then

$$\tau_{ycn} = \frac{\beta}{RT_h} l_{np} . \quad (12.17)$$

For the given propellant components and design of the head, which determined the mixing quality, ratio  $\beta/RT_h$  can be considered constant. Consequently, the arbitrary stay time of the gas in the combustion chamber and the reduced chamber length are directly proportional to one another.

The values of  $\tau_{ycn}$  and  $l_{np}$  are determined mainly by the propellant, the head design, and the type of LPRE scheme; for most engines  $\tau_{ycn} = (1.5-5.0) \cdot 10^{-3}$  s and  $l_{np} = 1.0-3.5$  m. A smaller value of  $\tau_{ycn}$  corresponds to chambers with higher pressure  $p_h$ . An increase in the reduced length of the combustion chamber brings about an increase in specific impulse, but simultaneously the chamber dimensions increase, which complicates its cooling.

For preliminary calculations, we can assume reduced lengths of 1.5-2.5, 1-1.5, and 0.5-1 m for the combustion chambers of LPRE's operating on the scheme "liquid-liquid" with propellants  $O_2 +$  kerosene,  $F_2 + NH_3$ , and  $O_2 + H_2$ , respectively [4, 17].

In LPRE's with afterburning of the generator gas, part of the propellant components first burn in the gasifier; therefore the required reduced length of their afterburners is 1.3-1.8 times less

than for the combustion chambers of LPRE's operating on the scheme "liquid-liquid."

When selecting the optimum ratio between the length and the diameter of a combustion chamber (afterburner) we use its relative area  $\bar{f}_K$ .

Besides the disadvantages noted in §12.2, with a decrease in  $\bar{f}_K$  there are additional complications in organizing efficient atomization of the propellant components because of reduced area of the surface on which the injectors are located. Therefore, with a de-

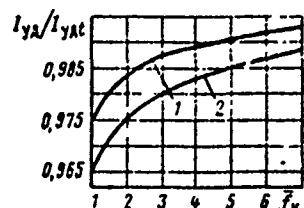


Fig. 12.15. Ratio  $I_{yA}/I_{yAt}$  vs. the value of  $\bar{f}_K$  with  $\epsilon_c = 100$  (curve 1) and  $\epsilon_c = 10$  (curve 2).

crease in relative area  $\bar{f}_K$ , the specific impulse of the chamber drops (Fig. 12.15), which is noticeable when  $\bar{f}_K < 3$  (particularly when  $\bar{f}_K \approx 1$ ). The influence of the relative area of the combustion chamber (afterburner) on the specific impulse when  $\bar{f}_K > 3$  can be disregarded, particularly with a high gas-expansion ratio  $\epsilon_c$ .

Some of the advantages of selecting a small relative area  $\bar{f}_K$  include a decrease in chamber mass and facilitation of its cooling (a decrease in the required thickness of the combustion chamber walls and its surface to be cooled).

The relative area  $\bar{f}_K$  can be determined from the selected flow intensity of the combustion chamber using equation (12.2) which, with consideration of (4.14) and (12.1), can be written in the following form:

$$r = \frac{p_K}{f_K^3}. \quad (12.18)$$

Since for a given propellant complex  $\beta$  can be considered constant, with increasing pressure  $p_K$  the flow intensity for the combustion chamber also increases.

Ratio  $r/p_K$  is called the *relative flow intensity* and is desig-

nated  $r_p$ , i.e.,

$$r_p = \frac{r}{p_k}, \quad (12.19)$$

or, considering (12.18),

$$r_p = \frac{1}{\bar{f}_k^3}. \quad (12.20)$$

If, for the propellants used, complex  $\delta$  is 1700-2400 N·s/kg [ $\approx 170-240$  kgf·s/kg], then when  $\bar{f}_k = 2-6$  the relative flow intensity is  $(0.1-0.2) \cdot 10^{-3}$  kg/N·s [ $\approx (1-2) \cdot 10^{-3}$  kg/kgf·s] [17].

The indicated value of  $\bar{f}_k$  for cylindrical chambers has a corresponding ratio of the length of the combustion chamber to the diameter of its cylindrical part of  $l_k/d_k = 1.0-1.5$ .

## CHAPTER XIII

### SYSTEMS FOR FEEDING LIQUID PROPELLANT COMPONENTS

† † †

#### §13.13. Basic turbine parameters

The following are among the basic turbine parameters.

1. Available turbine power, i.e., the turbine shaft horsepower; this should equal the sum of the powers required by the oxidizer and fuel pumps, and also by the pumps for the auxiliary propellant components (if used), i.e.,

$$N_{typd} = N_{HAC,OK} + N_{HAC,F} + N_{HAC,aux}$$

and defined by the formula

$$N_{typd} = \eta_t L_{ad} \dot{m},$$

where  $\eta_t$  is the effective efficiency of the turbine (see §13.14);  $\dot{m}$  is the per-second flow of gas entering the turbine;  $L_{ad}$  is the adiabatic work of expansion of 1 kg of gas, calculated from the formula

$$L_{ad} = \frac{k}{k-1} RT_0 \left[ 1 - \left( \frac{p_2}{p_0} \right)^{(k-1)/k} \right].$$

2. Pressure differential in the turbine (gas expansion ratio in the turbine), equal to the ratio  $p_0/p_2$ . A distinction is made between *high-differential* ( $p_0/p_2 = 15-40$ ) and *low-differential*

$(p_0/p_2 = 1.3-1.8)$  turbines. Pressure  $p_2$  is called *counterpressure*.

High-differential turbines include those with discharge of exhaust gas to the ambient medium; a supercritical gas-pressure differential is generated in the nozzles of their nozzle ring. To increase turbine power it is desirable to provide greater gas expansion; with constant pressure  $p_0$  this can be achieved by lowering pressure  $p_2$ . But in order that the turbine operating regime and, consequently, that of the TPA as a whole, not be influenced by a change in pressure of the ambient medium, pressure  $p_2$  must be selected higher than the maximum pressure of the ambient medium:  $p_2 \approx 1.3p_{h \max}$  (with consideration of the possibility of operation of the turbine exhaust pipe Laval nozzle in an overexpansion mode [17]). In this case, a supercritical pressure differential is assured at the nozzle of the turbine exhaust pipe, as a result of which, as noted in §9.1, the nozzle develops a certain thrust. The specific impulse  $I_{y_d}$  of the exhaust pipe nozzle is lower than that of the chamber, and with an increase in gas flow through the turbine the value of  $I_{y_d}$  for the engine drops. Therefore, the given power of high-differential turbines should be obtained with the lowest possible gas flow through them.

For the turbines of LPRE's operating on the scheme "gas-liquid" or "gas-gas" a high gas flow-rate is characteristic: for example, for the scheme "gas-liquid" it is usually equal to the total flow of one of the propellant components and part of the flow of the other component. Therefore, for such LPRE's we use turbines which develop sufficient power with a subcritical pressure differential, i.e., low-differential turbines.

3. Temperature of the gas at the turbine inlet  $T_0$ . Temperature  $T_0$ , together with the gas expansion ratio, determines the adiabatic work of expansion of 1 kg of gas, increasing as it does. Depending on the blade material and engine operating duration, temperature  $T_0$  is selected within the limits of  $750-1200^{\circ}\text{K}$ .

4. Turbine shaft rpm  $n$ . The number of revolutions  $n$  with single-shaft TPA design is determined from the condition of cavitation-free operation of the pumps; with multi-shaft design it is determined from the condition of maximum turbine efficiency and smallest size.

In turbine calculations we use the peripheral velocity  $U$  - the velocity of a point located midway on the blade (on diameter  $D_{cp}$ ); here

$$U = \frac{\pi D_{cp} n}{60} \text{ m/s.}$$

#### §13.14. Turbine efficiency and selection of the ratio $U/c_1$

The following losses occur during turbine operation:

- a) in the nozzle ring nozzles;
- b) on the moving blades;
- c) with exhaust velocity;
- d) friction of the disk against the gas, and ventilation losses;
- e) mechanical.

The *effective efficiency* of a turbine takes all these losses into account.

The losses in the nozzle ring nozzles and on the moving blades depend on the degree of perfection of the turbine blading, including the surface finish of the nozzles and moving blades and their profiles.

Losses with exhaust velocity are explained by the fact that the gas at the exit from the moving blades has a certain velocity  $c_2$ , i.e., the kinetic energy of the gas is not completely used in the turbine.

For the given values of gas velocity  $c_1$  and the slope of the velocity vector  $c_1$  to the plane of the turbine disk  $\alpha_1$ , the lowest velocity  $c_2$  and, consequently, the smallest losses with exhaust velocity are achieved with a ratio  $U/c_1$  defined by the formula

$$\frac{U}{c_1} = \frac{\cos \alpha_1}{2}. \quad (13.4)$$

Usually, in the impulse turbines of TPA's  $\alpha_1 = 15-20^\circ$  and velocity  $c_1 = 1000-1400$  m/s; here the required peripheral velocity  $U$ , calculated from formula (13.4), is inadmissibly high; in particular, the dimensions and mass of the turbine sharply increase. Therefore, in high-differential turbines the peripheral velocity  $U$  is usually selected within limits 250-350 m/s, while ratio  $U/c_1 = 0.1-0.3$ , which causes losses with exhaust velocity.

With low values of  $U/c_1$ , which are advisable to use in TPA turbines, the efficiency of a two-stage turbine is substantially higher than that of a single-stage turbine.

While losses to friction of the disk against the gas are inherent in all turbines, ventilation losses are characteristic only of partial-admission turbines; these losses increases with decreasing admission of the turbine.

The effective efficiency of high-differential turbines is within the limits of 0.3-0.7, while that of low-differential turbines, for which  $U/c_1 = 0.4-0.6$ , is higher.

For the most part, *axial* turbines are used in LPRE's; in them the gas moves in parallel with the shaft axis.

So-called *radial* turbines are of specific design; in them the gas moves along the radius of the disk to the shaft axis (*centripetal* turbines) or from the shaft axis to the periphery of the disk (*centrifugal* turbines). The most widely used radial turbines are the low-differential centripetal ones.

### §13.15. Liquid gasifiers

The liquid gasifier of the TPA turbine feed system generates a gas which has quite high pressure and temperature.

LPRE's use one- and two-component liquid gasifiers which, as shown in §9.1, can operate on the basic as well as the auxiliary propellant components.

Two-component gasifiers, operating on the basic propellant components, are the most widely used. In an LPRE with discharge of the exhaust gas from the turbine into the ambient medium, a small part (usually 2-3%) of the total flow of basic propellant components is taken at the pump exit for operation of the two-component liquid gasifier.

The temperature of the generator gas usually does not exceed 1200°K. If higher-temperature gas is fed to the turbine, the strength of the blade material is noticeably reduced, or the blades and other elements along the generator-gas line melt. The required

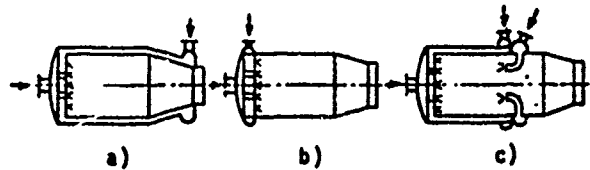


Fig. 13.29. Two-component liquid gasifiers: a - cooled, single-zone; b - uncooled, single-zone; c - cooled, two-zone.

gas temperature of two-component liquid gasifiers is assured with a significant excess of oxidizer or fuel (see §9.1).

A distinction is also made between single-zone and two-zone liquid gasifiers (Fig. 13.29).

In *single-zone* liquid gasifiers the flow of propellant components comes from the head, i.e., just as in the main chamber of an LPRE.

In *two-zone* liquid gasifiers, part of the excess propellant component is introduced into the gasifier through an additional band of injectors located in the central part of the gasifier. In such a liquid gasifier we can distinguish two zones: one high-

temperature (2000-3500°K) zone (from the head to the section containing the additional band of injectors), and the zone with a substantially lower temperature (from this band to the gasifier exit).

Designwise, two-zone gasifiers are more complex than single-zone gasifiers, and are used when one-zone gasifiers cannot assure stable burning or they are long because of an insufficiently active burning process caused by an excess of one of the propellant components.

To balance the temperature field at the gasifier exit, which is very important for excluding melting along the generator-gas line, the reduced length for the gasifier is longer than for the combustion chamber.

Ordinarily, liquid gasifiers have external circulation cooling, which assures their reliable and prolonged operating life; when the generator gas has a relatively low temperature, there is no need for such cooling.

**Single-component liquid gasifiers.** In a number of cases it is more advisable to use single-component instead of two-component gasifiers; in these there is, in the presence of a catalyst, decomposition of the liquid monopropellant (e.g., hydrogen peroxide) with the release of heat and the formation of gaseous products; such decomposition is called *catalytic decomposition*.

Either solid or liquid catalysts can be used; the latter should be continuously fed to the gasifier (such a gasifier is actually a two-component gasifier). The solid catalyst is placed directly in the gasifier in the form of a packet (Fig. 13.30). Gasifiers with a solid catalyst are simpler in design and are more widely used.

The packet of solid catalyst for decomposing hydrogen peroxide consists of grains of a solid carrier/base (gypsum, cement, etc.)

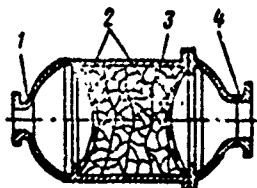


Fig. 13.30. Single-component liquid gasifier: 1 - intake pipe; 2 - grid for holding solid catalyst; 3 - packet of solid catalyst; 4 - exhaust pipe.

impregnated with catalytically-active salts (e.g.,  $\text{KMnO}_4$ ) or a compressed screen of an active metal (nickel, Monel metal, brass, and others).

The catalyst for hydrazine decomposition can be screens made of metals of the platinum group.

The temperature of the forming hydrogen peroxide decomposition products (a mixture of water vapor and gaseous oxygen) increases with an increase in hydrogen peroxide concentration, and is 720-1030°K at 80-90% concentration. The temperature of hydrazine decomposition products can be obtained within the limits from 875° to 1475°K by changing the time that the hydrazine remains in the catalyst packet and changing the length of the gasifier (by controlling the degree of decomposition of the hydrazine).

The following specific parameters are used to calculate the dimensions of the solid catalyst packet:

1. The specific surface of the catalyst - the area of the active surface of the catalyst per unit volume. For a number of catalysts that are used, the specific surface is 8-80  $\text{cm}^2/\text{cm}^3$ .

2. The specific load of the catalyst - the maximum permissible flow of liquid propellant component per 1 kg of catalyst,

$$s = \frac{\dot{m}_{\text{cat}}}{m_{\text{cat}}} \frac{\text{kg/s}}{\text{kg}}$$

For example, for a solid catalyst consisting of calcium permanganate  $\text{CaMnO}_4$  and calcium chromate, the value of  $s = 2.5-2.6$   $\text{kg/s/kg}$  with 80% hydrogen peroxide.

With an increase in the specific surface and specific load of the catalyst there is a decrease in the required volume of the catalyst packet and, consequently, in the volume and mass of the gasifier.

## CHAPTER XIV

### SYSTEMS FOR LPRE START-UP, MODE CHANGE, AND SHUTDOWN. SYSTEMS FOR CREATING CONTROLLING FORCES AND MOMENTS

#### §14.1. Systems for LPRE start-up

The system for LPRE start-up should assure sufficiently rapid but gentle (without great oscillations of pressure  $p_h$ ) and reliable runup of the engine to the rated operating mode with low nonproductive expenditures of propellant.

Conditions for reliable LPRE start-up include the following:

- a) no overshooting of pressure  $p_h$  above the permissible value (this can be caused by the accumulation of a large quantity of propellant components in the chamber before they ignite); in addition, no explosive mixture should form in the chamber;
- b) low level of pulsations of the pressure of the combustion products in the chamber and gasifier;
- c) slight deviation of coefficient  $\alpha$  in the chamber and gasifier from the calculated values.

Start-up of the engine is the most complex and critical period of its operation. The greatest number of engine failures occurs during just this period. The parameters in the chamber and gasifier are constantly changing, and the engine passes through a number of

regimes, each of which is practically impossible to check and study. Therefore, development of start-up usually causes great difficulties, which increase with increasing chamber dimensions.

**Methods for LPRE start-up.** Two methods of LPRE start-up are distinguished: *nonstepped* (smooth or "full-flow") and *stepped* (Fig. 14.1).

With nonstepped engine start-up the flow of propellant components to the chamber continually increases, smoothly (*smooth start-up*) or abruptly ("full-flow" start-up).

A smooth increase in propellant component flow is assured by special throttles, driven electrically or hydraulically, installed

in the propellant component lines.

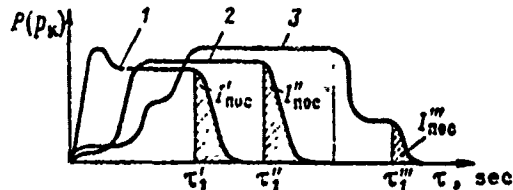


Fig. 14.1. Change in thrust (pressure  $p_k$ ) for various types of start-ups and shutdowns of an LPRE: 1 - abrupt ("full-flow") start; shutdown without final stage; 2 - start with preliminary stage; shutdown without final stage; 3 - start with preliminary and intermediate stages; shutdown through final stage.

With "full-flow" start-up there is the danger of hydraulic shocks and an impermissible overshoot of the pressure of the combustion products. Therefore, such start-up, in its pure form, is not used. The use of non-

stepped start-up simplifies the scheme and design of the engine, reducing to a minimum the nonproductive expenditure of propellant components and delay in the launch of the rocket vehicle (the time from the moment the command is given up to the launch of the vehicle). Nonstepped start-up is used mainly for low- and medium-thrust engines with pressure and pump feed.

For a high-thrust LPRE with pump feed, *stepped* start-up is used in a number of cases; this is accomplished through the preliminary or intermediate stage. The *preliminary* stage is characterized by the fact that before full flow of the propellant components to the chamber there is slight flow by hydrostatic pressure and by the

boost pressure of the tanks; in this case the TPA does not operate. Here a reliable burning fuel spray is formed in the chamber.

The *intermediate* stage is characterized by the fact that the TPA and the engine operate for a certain length of time under non-full-flow conditions before stabilizing in the rated mode; this can be necessary, e.g., to decrease the rate of increase of propellant component flow to the chamber.

To start up an LPRE with a TPA it is first necessary to start the pumps rotating; for this, the turbine is fed auxiliary gas and the propellant component tanks are supercharged by means of some auxiliary supercharging system (ordinarily, the system for supercharging the tanks of the power plant begins to operate several seconds after the command for engine switch-on).

Preliminary supercharging of the tanks and switch-on of the TPA of the engines of the first stage of the rocket can be accomplished from a ground starter, while for the second and subsequent stages these can be accomplished from the previous stage. However, the most efficient start-up systems are those included in the power plants of the appropriate stages.

For TPA start-up, its turbine is fed the following:

1. Gas (helium, nitrogen, air, or hydrogen) located in the starter bottle.
2. The combustion products from the two propellant starting components or the products of the decomposition of one propellant starting component, formed in the main liquid gasifier. The starting components are fed to the gasifier from the starter tanks by the compressed-gas generator. Such a system is quite efficient; it allows for multiple engine burn.
3. The combustion products of a solid-propellant charge located in the cartridge starter, or by the start-up solid-propellant gasifier. It is designed for short-term burning of the charge (up

to 1 second), sufficient for bringing the TPA to rated conditions. During rotation of the turbine by the starter the pumps create the necessary pressure for the propellant components; these begin to enter the liquid gasifier. The gasifier is brought to the rated conditions, and the turbine automatically switches from starter power to liquid-gasifier power.

The combustion products of the starter charge are usually fed to the main turbine. However, LPRE's are used which have a TPA containing an additional starter turbine which operates only during engine start-up.

Powder starters are basically used for launching single-burn LPRE's. The scheme of the engine in this case is simpler than when liquid starter propellant components.

4. The combustion products of the basic propellant components, fed from the tanks under hydrostatic pressure and the pre-launch tank supercharge pressure. As the combustion products begin to form in the liquid gasifier and they begin to enter the turbine, the pumps begin to operate, leading to a constant increase in flow of propellant components to the gasifier. If, during the entire start, the available power of the turbine is greater than the power required by the pumps, the liquid gasifier and the engine as a whole are brought to rated operating conditions. With such start-up (called *self-starting*) we are assured maximum simplicity of both single and multiple engine burns.

An electric motor can be used to start the TPA's of auxiliary aircraft LPRE's.

**Features of starting LPRE's under various ambient conditions.**  
The engine start-up system depends essentially on the start conditions: on the ground, at high altitudes, in outer space, etc.

When starting an engine on the ground, if abnormalities develop it can be shut down, if the engine thrust has not exceeded the launch

weight of the rocket, i.e., if the rocket has not started to move in the launcher.

The rocket can be held in the launcher, with its engines at full thrust, by special supports (levers) or exploding bolts (these break when the given engine thrust is attained). Disadvantages of such a launch system include high nonproductive expenditures of propellant components before the launch and impact loads on the bottoms of the tanks at the moment of launch.

Especially high requirements are imposed on the reliability of the starting systems of engines of the second and successive stages of a multistage rocket, and also the engines of space vehicles, which are started in a deep vacuum. If the engine does not start for some reason, or is damaged during start-up, failure of the rocket or vehicle is unavoidable. For example, repeated insertions of a satellite into orbit using the Europa booster ended in failure because the engines of the upper stages would not start.

The smoothness of engine start-up in outer space depends on a vast number of factors, mainly the pressure at which ignition of the propellant occurs, and also on the temperature of its components, the injectors of the head, and the walls of the combustion chamber.

Gentler start-up and reliable ignition of the propellant is assured with pressure in the combustion chamber. Therefore, the critical section of the chamber usually contains a plug to retain atmospheric pressure in the chamber before engine start-up. As the pressure of the combustion products rises, the plug is ejected from the nozzle.

The temperature of the head injectors and the chamber walls should be such as to prevent freezing of the propellant components during engine start-up, which would lead to chamber explosion.

Smoothness of start-up is also influenced by the properties of

the propellant components and the order in which they enter, the design of the chamber head, and other factors. For example, hypergolic propellants should have a short self-ignition delay period.

Start-up of the engines of the second and subsequent stages of a multistage rocket depends on the *type of stage separation*. Usually the stages of a rocket are rigidly connected by explosive bolts that burst when fed an electric current at the required moment.

A distinction is made between cold and hot staging. In *cold* staging the main engine of the upper stage does not operate; the stages are separated by the retro engines of the lower (burnout) stage or the boost engines of the upper (next) stage.

*Hot* staging is assured by the thrust of the main engine of the upper stage, which simplifies the scheme and design of the rocket (rétro and boost engines can be eliminated). However, such staging is complex to develop because of the appearance of perturbing forces and moments in the upper stage, which should be eliminated by the guidance system.

To decrease the perturbing forces and moment in hot staging we can use stepped start-up of the primary engine of the upper stage: first the engine operates in a reduced mode, going to the rated mode after staging.

With hot staging, the primary engine combustion products must be removed from the compartment between stages; in addition, more heat shielding of the engine is required.

The engines of satellites and space vehicles should start reliably under conditions of deep vacuum and weightlessness after prolonged orbital (satellite) or interplanetary flight. To start the engines with a TPA under weightlessness it is necessary to raise the pressure of the propellant components at the pump inlet. In addition to other methods, for this purpose boost engines are used

(particularly in large rockets). LPRE's operating on cryogenic propellant components can be started, under weightlessness, by feeding their vapors from the gas cushions of the main tanks to the chamber, i.e., use these vapors as starting components.

Start-up of an LPRE with displacement feed under weightlessness presents fewer difficulties. Separators are used in such engines to feed the propellant components in liquid form, not as an emulsion with the displacing gas.

The most difficult to assure is multiple burn of the engines of space vehicles, particularly if the interval between burns is long (this can reach several years). During the first engine burn there is air pressure in its chamber, hermetically plugged, while with subsequent burns the inner cavities of the chamber are under vacuum, which changes the nature of mixing of the propellant components.

The design and schemes of engines with multiple burns are, of necessity, complex; in particular, we must deal with the fact that after engine shutdown the heat is transmitted from the chamber and the liquid gasifier to the colder units, causing them to overheat, which makes subsequent engine burn impossible. The heat fluxes are particularly high, if there is a nozzle adapter with radiation cooling. In a chamber with external circulation cooling, the coolant can boil in its loop; if the coolant vapors cannot condense before the next start-up, its reliability also cannot be guaranteed. Therefore, for condensation of the vaporized coolant the time interval between shutdown and the next start-up should be sufficiently long; otherwise, the cooling loop must be purged. To decrease heat transfer from the chamber to cooler units of the engine we can use spacers made of nonheat-conducting material, and also reduce the engine thrust during the last seconds of its operation.

The chamber of impulse LPRE's operating on hypergolic propellants usually does not have a cooling loop; the main valves of the

engine are electrically driven and are placed directly on the chamber head, which assures a short duration of the transient operating modes and creation of very slight control pulses. With a decrease in the volume of the lines behind these valves there is a reduction in the time for the engine to come up to the rated mode during start-up and a reduction in the aftereffect pulse during shutdown.

A layer of heat insulation is placed on the pipelines and the chamber head to prevent freezing of the propellant components after engine shutdown (due to intense cooling in outer space). To hold the temperature of the propellant components within the required limits, the engines of a space vehicle can have special shields to protect them from solar heating.

The propellant components can freeze after engine shutdown when the valves are not tightly seated; the leaking component boils in a vacuum; the heat lost to vaporization lowers the temperature of the component below its freezing point.

Repeated engine burns in outer space can sharply increase the pressure  $p_{\mu}$ , and cause chamber destruction. The pressure rise can be caused by deposition of the propellant components, evaporated from the chamber head cavity, on the chamber walls after engine shutdown; therefore, the chamber temperature must be held within specific limits after engine shutdown.

An analogous phenomenon is observed with multiple burns of LPRE's operating on  $N_2O_4$ -based hypergolic propellants ( $N_2O_4 + MMH$ ,  $N_2O_4 + UDMH$ ;  $N_2O_4 + aerozine-50$ ,  $N_2O_4 + N_2H_4$ ), under outer-space conditions, and is explained by the formation of intermediate dangerously explosive products in the chamber in the period preceding ignition. It has been established that the temperature of the propellant components and the chamber before another engine burn should be at least  $224^{\circ}K$  [ $21^{\circ}C$ ] [1].

To assure gentle start-up of LPRE's operating on hypergolic

propellants, various additives are effective under space conditions.

The start-up of a *monopropellant* LPRE has its peculiarities. For example, when starting a hydrazine engine it is necessary to first heat the catalyst packet by feeding to the chamber a starting flow of nitrogen tetroxide. After the catalyst has heated up, the engine operates stably on hydrazine alone.

Systems for chilling the engine lines. If the temperature of the propellant components (e.g., cryogenic components) is lower than the ambient temperature, before starting the engine its lines are chilled (pumps, valves, pipelines, etc.). Otherwise, the liquid propellant components will be preceded in the chamber and liquid gasifier by their vapors and then by a mixture of vapors and liquid components. As a result, the engine comes up to its rated mode more slowly, while coefficient  $n$  will differ substantially from its rated value.

Products of intermediate chemical reactions, tending to detonate, can form in the chamber; detonation is also possible in the vapors of the propellant components. These phenomena can lead to explosion of the chamber or gasifier when the engine is started.

The engine lines must also be chilled to prevent cavitation of the pumps for the cryogenic propellant components.

The engine lines are cooled most simply by passing propellant components through them; these come from the tanks under hydrostatic pressure and boost pressure, flow along the engine lines and through the open bypass valves at the chamber and gasifier inlets, and are exhausted outside the vehicle. If the line of one propellant component must be chilled, it can be passed directly into the chamber; the liquid component discharges from the chamber nozzle, vaporizing to some extent. However, with such a system the unproductive flow of propellant components is increased.

Special systems can be used for chilling the lines, which include separate-drive recirculation pumps; the propellant component is fed by pump from the tank into the line, it is cooled, and it is then fed back to the tank through the open bypass valve. The system is switched on several minutes before the engine. After chilling has been accomplished, the bypass valve is closed and the command is given to start the engine. Since the propellant component absorbs heat fluxes as it passes along the engine line, it must first be supercooled.

The time required for chilling the units and pipelines is reduced by using a layer of thermal-insulating material (e.g., a plastic) on the surface in contact with the cryogenic propellant components.

The sequence in which the propellant components enter the chamber. In the process of developing an engine we select that sequence with which one propellant component enters the chamber ahead of the other so as to assure a gentle start-up. The valves should operate at very specific moments of time, which can differ for the oxidizer and fuel valves.

Selection of the sequence with which the components enter the chamber depends on the type of component. For example, it has been established that when working with a propellant consisting of RFNA + UDMH, the oxidizer should be fed to the chamber ahead of the fuel; smooth engine start-up is assured by the absorption of heat, released in the initial phase of burning, by the excess oxidizer.

In hydrogen LPRE's, for this purpose the fuel (hydrogen) is fed to the chamber before the oxidizer.

**Purging systems.** Before the start-up of certain engines, the lines for propellant feed are purged by an inert gas (nitrogen or helium). For example, in oxygen LPRE's the chamber and liquid-gasifier LOX lines are usually purged, as is the LOX pump seal.

Purging prevents the entry of fuel, which can result in explosion of the engine, and prevents the accumulation of a vast quantity of propellant components in these units.

When starting a rocket from a surface launcher, purging can be done from a ground compressed-gas cylinder, while in the engines of the second and subsequent stages of the rocket it can be done from a cylinder in the previous stage.

#### §14.2. Ignition systems

LPRE's operating on nonhypergolic propellants use a special system which, at the moment of engine start-up, feeds heat to the first portions of propellant components entering the chamber and the liquid gasifier; this results in their ignition.

All remaining amounts of propellant components go to the stable fuel burn spray and are ignited by the combustion products of the previous portions.

For reliable ignition of the propellant components under engine operating conditions (on the ground, in outer space, etc.), the ignition system should produce a sufficient quantity of heat in the largest possible chamber or liquid-gasifier volume. As the amount of heat increases, the ignition delay period decreases, which excludes the possibility of accumulation of propellant components in the chamber and gasifier during engine start-up.

The ignition system for a multiple-burn LPRE should assure ignition of the propellant components during each engine start-up; this complicates its design.

Selection of the ignition system depends on the properties of the propellant components and on the design and operating conditions of the engine. A distinction is made between *built-in* and *inserted* ignition systems. A system of the first type is built into the

chamber or gasifier and is ordinarily used in multiple-burn LPRE's. Systems of the second type are introduced into the chamber through the nozzle; they are part of the launch system or are installed on a brace attached in the nozzle throat. They can be used only in single-burn engines.

The ignition system should begin to operate before the propellant components enter the chamber or gasifier. In some cases, blocking is used which makes it impossible for the propellant components to enter the chamber or gasifier if the ignition system, for some reason or other, does not operate. The blocking system prevents launching of the rocket with one inoperative engine in a power plant consisting of several engines, or with one inoperative chamber in a multichamber engine.

The built-in type ignition system must be used in the gasifiers of both single- and multiple-burn engines.

Different types of ignition include pyrotechnic, chemical, electrical, thermal, and combination.

**Pyrotechnic ignition.** The pyrotechnic-ignition system creates a flame in the chamber or gasifier as a result of the burning of a charge of solid propellant. To increase the amount of heat released, and to increase the reliability of the ignition system, several solid-propellant charges can be used (Fig. 14.2).

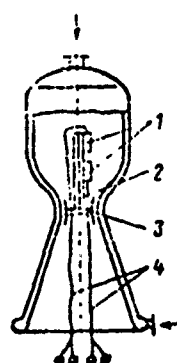


Fig. 14.2. Chamber with inserted system of pyrotechnic ignition or propellant components: 1 - ignition cylinder; 2 - brace; 3 - plug; 4 - electric leads.

The pyrotechnic-ignition system is distinguished by its simplicity and high reliability; the electric power required to trigger the ignition cylinders (which replace the solid propellant charge) is low. However, this system has a limited range of application (for a single-burn LPRE) and requires precautionary measures to avoid its chance triggering during engine tests.

**Chemical ignition.** The chemical-ignition system creates a flame by feeding, to the chamber or gasifier, components of the starting hypergolic propellants; they enter the chamber through its head or through an igniter in the nozzle.

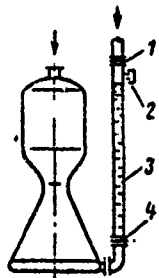


Fig. 14.3. Chamber with systems of chemical ignition of propellant components: 1,4 - free-space diaphragms; 2 - fill pipe; 3 - starting propellant component.

Chemical-ignition systems often use a liquid starting component, which ignites on contact with one of the primary propellant components (Fig. 14.3); with a rise in their pressure during engine start-up the diaphragms, between which the starting fuel is located, break. The starting flame is formed in the chamber upon the interaction of the starting fuel with the primary oxidizer, after which the primary fuel begins to enter.

The flow of starting propellant component per unit area of the chamber nozzle throat should be sufficient for reliable ignition of the primary components.

For multiple-burn LPRE's the starting propellant component, during start-up, enters the chamber from a special tank along the pipeline through an open valve. Then the valve closes and the line is purged by an inert gas.

In hydrogen LPRE's, triethyl aluminum or gaseous fluorine is used as the starting fuel; these are hypergolic in contact with liquid hydrogen.

The chemical ignition system assures multiple engine burn and fast run-up to the rated mode; it is reliable, quite simple, and widely used in modern LPRE's.

The disadvantages of such a system include the use of a dangerously explosive and toxic starting component and increased requirements on its valves during their opening and closing to prevent

abrupt start-up and explosion of the engine.

**Electrical ignition.** An electric spark plug serves as the ignition initiator.

The electrical ignition system permits multiple burns and can be used after the engine has been in long-term storage; it is quite simple and safe to handle. However, the dimensions of the igniter (spark) are small, and the contacts of the plug can foul and short circuit and also rapidly burn out. In addition, operation of such a system requires a rather high-powered electric source.

**Thermal ignition.** If the oxidizer is hydrogen peroxide, for ignition of the propellant we can use its decomposition products that form in the precombustion chamber. The chamber is first fed the hydrogen peroxide decomposition products and then, after their pressure is raised to the given value, the fuel. Such ignition is called *thermal ignition*. It excludes the possibility of the accumulation of propellant components in the chamber during engine start-up and is the safest and most reliable method of ignition.

**Combination ignition.** This is ignition in which a small part of the primary propellant components (or starting component) is fed,

during engine start-up, to the precombustion chamber and ignited in it using some type of ignition system (e.g., electrical). The combustion products that form enter the chamber and ignite the main portion of the components (Fig. 14.4). The precombustion chamber, creating the starting flame, in a number of cases facilitates start-up conditions.

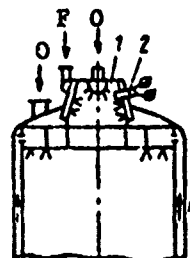


Fig. 14.4. Chamber with combination system for ignition of propellant components: 1 - precombustion chamber; 2 - electric spark plug.

Chemical and pyrotechnic ignition systems are used most often, particularly in high-thrust engines, while electrical and combination ignition systems are used in aviation LPRE's.

### §14.3. Systems for changing the operating mode

If the engine is not equipped with special systems, it runs up to the nominal mode with a greater or lesser deviation of combustion-chamber pressure  $p_K$  and coefficient  $\kappa$  of the propellant component ratio (and, consequently, thrust) from the calculated values.

The deviations of pressure  $p_K$  and coefficient  $\kappa$  from the rated values are not identical for various engine samples due to the influence of a number of factors: changes in density of the propellant components depending on the ambient temperature, disparities in the characteristics of the pumps and hydraulic resistances of the lines, the influence of linear acceleration of the rocket vehicle on TPA operation, etc.

In addition, the engine operating mode is influenced by the gaseous inclusions that form in the propellant components as the tanks are filled or as a result of their saturation with the displacement gas (in the absence of separators in the tanks).

Engine thrust can be varied on command from the vehicle guidance system or spontaneously. A spontaneous change in thrust can be caused, in particular, by a decrease in the flow cross section of the line for feeding the turbine with working fluid (gas) due to the settling of solid carbon-black particles on the walls, a decrease in the flow section of the cooling loop of the chamber due to deposits of particles of decomposed fuel on the loop walls, etc. These result in changes of propellant flow  $m$  and coefficient  $\kappa$ , leading to a reduction in specific impulse, an increase in the terminal mass of the vehicle (the rocket stage), and other undesirable consequences.

Engine control systems can be broken down as follows, according to their features.

1. Engines with control systems which are functions of the vehicle flight peculiarities. The operating mode of such engines

is varied by signals from the vehicle control system sensors (from the so-called *current signals* of the control system) or by signals from the programmed sensors according to a previously set program (from the *programmed signals* of the control system).

2. Engines with control systems that get signals only from sensors in the engine. Such control systems are called *intraengine* systems. They maintain the rated engine mode.

3. Engines having no control systems. Their operating mode during the initial period is "built-in" during assembly, but during further operation this mode can change spontaneously (see p. 117). In order that deviations of pressure  $p_K$  and coefficient  $\kappa$  from the rated values be slight, the chamber and gasifier feed lines are filled with propellant components and adjustment washers are placed in these lines at the pump exits. By changing the pressure differential on the adjustment washers we can assure identical (with low error) hydraulic resistance of the lines of all sample engines of the given type.

Control systems improve the engine characteristics: increase in engine reliability and service life, decrease in losses of specific impulse, compensation for inaccuracies in manufacture of various samples of the engines and the influence of external factors (vehicle acceleration, ambient temperature, etc.).

The control system includes the following elements:

- 1) sensors to measure the controlled value or the value proportional to it;
- 2) comparators, to determine the deviation of the controlled value from the programmed one or from that value generated by the vehicle control system, and to produce the command signal;
- 3) executive units, assuring a change in the controlled value as a function of the sign and magnitude of the command signal.

The executive unit can be the engine as a whole, as well as its regulators, controlled by special electric drives.

The power plants of rocket vehicles use the following types of control systems: combustion-chamber control system, tank-emptying system, system for maintaining constant  $p_h$  or TPA rpm, etc.

Control systems associated with a change in propellant flow  $\dot{m}$ . The combustion-chamber control system. If the engine is the executive unit of the control system, the engine thrust should vary with its signals. The thrust of an LPRE is determined by the flow rate of propellant components  $\dot{m}$  into the chamber.

Flow rate  $\dot{m}$  can be varied

a) by changing - with displacement feed - the pressure in the propellant component tanks (it should be noted, however, that due to large gas inclusions in the tanks the pressure rises or falls very slowly);

b) by changing - with pump feed - the TPA shaft rpm;

c) by changing - with displacement and pump feed - the pressure differential at the throttles installed in the engine lines ahead of the chamber and controlled by electric drives. With an increase or decrease of the pressure differential on the throttle, movements of the moving elements of the throttle cause a change in pressure of the propellant component ahead of the chamber and, consequently, a change in its flow rate. The throttles should assure a variable (rather large) pressure differential, which leads to an increase in the required power of the system for feeding propellant to the chamber.

The possibilities for a change in engine thrust are limited, if the cross-sectional area of the injector and chamber nozzles remains unchanged; with a decrease in thrust there is a decrease in pressure differential on the injectors, which has undesired results:

burning of the propellant becomes more unstable (shifts to the unstable zone) and less complete (decrease in coefficient  $\phi_\beta$ ), etc.

The basic conditions to assure stable and complete burning with a reduction in engine thrust include simultaneous retention of the pressure differential in the injectors ( $\Delta p_\phi = \text{const}$ ) and the pressure of the combustion products in the chamber ( $p_H = \text{const}$ ); it is much more difficult to carry out the second condition  $p_H = \text{const}$ .

The condition  $\Delta p_\phi = \text{const}$  can be assured, when creating varying thrust, by changing

- 1) the number of injectors through which the propellant components are sprayed into the chamber (a head with a variable number of working injectors);
- 2) the area of the through-section of each injector (injectors with variable geometry);
- 3) the degree of saturation of the propellant components with gas (the degree of their aeration);
- 4) pulse duration (in pulsed LPRE's); and
- 5) the coefficient  $\alpha$ .

In heads with a variable number of working injectors, the injectors are grouped, and to decrease the thrust a certain number of injector groups are shut off by closing the valves in the lines that feed them.

*Injectors with variable geometry were examined in §12.2.*

The openings in jet injectors can be closed, to a certain extent, by angular turning of the disk with the openings on the chamber head.

The use of chambers equipped with variable-geometry injectors makes it possible to reduce the thrust in a ratio of 10:1 and more.

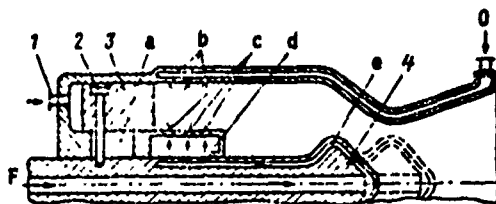


Fig. 14.5. Chamber with simultaneous proportional change in area of the nozzles of the propellant component injectors and the area of the critical section: 1 - feed pipe for control fluid; 2 - pin; 3 - piston; 4 - needle. a - notch in chamber housing; b - oxidizer injectors; c - fuel injectors; d - cavity ahead of fuel injectors; e - needle cooling loop.

Figure 14.5 shows a diagram of a chamber with a simultaneous proportional change in area of the injector nozzles (the number of injectors) and the area of the critical section, which assures constant pressure in the combustion chamber and a constant pressure differential in the injectors with a reduction in thrust.

The oxidizer flows along the cooling loop of the chamber, and enters the combustion chamber through the injector openings in the inner wall. The fuel is fed to the inner channel of needle 4, passes along its cooling loop e, and enters cavity d through openings in the outer wall of the needle; from here it flows through injector openings c into the combustion chamber. The needle is rigidly coupled to piston 3 and pin 2; it can move to the right under the influence of the pressure of the liquid working substance introduced through pipe 1, and to the left under the action of the pressure of the combustion products on the piston.

When the piston and needle move there is a simultaneous change in both the number of injector openings for oxidizer and fuel and the area of the critical section. Therefore, pressure  $p_K$  remains constant with a change in thrust.

One of the ways of changing the flow rate  $\dot{m}$  is to feed a special gas to the engine lines ahead of the chamber or to its head cavities (i.e., directly into the propellant components).

*Saturation with gas (aeration)* reduces the density of the propellant components and their mass flow into the chamber while retaining the conditions of atomization and stable burning. An inert gas (helium or nitrogen) is used for blow-in; this can be fed from a separate cylinder or taken from the compressed-gas generator tank.

In addition to inert gases, gaseous hydrogen can be blown into the fuel. The gas for saturation can be taken from the primary gasifier or produced in a supplementary liquid gasifier operating on the main propellant components. By increasing the flow of gas for aeration of the propellant components, the engine thrust can be reduced from a 10:1 to a 300:1 ratio.

The (time) average thrust of an engine operating in the pulsed mode can be increased or decreased by *changing the pulse duration* (from tenths of a second to tens of seconds) or by various *on-off time ratios*, i.e., by operating the engine for various lengths of time during each burn.

The change in thrust with adherence to the condition  $\Delta p_\phi = \text{const}$  is used mainly for relatively low-thrust engines.

Various values of the thrusts of certain LPRE's are obtained by *changing the coefficient  $\kappa$* . For example, to increase or decrease the thrust of the J-2 oxygen-hydrogen LPRE used in the American Saturn-5 booster, the coefficient  $\kappa$  is varied from 4.5 to 5.5, i.e., by  $\pm 10\%$  of the rated value; for this, part of the oxygen flow is bypassed from the line at the pump outlet to its inlet. Such a method makes it possible to rapidly change the thrust of the engine while lowering its characteristics only very slightly due to a shift in coefficient  $\kappa$ .

If varying thrust of an LPRE with pump feed is assured by changing the rpm of the component pumps, the TPA turbine should have a system to control its power. Temperature, flow, and hybrid methods of changing TPA turbine power are used.

The temperature method is used for bipropellant liquid gasifiers and consists in changing the temperature of the generator gas fed to the turbine; for this, in one of the gasifier feed lines there is installed a special electric-drive throttle, making it possible to increase or decrease the flow of one of the components to the gasi-

fier and, consequently, the coefficient  $\kappa$  of the generator gas.

The *flow* method consists in changing the flow rate of gas through the turbine, keeping its temperature constant. Such a method can be used for LPRE with mono- and bipropellant liquid gasifiers, and also for engines with gas (e.g., hydrogen) taken from the cooling loop of the chamber to drive the turbine.

Using the flow method of changing turbine power in an LPRE with a bipropellant liquid gasifier, throttles are installed in both feed lines; here the coefficient  $\kappa$  of the generator gas is kept constant. A special stabilizer is sometimes used for this purpose; this is controlled by a throttle located in the line of one of the components, and changes its flow as a function of the flow rate of the second component such that coefficient  $\kappa$  of the generator gas remains constant.

In the *hybrid* method of changing turbine power, the temperature and flow of the gas fed to the turbine are changed simultaneously.

Control systems associated with coefficient  $\kappa$ . The synchronous tank-emptying system. In 52.4 it was shown that the mass of the residue of rocket-vehicle (rocket-stage) propellant components should be low. In the absence of a special control system, cases are possible where a deviation of coefficient  $\kappa$  from the given value causes an increased flow of one of the components. As a result, one component is completely expended before the vehicle reaches its given velocity increase (or decrease, during deceleration), while a large amount of the other component remains unused in the other tank. In order that this not occur we can fill the tanks with a larger amount of components, i.e., increase their guaranteed residues in the tanks. These increase with an increase in the error with which coefficient  $\kappa$  is maintained, and lead to a reduction of the characteristic velocity of the vehicle (stage).

With a deviation of coefficient  $\kappa$  from its rated value there is

a decrease in the total impulse of the engine and the characteristic velocity of the rocket vehicle (the engine operating time for given masses of fuel and oxidizer in the tanks is maximum with strictly proportional expenditures of propellant components); in addition, there is a decrease in the specific impulse of the engine - however, this decrease is insignificant because of the slight steepness of the characteristic curve  $I_{yA} = f(n)$ .

Two types of control systems are associated with coefficient  $n$ :

- 1) the system for maintaining coefficient  $n$  constant ( $n = \text{const}$ );
- 2) the system for synchronous tank emptying, changing to some extent the coefficient  $n$  in order that the residual propellant components in the tanks be minimum at the moment of engine shutdown (up to 0.1% of the full amount).

Figure 14.6 shows a diagram of a system that assures the condition  $n = \text{const}$ . The oxidizer and fuel lines contain flow meters

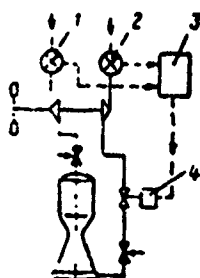


Fig. 14.6. Scheme of LPRE with control system assuring constant value of coefficient  $n$ : 1 - flow meter in oxidizer line; 2 - flow meter in fuel line; 3 - comparator; 4 - electric-drive fuel throttle.

through section and eliminates the deviation of coefficient  $n$  from the calculated value.

Figure 14.7 shows a diagram of the synchronous tank-emptying system. Its sensors are level sensors placed in the tanks, capacitance-type sensors, to be specific; these are two concentric pipes of different metals (to assure temperature compensation for a change

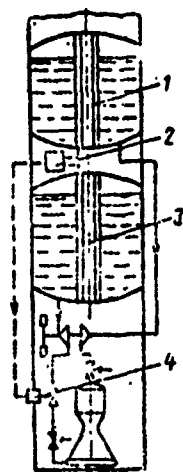


Fig. 14.7. Scheme of a power plant with tank-emptying system: 1 - capacitance-type sensor for oxidizer-tank level; 2 - comparator; 3 - capacitance-type sensor for level in fuel tank; 4 - electric-drive fuel throttle.

in density of the propellant components). The space between the walls of the inner and outer pipes is determined by plastic spacers.

The synchronous tank-emptying system operates in conjunction with the combustion-chamber control system. With a mismatch in emptying of the tanks the synchronous tank-emptying system comes into play, varying the coefficient  $\kappa$  and, consequently, the engine thrust to some extent. If in this case the measured apparent velocity of the vehicle deviates from the programmed value for a given moment of time, the chamber control system begins to operate, changing the thrust appropriately. In this case the coefficient

$\kappa$  might change, necessitating the operation of the synchronous tank-emptying system, and so forth.

Above we examined automatic systems for changing the mode and controlling the engines. Aircraft engines and those of manned space vehicles have, besides the automatic systems, a manual system for remote engine control, making it possible to change the engine operating mode by changing the flow of propellant components and coefficient  $\kappa$ , and also to start up and shut down the engine.

#### §14.4. Systems for creating controlling forces and moments

During flight in the atmosphere a rocket vehicle, analogous to an airplane, can change its flight direction by a deflection of the aerodynamic surfaces (air vanes) located on its body; in the rarefied layers of the atmosphere and in outer space this change can be made only by deflections of the reactive jet.

The system for creating controlling forces and moments should have low mass and introduce the least complications into the scheme for the power plant and the least reduction of its specific impulse.

To create controlling forces and moments we can use the following:

- 1) moveable elements placed in the flow of combustion products exhausting from the chamber nozzle;
- 2) chambers or motors on swivel or Cardan suspensions;
- 3) auxiliary (vernier) motors;
- 4) turnable nozzles on the turbine exhaust pipe;
- 5) redistribution of the flow of turbine working substance (after use in the turbine) through several fixed nozzles on the turbine exhaust pipe;
- 6) injection of liquid or blow-in of gas into the nozzle;
- 7) a change in the thrust created by various engines (for a power plant consisting of several engines).

Moveable elements placed in the flow of combustion products exhausting from the chamber nozzle. These elements include gas vanes, deflectors, and trim tabs that can be deflected using electrical or hydraulic steering motors. These change the direction of flow (partially or completely) of the combustion products discharging from the chamber nozzle, thus creating controlling forces and moments. Gas vanes, deflectors, and trim tabs lower the specific impulse of the power plant since they retard part of the flow of combustion products, and they have a limited operating life: these elements are washed by the combustion products which have, at the nozzle exit, high velocity and relatively high temperature; therefore they are made of heat- and erosion-resistant materials (graphite and special types of plastics).

*Gas vanes* (Fig. 14.8) reduce the velocity of part of the flow of combustion products not only when in the deflecting position but also in the initial position (parallel to the flow); therefore, gas vanes are used only rarely in modern rocket vehicles.

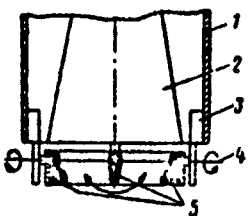


Fig. 14.8. Power plant with gas vanes: 1 - rocket body; 2 - chamber nozzle; 3 - gas-vane drive system; 4 - gas-vane turn axis; 5 - gas vanes.

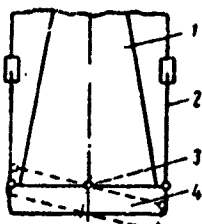


Fig. 14.9. Chamber with cylindrical deflector: 1 - chamber nozzle; 2 - control thrust; 3 - deflector turn axis; 4 - deflector.

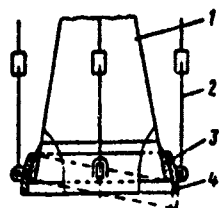


Fig. 14.10. Chamber with spherical deflector: 1 - chamber nozzle; 2 - control thrust; 3 - spherical nozzle fitting; 4 - spherical deflector.

Deflectors, or swivel rings, are installed at the exit from the chamber nozzle or the turbine exhaust manifold. Deflectors can be cylindrical (Fig. 14.9) or spherical (Fig. 14.10). The cylindrical deflector can turn in only one plane, while the spherical deflector can turn in two mutually perpendicular planes.

A more complex, but more economical, system involves the use of *trim tabs*, or telescoping panels, which move into the flow of the combustion products only when it becomes necessary to create controlling forces or moments.

**Deflectable chambers and motors.** The entire chamber or motor can be mounted on swivel or Cardan suspensions and deflected by a certain angle (usually not more than  $10^\circ$ ) from the standard position. The *swivel suspension* permits deflection of the chamber or motor in some *one plane*. If the power plant (engine) consists of four swivel-mounted engines (chambers), the swivels can be attached to a common frame; here the axes of the suspensions intersect in the center (Fig. 14.11). Such installation of the engines (chambers) makes it possible to create forces and moments for controlling the roll, pitch, and yaw of a rocket vehicle; e.g., to control roll, all four engines (chambers) should be turned in one direction around the circle.

A more effective, but more complex, system is Cardan suspension of the chamber (or engine) (Fig. 14.12), in which the chamber

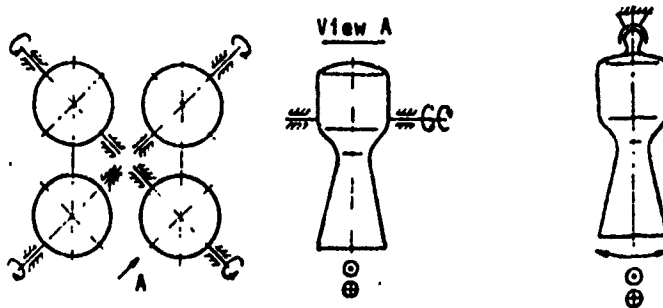


Fig. 14.11. Diagram of the positioning of the chambers of a four-chamber engine, with swivel suspension.

Fig. 14.12. Diagram of chamber installed on cardan suspension.

can be deflected simultaneously in two mutually perpendicular planes; here the longitudinal axis of the chamber can occupy any position within a certain cone.

With Cardan suspension of one engine, forces can be created for controlling the pitch and yaw of a vehicle. Roll is controlled by a separate system, e.g., a cold-gas rocket engine having several nozzles; these are located in a plane perpendicular to the longitudinal axis of the vehicle, and can create a turning moment.

If two engines of the power plant are mounted in the Cardan suspension, their deflection creates forces for controlling the roll, pitch, and yaw of the vehicle.

Average- and large-sized engines are deflected using hydraulic steering motors, small and light, using as the energy source the system for feeding the primary propellant components; most often, for this purpose, part of the flow of fuel at the exit from the TPA pump is tapped. The engine deflection system can operate from an independent TPA. Small engines can be deflected by steering motors operating from an individual electric pump, or by electric steering motors.

Swivel and Cardan suspension of LPRE's assures a simple scheme and design, and reduces the specific impulse only slightly (due only to deflection of the engine).

However, for deflection of chambers or the engine as a whole, great power is needed. Some difficulty is also involved in feeding the propellant components to the deflectable chambers and engines.

**Steering motors.** The main motors can be rigidly attached, provided that the power plant has auxiliary motors, usually placed symmetrically outside the tail section of the vehicle on swivel or

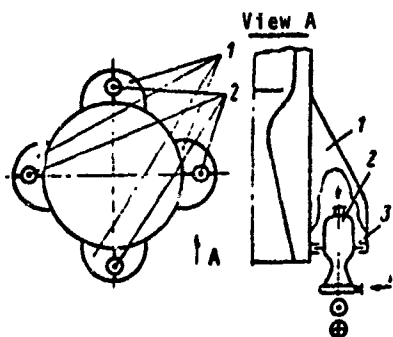


Fig. 14.13. Power plant with verniers:  
1 - aerodynamic cooling; 2 - vernier;  
3 - vernier swivel suspension.

Cardan suspensions (Fig. 14.13). Such motors (called *steering*, *controlling*, or *vernier*) can be deflected by a certain angle and thus create forces and moments for controlling the roll, pitch, and yaw of the rocket vehicle.

The steering motors can operate continuously or in a pulsed mode; for their operation it is most expedient to tap off some of the flow of main propellant components at the exit from the TPA pumps of the primary engines. Such a scheme is used, in particular, in the power plants of the first and second stages of the Vostok booster. However, steering motors can also operate from the TPA itself.

Steering motors complicate the scheme and design of the power plant, reducing its reliability to some extent. There is an insignificant decrease in the specific impulse of the power plant when steering motors are used.

For example, the steering motors of the first and second stages of the Vostok booster reduce the specific impulse of the power plant by 1 N·s/kg [ $\approx 1$  kgf·s/kg].

**Turnable nozzles.** Controlling forces and moments can also be created by steerable nozzles operating on the gaseous working substance of the TPA turbine (in an LPRE with discharge of the working substance, after operation in the turbine, into the ambient medium).

In this case the chamber and the engine as a whole are rigidly installed in the rocket vehicle. The following variants of such nozzles are possible:

1. Exhaust pipes, terminating in fixed nozzles (see Fig. 2.15), are connected to the turbine exhaust manifold; there are two pitch nozzles, two yaw nozzles, and two pairs of roll nozzles. The lines for each pair of nozzles contain an electrically-driven gas distributor. Controlling forces are created by redistribution of the gas flow between like nozzles.
2. One or two exhaust pipes of the turbine terminate in a nozzle which is swivel- or Cardan-suspended from the pipe.

Injection of liquid or blow-in of gas. To create comparatively low controlling forces and moments it is possible to introduce a working substance (inject a liquid or blow in a gas) into the expanding part of the nozzle through openings (nozzles) located in

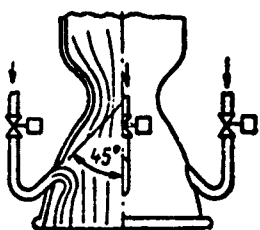


Fig. 14.14. Chamber with four nozzles for introducing the controlling working fluid to the main nozzle.

the wall of the nozzle, equidistant in a circle in any cross section (Fig. 14.14). There can be from 4 to 24 and more nozzles, i.e., there are one or several nozzles in each quadrant of the nozzle section. Four nozzles are sufficient to create lateral forces for pitch and yaw control. The nozzles of each quadrant begin to operate after the valve, located in the line feeding the liquid or gas, has opened.

When introducing the working substance through the nozzle, the gas or liquid vapors penetrate the flow of combustion products. An oblique shock front is created at the point of introduction of the working substance. This results in the occurrence of a lateral force directed toward the nozzle through which the substance is introduced.

The lateral force depends not only on the flow of introduced substance, but also on the slope of the nozzles to the axis of the

chamber nozzle, and also on the number of nozzles and the area and shape of their cross sections. This angle can be anywhere from  $90^\circ$  to  $45^\circ$ ; if  $45^\circ$ , the working substance is introduced counter to the flow of combustion products, and greater lateral force is created.

Round nozzles are more efficient than slotted nozzles. An increase in the number of nozzles complicates the design of the system, but a lesser flow of working substance is required to create an identical lateral force.

The lateral force that occurs also depends on the composition of the working substance introduced and on the basic combustion products.

To decrease the amount of heat removed from the flow of combustion products by the liquid working substance, its heat capacity, boiling point, and vaporization point should be low.

Of the gas blow-in systems the most efficient, from the standpoint of creating lateral forces, simplicity of engine scheme, and lowering of engine mass, is the system for bypassing the combustion products from the combustion chamber or the convergent part of the nozzle to its expanding part; however, this is not used because of the difficulty of obtaining refractory materials, particularly for the regulators.

Systems with the introduction of working substance into the nozzle, as noted above, can create relatively low controlling forces and moments.

However, these systems are also advantageous for the following reasons:

a) an increase in engine thrust because of the introduction of additional working substance into the main flow of combustion products;

- b) high reliability;
- c) short lag time.

Mismatch of the thrust of the engines making up the power plant. If we change the thrust of diametrically opposed engines in a power plant, we can create a controlling moment relative to the center of mass of the rocket vehicle and turn it in the pitch and yaw planes, even though the engines are rigidly attached. Such a system is relatively simple and causes only slight losses of specific impulse of the power plant (caused only by a departure of the engines' operating regime from the rated mode).

#### §14.5. Systems for LPRE shutdown

The system for LPRE shutdown should assure the following:

- a) most complete depletion of the propellant components;
- b) low aftereffect pulse;
- c) smooth cut-in;
- d) the possibility of using the engine (after its bench test);
- e) the required sequence of switching off the engines in a power plant consisting of several engines;
- f) emergency shutdown of the engine, allowing for the possibility, in a number of cases, for its further use;
- g) multiple shutdown (for LPRE's with multiple burn).

It is very complex to assure simultaneous complete depletion of both propellant components. Therefore, a sequence of engine shutdown is used in which one of the components, usually the oxidizer, is totally depleted, i.e., the engine is shut down with excess fuel on a signal that the oxidizer has been totally depleted; the signal is given by the signaller with a reduction in pressure at the exit from the oxidizer pump or by a residue sensor located in the tank.

Certain engines (e.g., LPRE's for anti-aircraft guided missiles and certain meteorological rockets) operate up to total depletion of components from the tanks, and require no shutdown system.

With an increase in aftereffect pulse there is an increase in the absolute value of its scatter, which increases the error in the resultant terminal velocity of the vehicle and, consequently, an error in its landing on target, inserting a satellite into orbit, etc.

'The aftereffect pulse of an LPRE is decreased by:

- a) switching the engine to its final stage of operation before its shutdown;
- b) installing cutoff valves as close as possible to the cavities of the chamber injector head, and their rapid triggering;
- c) draining the propellant components from the cavities behind the cutoff valves into the ambient medium;
- d) installing an insert in the chamber head.

The aftereffect pulse with engine shutdown through the terminal stage is substantially less than with shutdown directly from the rated mode (see Fig. 1.9). If the power plant includes steering motors, the aftereffect pulse is decreased considerably if the primary engines are shut down first as the vehicle approaches its given velocity, and then the steering motors are turned off.

The cutoff valves in the chamber feed lines are installed such that the volume of propellant components from the valves to the chamber injectors is as small as possible. If the chamber has no cooling loop (i.e., in pulse LPRE's), the cutoff valves are located on or inside the head.

In a chamber with a cooling loop the cutoff valve can also be positioned immediately in front of the head and in the line for the propellant component flowing through the loop (Fig. 14.15).

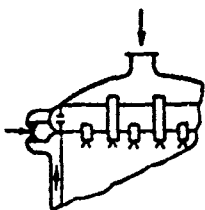


Fig. 14.15. Chamber with valve installed in line between cooling loop and head.

The propellant components are bled from the lines behind the cutoff valves into the ambient medium with opening of the drain valves located in these lines, which substantially reduces the quantity of components entering the chamber after the cutoff valves have been closed. An insert in the chamber head also reduces the quantity of one of the propellant components entering the chamber during engine shutdown; to reduce the chamber mass, the insert is made of a low-density material.

The smoothness of engine shutdown depends on the sequence of closings of the cutoff valves. The command for their closing can be given simultaneously, or at different times. The time for engine shutdown, i.e., a drop in thrust, is usually short (no more than 2-3 seconds); it is determined by the cutoff-valve closing time. If this time is short, the aftereffect pulse is also small; however, a very abrupt closing of the cutoff valves is not permissible, since it leads to hydraulic shocks in the engine lines, resulting in their destruction.

The main or cutoff valves, during engine shutdown, should be air-tight against their seats after closing. Otherwise, the propellant components leak through the valve, which can cause the chamber to explode.

The fuel cavities of the chamber and the gasifier of oxygen LPRE's are purged, during their shutdown, with an inert gas (nitrogen or helium) to prevent the hot combustion products from getting into the fuel injectors and melting them. Such purging is particularly necessary for LPRE's with multiple burn; if there is no purging, the fuel can remain in the fuel cavity of the chamber and gasifier and, with repeated start-up, lead to explosion of the chamber or to intolerable overshoots of temperature in the gasifier; these are particularly dangerous for LPRE's with afterburning of the generator gas (the TPA turbine blades can be damaged).

The purging system should be arranged so that the quantity of fuel displaced by the purging gas into the chamber and gasifier after engine shutdown is small.

When shutting down LPRE's with pump feed, there should be, in addition to the command to close the cutoff valves in the chamber feed lines, a command to close the cutoff valves in the gasifier feed lines. In certain cases there must be, in addition, opening of the valve that bypasses the generator gas to the turbine bypass.

The following types of engine shutdown are distinguished:

- a) normal and emergency;
- b) manual and automatic.

*Normal* engine shutdown is provided by a programmed control system. The engine of the last stage of a ballistic or space missile is shut down after the missile reaches a given velocity; the retro engine of a space vehicle is shut down after its velocity has dropped to a given value.

*Emergency* engine shutdown (EES) occurs when some abnormality is observed during its start-up. The engine includes a special system for detecting an emergency situation. Its sensors measure parameters which, when they deviate from their norms or from the programmed values, are taken as an emergency situation: flight altitude and velocity of a rocket vehicle; roll, pitch, and yaw angles; vibration acceleration of the chamber or pulsations in the engine lines; TPA shaft rpm; etc.

The EES system makes it possible to save the engine by shutting it down before the appearance of destructive vibrations, pulsations, etc. For example, the vibrational-acceleration sensor, located in the chamber head, can send a shutdown signal when the head vibrates sharply. In this case, the engine, during a bench test or as part of the power plant of the first stage of a multistage rocket, can be

saved before it begins to move, and it can be reused, if we can determine the reasons for the increased chamber vibrations.

Manual shutdown can be done, during engine bench tests, by the operator running the test; for the engine of a space vehicle it can be done by a crew member.

However, both normal and emergency engine shutdown is most often done automatically.

As an example we have the EES system which uses a time relay and a sensor for the chamber pressure; if by a given time the engine has not entered the required operating mode (in particular, pressure  $p_h$  has not reached its given value), the time relay gives the command for engine shutdown.

The EES system should have very high reliability; in particular, there should be no possibility for shutting down a normally starting or normally operating engine.

## REFERENCES

1. «Авиационные и ракетные двигатели», РЖ, М., ВИИИТИ, 1965—1971.
2. Алемасов В. Е. и др. Теория ракетных двигателей. Изд. 3-е, переработ. и дополн. Под ред. д-ра техн. наук, проф. В. Е. Алемасова. М., «Машиностроение», 1969.
3. Базакуца В. А. Международная система единиц. Изд. 3-е, переработ. и дополн. Под общей ред. проф. Г. Д. Бурдина. Харьков, ХГУ им. Горького, 1970.
4. Баррер М. и др. Ракетные двигатели. (Пер. с англ.). М., Оборонгиз, 1962.
5. Бассард Р., Делаузэр Р. Ядерные двигатели для самолетов и ракт. (Сокращенный пер. с англ. под ред. д-ра техн. наук О. Н. Фаворского). М., Воениздат, 1967.
6. Ваничев А. П. Термодинамический расчет горения и истечения в области высоких температур. Технический отчет № 18. М., БНТ, 1947.
7. Васильев А. П. и др. Основы теории и расчета жидкостных ракетных двигателей. Под общей ред. В. М. Кудрявцева. М., «Высшая школа», 1967.
8. Волков Е. Б. Ракетные двигатели. М., Воениздат, 1969.
9. Волков Е. Б. и др. Жидкостные ракетные двигатели. Основы теории агрегатов ЖРД и двигателевых установок. М., Воениздат, 1970.
10. «Вопросы ракетной техники», М., «Мир», 1960—1971.
11. Вспомогательные системы ракетно-космической техники. (Пер. с англ. под ред. проф. И. В. Тишинина). М., «Мир», 1970.
12. Глушко В. П. Жидкое топливо для реактивных двигателей. Ч. I. Курс лекций, читаемых ВВА РККА им. Жуковского, М., 1936.
13. Гильзин К. А. Двигатели невиданных скоростей. М., «Машиностроение», 1965.
14. Гильзин К. А. Электрические межпланетные корабли. Изд. 2-е, переработ. и дополн. М., «Наука», 1970.
15. Гурвич Л. В. и др. Термодинамические свойства индивидуальных веществ. Справочник в двух томах. Изд. 2-е, полностью переработ. и расширен. Под ред. акад. В. П. Глушко, Л. В. Гурвича и др. М., изд. АН СССР, 1962.
16. Двигательные установки ракет на жидком топливе. (Пер. с англ.). М., «Мир», 1966.
17. Добровольский М. В. Жидкостные ракетные двигатели. Основы проектирования. М., «Машиностроение», 1968.
18. Нисаев С. И. и др. Основы термодинамики, газовой динамики и теплопередачи. Под общей ред. В. Н. Хвостова. М., «Машиностроение», 1968.
19. Квасников А. В. Теория жидкостных ракетных двигателей. Ч. I. Л., Судпромгиз, 1959.
20. Кондратюк Ю. В. Завоевание межпланетных пространств. Изд. 2-е. Под ред. П. И. Иванова. М., Оборонгиз, 1947.
21. Корлисс У. Р. Ракетные двигатели для космических полетов. (Пер. с англ. под ред. проф. В. К. Кошкина). М., ИЛ, 1962.

22. Королев С. П. Ракетный полет в стратосфере. М., Воениздат, 1934.

23. Космонавтика. Маленькая энциклопедия. Главный ред. акад. В. П. Глушко. Изд. 2-е (дополн.). М., «Советская энциклопедия», 1970.

24. Лангенак Г. Э и Глушко В. П. Ракеты, их устройство и применение. М., ОНТИ НКТП, 1935.

25. Левинсон Я. И. Аэродинамика больших скоростей (газовая динамика). Изд. 2-е. Под ред. Б. Я. Шумлянского. М., Оборонгиз, 1950.

26. Махин В. А. и др. Динамика жидкостных ракетных двигателей. Под ред. д-ра техн. наук, проф. В. А. Махина. М., «Машиностроение», 1969.

27. Мелик-Пашаев Н. И. Жидкостный реактивный двигатель. М., Вениздат, 1959.

28. Мелькумов Т. М. и др. Ракетные двигатели. Под ред. д-ра техн. наук, проф. Т. М. Мелькумова. М., «Машиностроение», 1968.

29. Мошкин Е. К. Нестационарные режимы работы ЖРД. М., «Машиностроение», 1970.

30. Овсянников Б. В. Теория и расчет насосов жидкостных ракетных двигателей. М., Оборонгиз, 1960.

31. Петрович Г. В. Развитие ракетостроения в СССР. У источников советского ракетостроения. М., «Наука», 1968.

32. Петрович Г. В. Развитие ракетостроения в СССР. Штурмы космоса ракетными системами. М., «Наука», 1968.

33. Петрович Г. В. Ракетные двигатели ГДЛ—ОКБ, 1929—1969. М., «Наука», 1969.

34. Рожков В. В. Ракетные двигатели твердого топлива. М., Всесоюз. изд., 1963.

35. Сарнер С. Химия ракетных топлив. (Пер. с англ. под ред. д-ра техн. наук В. А. Ильинского). М., «Мир», 1969.

36. Саттон Д. Ракетные двигатели. Основы теории и конструкции жидкостно-реактивных двигателей. (Пер. со 2-го американского изд.). М., ИЛ, 1952.

37. Справочник химика. Т. 1—2. Изд. 2-е перераб. и дополн. М.—Л., Госхимиздат, 1963.

38. Синярев Г. В. и Доброзвольский М. В. Жидкостные ракетные двигатели. Теория и проектирование. Изд. 2-е переработ. и дополн. М., Оборонгиз, 1957.

39. Синярев Г. В. Обобщенные системы уравнений для определения равновесного состава рабочего тела. Сб. «Некоторые вопросы механики». М., Оборонгиз, 1962.

40. Синярев Г. В. Универсальный метод решения системы уравнений для определения равновесного состава рабочего тела. Сб. «Некоторые вопросы механики». М., Оборонгиз, 1962.

41. Сушкин Ю. Н. Двигатели космических скоростей. М., Воениздат, 1962.

42. Федосеев В. И. и Синярев Г. В. Введение в ракетную технику. Изд. 2-е, исправл. и дополн. М., Оборонгиз, 1961.

43. Фридлендер Е. С. Будущее ракетных двигателей. М., Воениздат, 1963.

44. Чайлдер Ф. А. Проблема полета при помощи реактивных аппаратов. Межпланетные полеты. Сб. статей. Изд. 2-е (дополн.). Под ред. Л. К. Кориесса. М., Оборонгиз, 1961.

45. Чирковский К. Э. Труды по ракетной технике. Под ред. М. К. Тихонравова. М., Оборонгиз, 1917.

46. Чертов А. Г. Международная система измерений. Изд. 2-е, переработ. и дополн. М., «Высшая школа», 1967.

47. Шапиро Я. М. и др. Теория ракетного двигателя на твердом топливе. М., Всесоюз. изд., 1966.

48. Шестюк М. И. Теоретические основы проектирования жидкостных ракетных двигателей. М., Оборонгиз, 1960.

49. Штадлер Э. Ионные двигатели для космических полетов. (Пер. с англ. под ред. канд. техн. наук Л. И. Сорнина). М., Всесоюз. изд., 1966.

50. «Астронавтика и ракетодинамика». Экспресс-информация. М., ВНИИТИ, 1960—1971.

51. Jet, rocket, nuclear, ion and electric propulsion: theory and design. Ed. Loh W. H. T. (Appl. Phys. and Eng. 7). Berlin—Heidelberg—New York, Springer, 1968.

52. Williamson R. A., Jaumotte A., Bussard R. W. Nuclear, thermal and electric rocket propulsion. New York, Cordon and Breach, 1967.